



**CHALMERS**  
UNIVERSITY OF TECHNOLOGY

---



# Kraft cooking of *Eucalyptus Urograndis*

An investigation of the delignification kinetics of eucalyptus wood

Master's thesis in Innovative and Sustainable Chemical Engineering

Anders Ahlbom

Maria Bohman



# Kraft cooking of *Eucalyptus Urograndis*

An investigation of the delignification kinetics of eucalyptus wood

Master's thesis in Innovative and Sustainable Chemical Engineering

Anders Ahlbom  
Maria Bohman

Forest Products and Chemical Engineering  
Department of Chemistry and Chemical Engineering  
CHALMERS UNIVERSITY OF TECHNOLOGY

Gothenburg, Sweden 2018

Kraft cooking of *Eucalyptus Urograndis*

An investigation of the delignification kinetics of eucalyptus wood

ANDERS AHLBOM and MARIA BOHMAN

© ANDERS AHLBOM AND MARIA BOHMAN, 2018

SUPERVISORS:

Prof. Hans Theliander (Chalmers)

Ass. Prof. Merima Hasani (Chalmers)

EXAMINER:

Prof. Hans Theliander

Forest Products and Chemical Engineering  
Department of Chemistry and Chemical Engineering  
CHALMERS UNIVERSITY OF TECHNOLOGY  
Gothenburg, Sweden 2018

**Cover figure**

Photograph of the black liquor fraction 1 to 8 from H\_B cook in flow-through reactor (top), wood chips of *Eucalyptus Urograndis* (bottom left) and wood meal from *Eucalyptus Urograndis* (bottom right).

**Kraft cooking of *Eucalyptus Urograndis***  
**An investigation of the delignification kinetics of eucalyptus wood**

ANDERS AHLBOM and MARIA BOHMAN

Forest Products and Chemical Engineering  
Department of Chemistry and Chemical Engineering  
CHALMERS UNIVERSITY OF TECHNOLOGY

## ABSTRACT

---

Kraft pulping is the dominating pulping method employed worldwide. Although favoured for its pulp quality and efficient chemical recovery it suffers from low yield. Better knowledge on the process of delignification could be used to improve the Kraft pulping process and reduce the yield losses due to carbohydrate degradation through more efficient cooking. Recent studies on softwood have shown that mass transfer play an important part of the delignification process.

Eucalyptus is broadly used as a raw material in the pulp industry. Since it is a hardwood its composition and morphology is different from softwood and it is of interest to investigate whether the impact of mass transfer are applicable for eucalyptus as well. The hypothesis is that the conclusions are transferrable to eucalyptus and the motivation for this thesis is to test whether is true.

The main objective of this thesis was to investigate the impact of mass transport on the delignification kinetics on two length scales: cell wall and wood chip. First, wood meal from *Eucalyptus Urograndis* was cooked in a small flow-through reactor. Secondly, wood chips from *E. Urograndis* were cooked in an autoclave, which enabled comparison between the two length scales of wood material. The concentration of active cooking chemicals, OH<sup>-</sup> and SH<sup>-</sup>, and cooking temperature were kept constant whereas the ionic strength of the cooking liquor and cooking times were varied. Black liquor and pulp received from all cooks were analysed for carbohydrate and Klason lignin content. Furthermore, the molecular weight distribution and structure of the lignin was investigated with GPC and 2D-NMR.

The findings indicate that the delignification rate for eucalyptus wood meal cooked in a flow-through reactor is more rapid than that of wood meal from Scots pine. Moreover, the results imply a possibility that mass transport have a significant impact on the delignification rate of both wood meal and chips. Lastly, findings also indicate that increased ionic strength of the cooking liquor decreases the degree of delignification on both length scales, but the impact is more pronounced on the cell wall scale. However, further investigations are needed to establish these findings.

**Keywords:** *Eucalyptus Urograndis*, **Delignification, Kinetics, Kraft pulping, Mass transport, Flow-through reactor, Ionic strength**

## **Acknowledgements**

We would like to direct our gratitude to a number of people without whom the writing of this thesis would not have been possible.

**Professor Hans Theliander**, our examiner and supervisor at Chalmers University of technology, for giving us the opportunity of writing this thesis, as well as the valuable input and for showing great interest in our work

**Assistant Professor Merima Hasani**, our supervisor at Chalmers University of Technology, for the valuable knowledge and support during the project.

**Research Engineer Ximena Rozo Sevilla** for all guidance and assistance during the laboratory work and daily encouragement throughout the project.

**Dr. Huyen Lyckeskog** for the all help with the NMR analysis and guidance during the project.

**M.Sc. Axel Martinsson** for the help with the autoclave cooks and support when needed.

Finally, we would like to thank all the people at the division Forest products and chemical engineering for your help and encouragement when needed.

Gothenburg 2018-06-14

Anders Ahlbom and Maria Bohman

# TABLE OF CONTENTS

---

1	Introduction.....	1
1.1	Objective .....	2
1.2	Delimitations.....	2
2	Theoretical background.....	3
2.1	Wood.....	3
2.2	Hardwood .....	3
2.2.1	Cell wall structure and ultrastructure.....	4
2.3	Composition of components .....	5
2.3.1	Lignin .....	5
2.3.2	Other major constituents .....	6
2.3.2.1	Cellulose .....	6
2.3.2.2	Hemicellulose.....	7
2.3.2.3	Extractives.....	8
2.4	Eucalyptus .....	8
2.4.1	Eucalyptus Urograndis.....	8
2.5	Kraft pulping.....	8
2.5.1	Cooking chemicals .....	9
2.5.2	Steaming and Impregnation .....	9
2.5.3	Major reactions during Kraft pulping .....	9
2.5.3.1	Delignification.....	9
2.5.3.2	Carbohydrate reactions .....	11
2.5.4	Recovery cycle .....	13
2.6	Analytical methods .....	14
2.6.1	UV .....	14
2.6.2	NMR.....	14
2.6.3	HPAEC-PAD .....	14
2.6.4	GPC .....	15
3	Previous work on delignification kinetics .....	16
4	Method.....	19
4.1	Cooking liquor preparation and ABC-titration .....	19
4.2	Wood meal in continuous flow-through reactor .....	20
4.2.1	Continuous flow-through reactor .....	20
4.2.1.1	Preparation .....	20

4.2.1.2	Impregnation .....	20
4.2.1.3	Cooking.....	20
4.2.2	Chosen experiment parameters .....	21
4.3	Wood chips in batch reactor .....	22
4.3.1	Batch autoclave reactor.....	22
4.3.1.1	Preparation .....	22
4.3.1.2	Impregnation .....	23
4.3.1.3	Cooking.....	23
4.3.2	Chosen experiment parameters .....	23
4.3.3	Choice of chip dimensions .....	24
4.3.4	Separation of BL .....	24
4.3.5	Homogenisation of the pulp.....	25
4.4	Analytical methods .....	25
4.4.1	Klason lignin content.....	25
4.4.1.1	Pulp and wood meal.....	25
4.4.1.2	Black liquor .....	26
4.4.2	Carbohydrate analysis.....	26
4.4.3	Acid soluble lignin content .....	27
4.4.4	Precipitated lignin from BL .....	27
4.4.5	Molecular weight distribution (MWD).....	27
4.4.6	Nuclear magnetic resonance (NMR) .....	27
4.4.7	Number of samples.....	28
5	Results and Discussion .....	29
5.1	Klason lignin.....	29
5.1.1	Flow-through reactor .....	29
5.1.1.1	Constant ionic strength .....	29
5.1.1.2	Changed ionic strength .....	31
5.1.2	Autoclave reactor .....	33
5.1.3	Comparison between autoclave and flow-through cooks .....	35
5.2	Carbohydrates .....	36
5.3	Composition.....	40
5.4	Molecular weights.....	42
5.4.1	Flow-through cooks.....	42
5.4.2	Comparison of $M_w$ of lignin between autoclave and flow-through reactor cooks .....	44
5.5	NMR.....	44
5.5.1	L_B.....	46

5.5.1.1	Aliphatic region.....	46
5.5.1.2	Methoxy, Linkages and Carbohydrates region.....	46
5.5.1.3	Aromatics and alkenes region .....	47
5.5.2	HL_B_60 .....	47
5.5.2.1	Aliphatic region.....	47
5.5.2.2	Methoxy, Linkages and Carbohydrates region.....	48
5.5.2.3	Aromatics and alkenes region .....	48
5.5.3	Comparison between L_B and HL_B_60.....	48
6	Conclusions .....	50
7	Future work .....	51
Appendix I	.....	I
Calculations performed during ABC-titration.....		I
Calculations on which the added amount of Na <sub>2</sub> CO <sub>3</sub> was based.....		I
Appendix II	.....	II
Calculations of H-factor.....		II
Appendix III	.....	III
Calculations of Klason lignin in theoretical pulp .....		III
Appendix IV	.....	IV
Literature values for composition in <i>E. Urograndis</i> .....		IV
Appendix V	.....	V
MWD.....		V
Appendix VI	.....	XI
2D-NMR.....		XI
L_B samples.....		XI
HL_B_60 samples .....		XII

## ABBREVIATIONS

<b>ASL</b>	Acid Soluble Lignin	<b>Man</b>	Mannose
<b>Ara</b>	Arabinose	<b>MWD</b>	Molecular Weight Distribution
<b>BL</b>	Black liquor	<b>M<sub>w</sub></b>	Weight average molecular weight
<b>DMSO</b>	Dimethyl sulfoxide	<b>NMR</b>	Nuclear Magnetic Resonance
<b>GPC</b>	Gel Permeation Chromatography	<b>PAD</b>	Pulsed Amperometric Detection
<b>Gal</b>	Galactose	<b>PEG</b>	Polyethylene glycol
<b>Glu</b>	Glucose	<b>r.t.</b>	Room temperature
<b>HPAEC</b>	High Performance Anionic Exchange Chromatography	<b>SEC</b>	Size Exclusion Chromatography
<b>HSQC</b>	Heteronuclear Single Quantum Coherence spectroscopy	<b>UV</b>	Ultraviolet spectroscopy
<b>LCC</b>	Lignin-Carbohydrate Complex	<b>Xyl</b>	Xylose

## SAMPLE LABELLING

The labelling of the test series convey information of ionic strength and cooking time. For the flow-through reactor experiments the labels also contain information on the exchange time of cooking liquors. The labels are of the form YY\_X\_NN, where Y either is H or L which gives the ionic strength of the cooking liquor (H=high, L=low), X relates the cooking time (A=90 min, B=180 min, C=40 min, D=18 min, E=22 min and F=60 min) and N gives the exchange time. A, B and C cooking times were used in the flow-through reactor, whereas D, E and F cooking times were used in the autoclave reactor. Consequently:

- LH\_B\_30 means that the cook starts at low ionic strength. After 30 min this was changed to high ionic strength and the total cooking time was 180 min.
- HL\_A\_60 means that the cook starts at high ionic strength. After 60 min this was changed to low ionic strength and the total cooking time was 90 min.
- L\_B means that the cook was at low ionic strength for 180 min.
- H\_F mean that the cook was at high ionic strength for 60 min in the autoclave.
- TL samples are reruns of the L cook in the autoclave.

# 1 INTRODUCTION

---

In the following section the background to the project is presented. Next the overall aim is stated followed by the research questions. Finally the delimitations of the projects are stated.

Kraft pulping is currently the most dominant process method worldwide for pulp production used for various pulp products, such as paper and dissolving pulp, and have been so for more than a half a century. Both soft- and hardwoods are pulped with the Kraft process. The principle is that woodchips are cooked with an alkaline solution in which the active ions are hydroxide and hydrosulphide ions. The aim of the process is to remove lignin from the wood as selectively as possible.

Although favoured for its ability to produce strong pulp, Kraft pulping suffers from problems with low yield, roughly 50 % of the wood raw material is lost due to carbohydrate degradation and lignin dissolution. The alkaline environment in the Kraft cooking digester do not only degrade lignin in the wood but also the other major constituents, namely hemicellulose and cellulose (Dang, 2017). Degradation of the latter two compounds is undesirable since it lowers the yield of the process. Hence, optimisation of the cooking conditions is needed to selectively degrade the lignin in the wood while at the same time avoiding degradation of the other major constituents of the wood. Understanding the delignification kinetics of the Kraft process is therefore crucial to maintain a high yield in the process (Santos et al., 2011).

Kraft pulping have been extensively investigated and a good understanding of macroscopic level of delignification has been attained (Dang et al., 2016a). A pseudo-homogenous assumption of the kinetics of delignification is prevailing in these studies. The mass transport rate, desorption and solubility of reaction products is thus neglected and the delignification is described with a reaction kinetic expression. There are some models that include the influence of mass transport and manage to describe the delignification. For example Gustafson et al. proposed such a model (Gustafson et al., 1983). However, it has not been conclusively shown that the mechanisms used in these models govern the kinetics of overall delignification (Dang et al., 2016a). More recent work on the softwood species *Pinus Sylvestris*, Scots pine, performed by Dang have established mass transport to play a significant role during the delignification process at a cell wall level contrary to the common assumption of pseudo-homogenous kinetics (Dang, 2017).

While delignification kinetics in Kraft cooking of softwood thus have been shown to be dependent on mass transport, some parts of the delignification kinetics of hardwood remain unestablished. Studies have been conducted on the delignification kinetics in Kraft cooking of hardwood, but with focus on the lignin structure and how it effects the solubility of lignin. Comparing the delignification rate of wood chips to that of sawdust, no difference was found with the methods used by Santos et al., which implies that the delignification on this level is governed by reaction kinetics rather than mass transport (Santos et al., 2011). On the other hand Mattson et al. found that for Scots pine, the major lignin reactions occur rapidly and that the delignification thus is limited by mass transport on the cell wall level (Mattsson et al., 2017). What limits the delignification on cell wall level of hardwood remains an open question.

Eucalyptus is a genus consisting of several tree species. Many of these species display high forest productivity, thrive in short rotation plantations in tropical areas and result in high pulp yield (Silverio et al., 2007). Therefore, eucalyptus is the most predominant short fibre hardwood used in pulp and paper industry (Wimmer et al., 2008). In light of this, delignification kinetics of eucalyptus will be explored with focus on mass transport.

## 1.1 OBJECTIVE

The main scientific goal is to increase understanding of Kraft cooking kinetics by elucidating cooking behaviour of hardwood eucalyptus in relation to previous findings on softwood made by Dang (Dang, 2017) and Mattsson et al. (Mattsson et al., 2017). Improved knowledge on delignification kinetics, e.g. rate determining factors, governing conditions, etc., would open up for future improvements in one of the largest pulping processes.

- Is the delignification rate of *Eucalyptus Urograndis* limited by mass transport or reaction kinetics?
  - On which morphological level; chips size and/or cell/cell wall size?
  - If so, is the effect more or less pronounced than in the findings of (Dang, 2017) on Scots pine?
  - Does the cell structure, and in particular the vessels, affect the delignification rate?

## 1.2 DELIMITATIONS

- Experiments were performed with wood of *Eucalyptus Urograndis*. The wood came from all parts of the trunk from one specific tree. No softwood experiments were conducted.
- The laboratory work was conducted with wood meal in a flow-through reactor and wood chips in a batch autoclave reactor.
- Following the method of Dang, two parameters in the cooking of wood meal were tested: cooking time and ionic strength of the cooking liquor. The influence of changed ionic strength during the cook was also investigated.
- Dang made exchanges of ionic strength both at 30 and 60 min of cooking time in the same cook. In this work the ionic strength was only changed once in each cook, either at 30 or 60 min.
- On the wood chips, cooking time and ionic strength were the investigated parameters. The ionic strength was not exchanged during the cook, as opposed to the flow-through reactor cooks.
- The concentrations of the active cooking ions, namely  $\text{OH}^-$  and  $\text{HS}^-$ , were not varied.
- The characterization of the raw material and products from the cook, namely wood meal, black liquor and pulp, focused on lignin and sugar content. No investigation on extractives and ash was performed.

## 2 THEORETICAL BACKGROUND

---

This section will first introduce wood which is the raw material for Kraft pulping. A brief introduction to its morphological levels and composition is given, which is further developed in the next section on hardwood. Next comes a section with a more extensive description of the components building the cells of the wood. *Eucalyptus Urograndis*, the wood species used as raw material in this project is introduced afterwards and a brief overview of the Kraft pulping process is given. Finally a theoretical background to the characterisation methods used in the project is given.

### 2.1 WOOD

Wood is the most abundant source of biomass on earth and is a fibrous tissue building up the main part of the trees. It is a bio-composite consisting of different compounds, such as cellulose, hemicellulose and lignin. As all living organisms the wood is built from cells, with the objective of giving a strong and resilient structure. The trees need to transport nutrients and water from the ground upwards to the leaves and needles where the photosynthesis occur. Carbohydrates, formed by the photosynthesis, need to be transported downwards to be used as energy storage and building material for cells. To ensure efficient transport and stability, the trees are ordered on several morphological levels (Henriksson et al., 2009).

The majority of the wood material is located in the stem, hence the stem is the part of the tree predominantly used in pulping. The stem consists of different zones. Beneath the bark the *phloem*, in which transport of nutrients from the photosynthesising leaves or needles takes place, is situated. Next comes the *cambium* which is the growth zone of the tree together with the tips of the stem, roots and branches. Inside the *cambium* the wood tissue, *xylem*, is situated. This is divided into sapwood and heartwood, with the latter forming the core of the stem together with the juvenile wood created during the first years of growth. The heartwood is dead tissue and gives support to the stem. The sapwood serves to transport water and minerals upward to the leaves and needles (Henriksson et al., 2009).

The next morphological level is the macroscopic cell structure with different specialised cells for support and transport (Daniel, 2009).

### 2.2 HARDWOOD

Wood is generally divided into two main anatomical groups, hardwood and softwood. Hardwood trees are often flowering trees and have a more complex morphology than softwood with more specialised cells. Hardwoods are also more genetically evolved. Softwood, on the other hand, have a simpler morphology and are so called evergreen conifers. In general softwoods also have longer fibres than hardwoods which is suitable for pulp applications where strength is of importance. Shorter fibres from hardwood find applications in other types of products, such as printing paper (Henriksson et al., 2009).

As mentioned above, hardwood has a more complex anatomical structure, and consists of a larger number of cell types than softwood. The major cell types present in hardwood and their function are shown in Table 1. Softwood trees do not have the vessels and libriform fibres which are present in hardwood. Instead the functions of these cells are taken care of by the tracheids (Daniel, 2009).

Table 1. The major cell types in hardwood and their functions.

Cell type	Function
<b>Vessels</b>	Conduction
<b>Fibres</b>	
<i>Libriform fibres</i>	Support
<i>Fibre tracheids</i>	
<b>Tracheids</b>	
<i>Vascular tracheids</i>	Conduction
<i>Vasicentric tracheids</i>	
<b>Parenchyma</b>	
<i>Ray parenchyma</i>	Storage
<i>Longitudinal parenchyma</i>	

The presence of vessels in hardwood is one of the major structural differences between hard- and softwood. In hardwood the function of the vessels is to transport liquids in the wood. In a transverse cross sectional area of the wood, it is possible to observe the vessels with the naked eye as small holes. Hardwood is therefore called “porous wood”. The vessels can be arranged in different ways depending on in which climate zone the tree grows. The different arrangements are “diffuse porous” where the vessels are uniform in size and evenly distributed, “ring-porous” with much larger vessels in the earlywood<sup>1</sup> than in the latewood<sup>2</sup>, and “semi-ring porous” where the vessels in the earlywood is slightly larger than those in the latewood. Among these arrangements, diffuse porous is the most common among the hardwoods used in the paper industry (Daniel, 2009). Eucalyptus is an example of a hardwood with the “diffuse porous” arrangement of the vessels (Sreevani and Rao, 2015).

### 2.2.1 Cell wall structure and ultrastructure

Cell walls in wood are mainly composed of cellulose, hemicellulose and lignin in a skeletal matrix from which the lignin is removed during pulping. The cell wall is arranged in several layers: one primary and two to three secondary layers with different fibre orientation, shown in Figure 1. Besides being a part of the cell wall, lignin is also a major part of the middle lamella. The lignin in the middle lamella “glues” the cells together and increases the stiffness (Daniel, 2009).

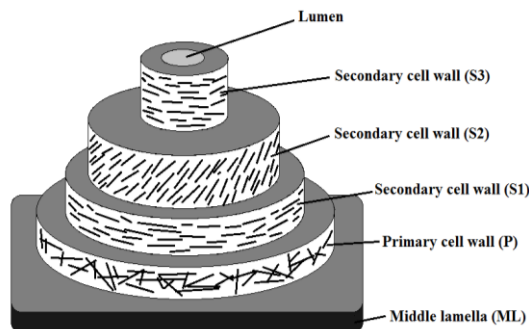


Figure 1. Scheme over the cell wall structure in wood. The lines in each layer represents cellulose fibres.

<sup>1</sup> Wood grown in spring.

<sup>2</sup> Wood grown in summer.

## 2.3 COMPOSITION OF COMPONENTS

The composition of components in wood varies between species but can also vary within a species and within different parts of a tree. A typical composition of *E. Urograndis* is presented in Table 2 as percentage of the wood.

Table 2. Composition of *E. Urograndis* wood. The values are presented in percentage of the total wood (Pinto et al., 2005).

	Klason lignin	Extractives	Glucose (Glu)	Xylose (Xyl)	Rhamnose (Rha)	Arabinose (Ara)	Mannose (Man)	Galactose (Gal)
<i>E. Urograndis</i>	27.9	1.91	52.1	11.4	0.2	0.4	0.7	1.2

### 2.3.1 Lignin

As previously mentioned in section 2.2.1, lignin “glues” wood cells together and contributes to the stiffness of the wood cells. Furthermore, lignin makes the cell wall hydrophobic and provides an efficient barrier against microorganisms. A lignified tissue is highly compact and simply too dense for microbes to enter. Therefore, lignin protects against microbial degradation by blocking the microbes from entering the wood structure (Henriksson, 2009). Lignin has the most complex structure of the naturally occurring polymers due to its mixture of aromatic and aliphatic parts and its branched structure, shown in Figure 2.

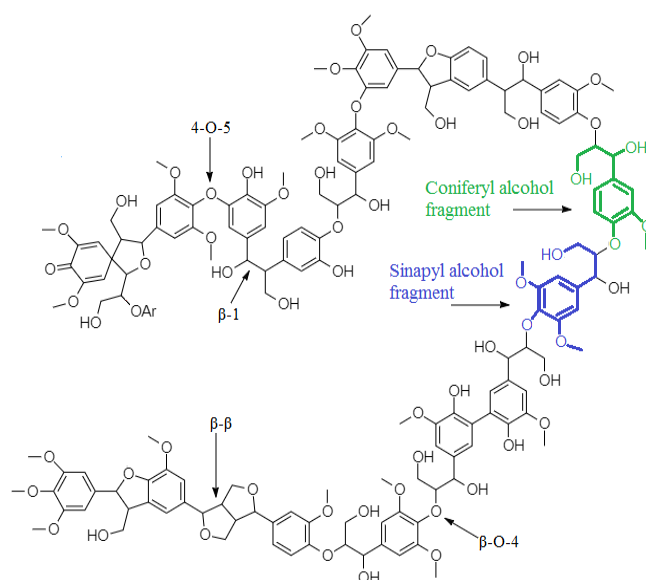


Figure 2. Simplified hardwood lignin structure showing both the most common monolignols and common bonds. Redrawn from (Zakzeski et al., 2010)

Lignin is polymerised from three different monolignol monomers. These monolignols are shown in Figure 3, and the ratio between them differ between hardwood and softwood. The atoms in these phenylpropane are conventionally labelled as shown in Figure 4, thus bonds between different monolignols may be named, e.g.  $\beta$ -O-4 and  $\beta$ - $\beta$  shown in Figure 2 (Henriksson, 2009).

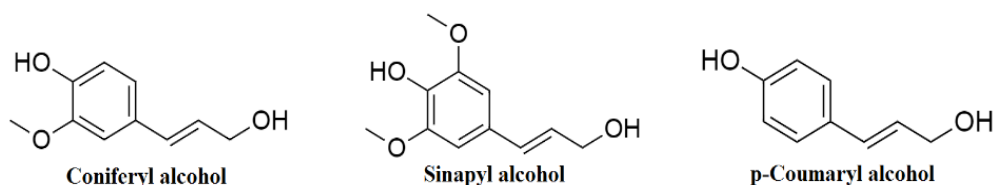


Figure 3. Structure of the most common monolignols in hardwood lignin

Hardwood lignin consists mostly of coniferyl and sinapyl alcohols, which is shown in Figure 2. When incorporated in the lignin structure the phenylpropanoid fragment from the coniferyl alcohol is denoted guaiacyl, G, and the corresponding sinapyl alcohol fragment is denoted syringyl, S. The S/G ratio is used as an indicator for ease of delignification where a higher S/G ratio generally means a swifter delignification. The amount of condensed structures in the lignin decreases with higher S/G ratio whereas the important  $\beta$ -O-4 bonds increase (Magaton et al., 2009). The ratio is thus used as a parameter in clonal breeding programs of eucalyptus for pulpwood. Different species of hardwood have different S/G ratios and in a study of industrially important hardwood species Santos et al. concluded that the eucalyptus together with birch had the highest S/G ratios, shown in Table 3. Eucalyptus was found to be easiest to delignify (Santos et al., 2011). Softwood contains no syringyl and, in general, hardwood is easier to delignify than softwood (Ek et al., 2009).

Table 3. S/G ratios of commercially important hardwoods and pine from (Santos et al., 2011)

Species	S/G ratio	Species	S/G ratio
<i>Eucalyptus Nitens</i>	2.59	Red alder	1.37
<i>Eucalyptus Urograndis</i>	1.76	Maple	1.27
<i>Eucalyptus Globulus</i>	2.73	Red oak	2.12
Cottonwood	1.41	Birch	3.15
Acacia	1.18	Pine	0

The  $\beta$ -O-4 bound, which is shown in Figure 4, is the most common bond between the monolignols in hardwood lignin. It is also the bond which is the easiest to break due to its low strength. Other common bonds include  $\beta$ -5, 5-5 and 4-O-5. Hardwood lignin contains a larger part of  $\beta$ -O-4 bounds than softwood lignin and is also believed to be more linear, which is one of the explanations to why hardwood lignin easier to degrade (Henriksson, 2009).

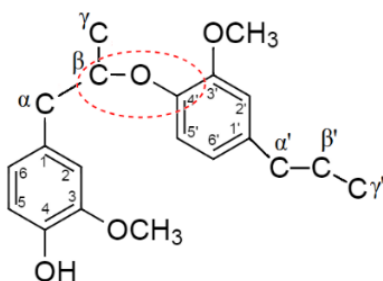


Figure 4. Illustration of the  $\beta$ -O-4 linkage, marked with a dotted ring. Also illustrated is the labelling of the phenylpropane atoms.

### 2.3.2 Other major constituents

Apart from lignin, wood also consists of the major components cellulose, hemicellulose and extractives. These will be briefly introduced in the following sections.

#### 2.3.2.1 Cellulose

Cellulose is the main component in the cell wall. It has a rather simple and ordered chemical structure, compared to e.g. lignin, with long unbranched chains consisting of glucose, it displays several scientific and technical properties, such as high mechanical strength, relatively high resistance to chemical derivatization. Hence, it is, together with hemicelluloses, the target product of pulping processes (Henriksson and Lennholm, 2009).

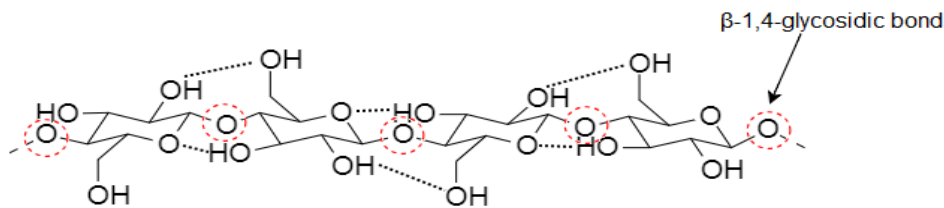


Figure 5. Primary structure of cellulose. The dashed lines indicate the  $\beta$ -1,4-glycosidic bonds.

When cellulose is biosynthesised from glucose the polymerisation occurs as a condensation reaction. Water is released as the glucose units are connected. The resulting chain consists of anhydrous glucose units. The primary structure of cellulose, shown in Figure 5, is hence a linear unbranched polymer of D-glucopyranose connected with  $\beta$ -1,4-glycosidic bonds. However, cellulose is not totally straight, rather it is a much extended helix with every second glucopyranose unit rotated approximately  $180^\circ$ . This rotation imposes a two-fold-helical conformation of the chain. Wood cellulose has often a high degree of polymerisation, around 8000. The cellulose chains are stabilised by intramolecular hydrogen bonds (black dashed lines in Figure 5) and connected with intermolecular hydrogen bonds, to form narrow sheets of cellulose. These sheets are stacked with van der Waals bonds connecting them which results in a crystalline structure, increasing the resistance to degradation (Henriksson and Lennholm, 2009). However, cellulose also contain more unorganized structures with irregular spacing between the chains and random relationship between chains. These unorganized structures can be either semi-crystalline or amorphous and are more sensitive to degradation than the crystalline parts (Brown and Saxena, 2007). The chains running through these amorphous, semi-crystalline and crystalline parts then form bundles called microfibrils, which in turn forms bundles, so called macrofibrils. Bundles of macrofibrils make up the fibres and these are shown as lines in Figure 1 (Henriksson et al., 2009).

### 2.3.2.2 Hemicellulose

Together with lignin and cellulose, the hemicelluloses are one of the main constituents in wood, representing between 20-35 % of dry the wood. Hemicellulose contributes to the strength of the wood and generally occur as hetero-polysaccharides. The degree of polymerization of hemicelluloses is up to 200, which is considerably lower than cellulose. The main building blocks of the chains are hexoses and/or pentoses; mannose, xylose, glucose, arabinose, galactose and rhamnose.

The most common types of hemicelluloses are glucomannans and xylans. Softwood contain more glucomannan than hardwood. Glucuronoxylan is the predominant hemicellulose in hardwoods, with small proportions of glucomannan also being present. Two common glucomannans are galactoglucomannan and glucomannan. Both are built from a backbone of  $\beta$ -1,4-linked D-gluco- and D-mannopyranose. D-galactopyranose and acetyl are present as side groups. Glucomannan contains less galactose but more mannose than galactoglucomannan (Teleman, 2009).

Examples of xylans include arabinoglucuronoxylan and glucuronoxylan. Both have a backbone of  $\beta$ -1,4-linked D-xylopyranose and side groups of 4-O-methyl-glucuronic acid. The former also have a side chain of L-arabinofuranose but is not acetylated as glucuronoxylan. Arabinoglucuronoxylan is present in softwoods whereas glucuronoxylan predominates in hardwoods (Teleman, 2009). In Figure 6, glucuronoxylan is shown. The acetyl groups are marked with Ac and the 4-O-methyl-glucuronic acid is the side chain to the right. It should be noted that softwood and hardwood xylans and glucomannans, not only differ in the types of side groups and their binding sites but also in the proportion of the sugar monomers. Eucalyptus species' hemicelluloses consists mainly of xylans. These xylans are especially rich in uronic acids (Magaton et al., 2009).

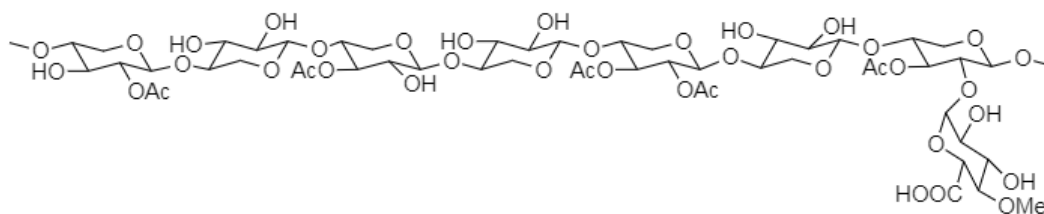


Figure 6. Structure of hardwood glucuronoxylan.

### 2.3.2.3 Extractives

Wood extractives are defined as compounds with low molecular weight which can be extracted with various neutral solvents depending on the sort of extractive. The composition and structure of extractives varies considerably between tree families and genera. Therefore, the extraction procedure must be specified based on which extractive that should be extracted. The extractives have different functions e.g. to act as fungicides, insecticides, hormones and as an energy source.

Extractives only make out a few percentages of the wood but can have an impact on the final pulp product quality and cooking outcome. The extractives are divided into three groups based on lipophilic components. The groups are: fats and fatty acids, terpenoids and terpenes, phenolic extractives (Björklund Jansson and Nilvebrant, 2009).

## 2.4 EUCALYPTUS

Eucalyptus is a genus belonging to the myrtle family and consists of more than 500 species. The eucalyptus trees has silver-green coloured leaves which contain an aromatic oil, known as eucalyptus oil. Some species has white or red flowers. Eucalyptus grows naturally in Australia and surrounding areas, but is also cultivated in tropical and subtropical areas. Some species of Eucalyptus can grow up 100 meters (Henriksson et al., 2009). Eucalyptus wood is becoming a more and more dominating short fibre source for pulp and paper industry. Especially in South America and the Iberian Peninsula, eucalyptus is used as a raw material for the Kraft pulp production. Eucalyptus is preferred due to its high growth rate, low requirement on pulping and bleaching conditions, and it has good papermaking performance (Evtugin and Neto, 2007).

### 2.4.1 Eucalyptus Urograndis

*E. Urograndis* is a hybrid of the species *E. Grandis* and *E. Urophylla*. These two have been chosen for cross breeding due to the rapid growth rate of *E. Grandis* and the disease tolerance of *E. Urophylla*. Therefore, *E. Urograndis* holds both of these properties and is preferred by the pulping industry (Leonardi et al., 2015).

## 2.5 KRAFT PULPING

Kraft pulping, also known as sulphate pulping, is the dominating pulping process today. Other pulping processes include sulphite pulping and mechanical pulping. The majority of all pulp is produced through Kraft pulping and it is unlikely to decrease. As active cooking chemicals, sodium hydroxide and sodium sulphide dissolved in water are used, where the active cooking species are  $\text{OH}^-$  and  $\text{HS}^-$  (Brännvall, 2009a). Prior to the cooking, the liquor is called white liquor (cooking liquor). Degradation of lignin occurs during the cook, which increases solubility and results in lignin removal from the wood. The removal of lignin enables fibre liberation (Dang, 2017). After treatment such as washing and defibrillation is performed followed by bleaching. Depending on the application of the pulp and the desired properties the bleaching degree is adjusted to yield the desired lignin content in the pulp (Brännvall and Annergren, 2009). The spent cooking liquor, commonly called black liquor, is then processed to recover the cooking chemicals and convert dissolved organics (mainly lignin) to heat.

Kraft pulping has lower demands than other pulping methods on which wood species and qualities that can be used as raw materials. It also requires relative short cooking times, has well established methods for processing the spent liquor, and yields superior strength properties of the pulp. However, some drawbacks exist, such as low yield due to carbohydrate degradation, dark colour of pulp and high installation costs of new equipment (Fengel and Wegener, 2011). In Figure 7, a simplified scheme of the Kraft pulping process is shown (Dang, 2017).

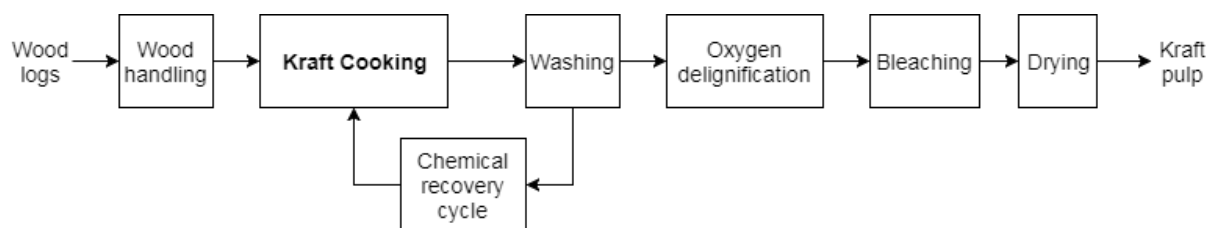


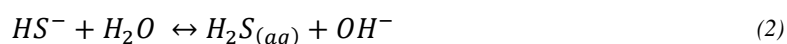
Figure 7. A simplified scheme of the Kraft pulping process.

### 2.5.1 Cooking chemicals

As mentioned in section 2.5, the cooking liquor used during Kraft cooking mainly consists of sodium hydroxide (NaOH) and sodium sulphide (Na<sub>2</sub>S) dissolved in water. Na<sub>2</sub>S is hydrolysed into both OH<sup>-</sup> and HS<sup>-</sup> when mixed with water, according to the equilibrium reaction shown in Eq. (1).



However, further hydrolysis of HS<sup>-</sup> can occur, as shown in equilibrium reaction Eq.(2), which means that S<sup>2-</sup> can exist as S<sup>2-</sup>, HS<sup>-</sup> or H<sub>2</sub>S. During alkaline conditions, the equilibrium in Eq. (1) is shifted to the right and generally HS<sup>-</sup> is the active ion of interest.



### 2.5.2 Steaming and Impregnation

Steaming and impregnation is used in order to achieve a homogeneously delignified pulp. If that is not achieved, the cooking chemicals will not reach the centre and the fibres will be unevenly cooked resulting in over and undercooked parts. During steaming the air within the wood is substituted with water in form of steam, which facilitates a better impregnation. The cooking chemicals are then distributed within the chip during impregnation by liquor penetration and diffusion (Brännvall, 2009b).

### 2.5.3 Major reactions during Kraft pulping

During the Kraft cooking, which occurs at high temperature (150-170 °C) and pH, several reactions occur. Some are desired, such as delignification reactions breaking the β-O-4 bonds, whereas other are not. Degradation of cellulose and hemicellulose are examples of undesired reactions. Hence, there is a trade-off between delignification and carbohydrate degradation (Gellerstedt, 2009a). In this section, the reactions that occur during the cook will be presented.

#### 2.5.3.1 Delignification

Delignification reactions degrade and dissolve the lignin in the wood. The degradation increases the solubility of the lignin since large lignin molecules are fragmented. Moreover, the degradation introduces ionisable phenolic groups in the large organic lignin structure which increases its solubility in the polar cooking liquor. Delignification reactions are hence desired since they enable removal of lignin from the wood. The lignin dissolves in the black liquor, but the solubility is highly pH dependent. By lowering the pH the lignin may be re-precipitated when deprotonated phenol groups are re-protonated (Gellerstedt, 2009b). Furthermore, the lignin dissolved from the wood may be connected to

carbohydrates in so called lignin carbohydrate complexes (LCC:s). These may be formed from breaking the lignin-carbohydrate network or condensation reactions between lignin fragments and carbohydrates (Henriksson, 2009).

Delignification can be described in three phases possibly having different rates, but there is debate about if this is a suitable description. The three suggested phases are as follows (Brännvall, 2009b):

1. Initial phase: Occurs at temperatures below 140 °C and the dissolution of lignin is rapid. This phase continues until a dramatic change in delignification rate occur, which happens when around 20 % of the lignin has been removed.
2. Bulk phase: The major part of the lignin is degraded and dissolve in this phase, while the dissolution of the carbohydrates is small. Hence, this phase has the highest selectivity. The bulk phase continues until approximately 90 % of the lignin has been dissolved or degraded.
3. Residual phase: The delignification in this phase is very slow and the cook is often interrupted before this phase begin due to the high loss of carbohydrates (Gellerstedt, 2009a).

Furthermore, delignification is a two-phase heterogeneous reaction system between the liquid cooking liquor and the solid wood. The reaction thus involves mass transport to and from the wood. Dang describes this as occurring in the following steps (Dang, 2017):

1. Mass transport of cooking liquor from the bulk to the wood chip surface
2. Mass transport of cooking liquor from the surface into the chip (pores and cell wall)
3. Reactions and dissolution of lignin, carbohydrates and other wood components
4. Mass transport of dissolved wood components from the pores to the surface
5. Mass transport of dissolved wood components from the surface to the bulk

Fragmentation of the lignin during the cook transpires through breaking of the dominant chemical linkage between the phenylpropanes, the so called  $\beta$ -O-4 bond, shown in the far left of Figure 8. The hydrosulphide ions fragments the phenolic  $\beta$ -O-4 structures extensively. However, phenolic  $\beta$ -O-4 structures make out less than 15 % of the total wood lignin (Chen et al., 1997). The fragmentation reaction with hydrosulphide is possible due to the alkaline cooking conditions in which quinone methide is formed from phenolic benzyl structures. Due to the presence of hydrogen sulphide ions, an equilibrium with a benzyl thioalcohol structure forms. Once the benzyl thioalcohol is formed, it attacks the  $\beta$ -carbon, which results in the formation of an episulphide and a phenolic end-group finalizing the cleavage of the  $\beta$ -O-4 bond. Episulphide is an instable structure and sulphur will hence be expelled to the cooking liquor.

However, other competing reactions transpires at the quinone methide intermediate, such as the loss of a  $\gamma$ -hydroxymethyl group which forms a stable enol ether without breakage of the  $\beta$ -O-4 bond, at the bottom of Figure 8. As a result of this competing reaction, the delignification rate will decrease. Other reactions that occur is reduction and condensation of the quinone methide intermediate. The condensation reactions introduce carbon-carbon bonds between the quinone methide and other lignin fragments or carbohydrates. The mentioned reactions is shown in Figure 8 (Gellerstedt, 2009a).



## Peeling reaction

During peeling reactions the reducing end-groups on the carbohydrate chains are rearranged and eliminated, which creates a new reducing end and the reaction sequence starts over. The result is that the carbohydrate polymer is shortened monomer by monomer. Temperatures from 100 °C and alkaline conditions promote the peeling reaction, seen in Figure 10, to occur.

In presence of alkali, an equilibrium will be formed between the aldehyde and keto form of the reducing end group sugar unit via an enediol rearrangement. A  $\beta$ -elimination may occur from both the aldehyde and the keto form, eliminating the first sugar unit by cleavage of the glucosidic bond in the 4-position. This reaction sequence will be repeated until a stopping reaction occurs, after elimination of approximately 50-100 monomers. Stopping reactions occur due to a rearrangement when the  $\beta$ -elimination transpires from an aldehyde, but not a ketone. This rearrangement forms alkali stable meta-saccharinic which stabilises the end-group.

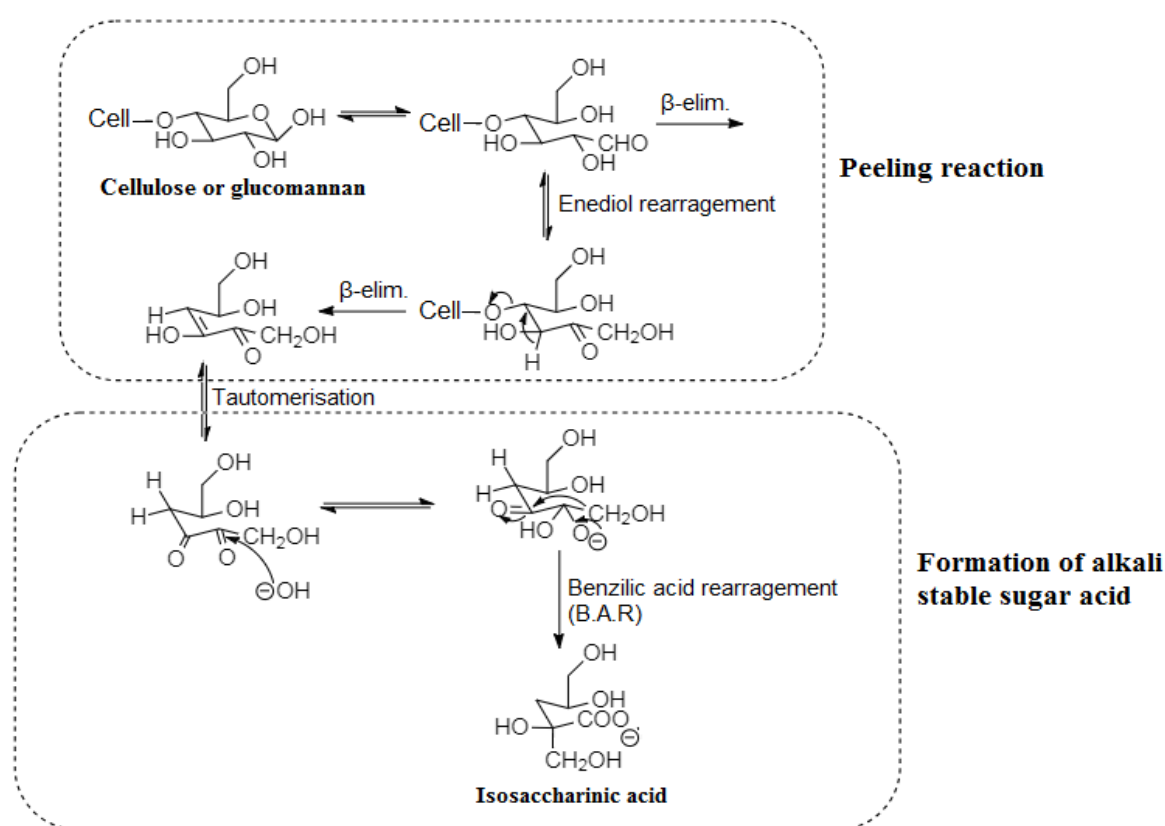


Figure 10. Mechanism for peeling reaction and a possible following formation of an alkali stable sugar acid. The " $\beta$ -elim." in the top right corner is also a peeling reaction. Redrawn from (Gellerstedt, 2009).

After the  $\beta$ -elimination the sugar unit removed from the carbohydrate chain may react further via a benzylic acid rearrangement creating alkali stable isosaccharinic acid. Certain carbohydrates are more protected against the peeling reaction than others. For instance, the hemicellulose xylan has side groups on its chain which protects it from extensive  $\beta$ -elimination by preventing the rearrangement of the reducing end. Also, cellulose is protected to some degree since it is partly crystalline and has a high degree of polymerisation, meaning that there are few end groups from which the peeling can occur. In contrast hemicelluloses, such as glucomannan, have more end groups, owing to their low degree of polymerisation leading to extensive peeling (Gellerstedt, 2009a).

## Alkaline hydrolysis

Alkaline hydrolysis of the glucosidic linkages may occur at elevated temperatures, around 170 °C, and results in further loss of cellulose. Unlike the peeling reaction which transpires from reducing end groups on the carbohydrate chains, the alkaline hydrolysis may occur at any glucosidic linkage along the chain. Hence, this reaction may cut the chain at almost any position. The crystalline parts of cellulose are more protected against alkaline hydrolysis than the amorphous parts. The reaction starts by change in the ring conformation (promoted by high temperature) and an attack of the C-2 hydroxyl group on the C-1 carbon which will expel an anhydroglucose unit and create a new reducing end-group, shown in Figure 11. Alkaline hydrolysis hence results in a rapid secondary peeling reaction (Gellerstedt, 2009a).

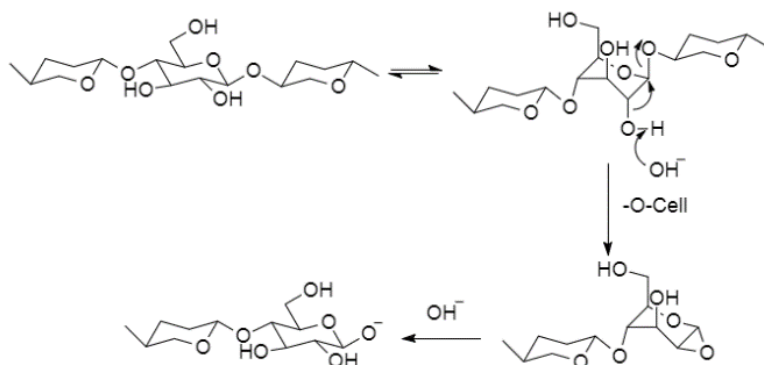


Figure 11. Alkaline hydrolysis of a glucosidic linkage. Redrawn from (Gellerstedt, 2009a).

### 2.5.4 Recovery cycle

The chemical recovery cycle is the part of the mill where the chemicals in the black liquor is converted back into white liquor, which is then recycled to the digester, shown in Figure 12. Furthermore, the latent heat in the dissolved organics is recovered and utilized. Black liquor is burned in the recovery boiler and a smelt, consisting of mainly sodium carbonate and sodium sulphide, is formed. Green liquor is formed when the smelt is dissolved in weak white wash, i.e. diluted white liquor. The green liquor passes through the slaker where CaO is added. The added CaO forms calcium hydroxide upon contact with water. The mixture then passes through the causticisation vessels where calcium carbonate is precipitated and hydroxide ions released. The liquor containing the hydroxide ions is sent back to the digester. The calcium carbonate is separated from the white liquor by filtering and then burned to reform CaO in the lime kiln. Figure 12 shows a simplified scheme of the recovery cycle (Theliander, 2009).

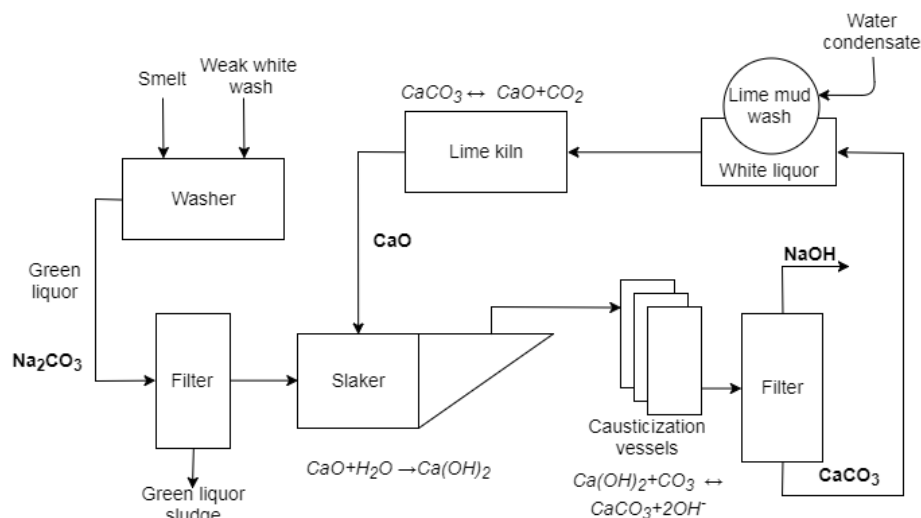


Figure 12. A simplified scheme of the chemical recovery cycle in a pulp mill.

## 2.6 ANALYTICAL METHODS

The technical background of the methods used for characterisation of the raw material and products are presented in this section.

### 2.6.1 UV

UV spectroscopy can be used for quantification of UV-active structures in a sample. Matter interacts with light due to excitation of electrons. Different molecules have different electronical configuration and hence light of different wavelengths interact with different types of matter. By measuring the absorbance of monochromatic light as it passes through a sample of a specific length, Lambert-Beer's law, Eq. (3), may be used to calculate the concentration of the molecules absorbing light at the chosen wavelength. (Christian and O'Reilly, 1978).

$$A = \epsilon l C \quad (3)$$

In Eq. (3),  $A$  is the absorbance,  $l$  is the length of the sample, i.e. the cuvette in the spectrophotometer used for the measurement,  $C$  is the concentration and  $\epsilon$  is the molar absorptivity.  $\epsilon$  is characteristic for each absorbing substance with a specified solvent and the wavelength of the light absorbed. Since lignin contain aromatic rings it may be detected and quantified with light in the UV spectrum (Lin et al., 1992).

### 2.6.2 NMR

Nuclear Magnetic Resonance, NMR, spectroscopy is a method used for analysing the structure of a molecule. Each atomic nucleus has specific magnetic properties and is electrically charged. By applying an external magnetic field, energy transfer to certain atomic nuclei, such as  $^1\text{H}$  and  $^{13}\text{C}$ , is facilitated. Then the nuclei are excited to a higher level and the energy needed is dependent on the surroundings of the atomic nuclei. Energy will later be emitted when the nuclei returns to its base level. The emitted energy corresponds to a signal which is measured to produce a NMR spectrum. The NMR spectrum shows the chemical environment in which the nuclei exists, from which the structure can be interpreted (Khopkar, 2011).

### 2.6.3 HPAEC-PAD

High performance anionic exchange chromatography, HPAEC, is a type of liquid chromatography which separates ions depending on their charge. A positively charged stationary phase in the chromatographic column serves to retain anions in the mobile phase which is pumped through the column. Depending on the charge of these ions different retention times are displayed since they interact differently with the stationary phase. This technique may be used to separate sugar monomers. Due to their hydroxyl groups the sugar monomers act as weak acids with a pKa around 12. The alkaline eluent used in the chromatograph deprotonates hydroxyl groups present on the sugar monomers thus enabling the ionic chromatography. Depending on the size and structure of these sugar monomers the shielding and hydration of the monomers are somewhat different which results in different retention times for the different monomers as they pass through the column. Large carbohydrates eluate slower than small ones (Lee and Bunker, 1989). The carbohydrate fucose may be used as internal standard for quantification of the different monomers.

Sugars do not generally absorb light over 210 nm and hence detection with spectroscopy, as in the case of lignin, is not suitable (Lee and Bunker, 1989). Instead amperometric detection may be employed to measure the sugar monomers as they elute from the HPAEC column. This is used in pulsed amperometric detection, PAD. A gold electrode oxidises the sugar monomers employing a fixed voltage. Measuring the current in the electrode it is thus possible to detect the monomers as they eluate from the chromatography column. The potential in the electrode is then raised to oxidise the gold in the

electrode and clean it since it is poisoned during the oxidation of the sugars. To restore the gold surface the potential is then lowered again to reduce the gold oxide. The electrode is at that time ready for a new cycle of measurement. These changes in the voltage are the pulses referred to by the name PAD (Rohrer, 2012).

#### **2.6.4 GPC**

Gel permeation chromatography, GPC, also called size exclusion chromatography, SEC, can be used to determine molecular weight distribution of lignin and polysaccharides. It is a liquid chromatographic technique which separate polymers depending on their size. A detector at the outlet measure the intensity of the response as the sample eluates which corresponds the concentration. The detector may for instance be a UV detector when lignin is measured, or a refractive index, RI, detector when carbohydrates are measured.

The sample is dissolved and the solution is pumped through a molecular sieving material which is porous. Since smaller molecules will enter the pores of the stationary phase, i.e. the packing material of the column, more easily, they will have a longer retention time in the column. Therefore, the largest molecules will eluate first and then the molecules will exit in order of decreasing molecular size. Measuring the intensity with a suitable detector as the polymers eluate is thus possible to calculate the molecular weight distribution by comparing with a set of standards with known molecular weights. From the molecular weight distribution the average molecular weight may be determined (Gellerstedt, 2009c).

### 3 PREVIOUS WORK ON DELIGNIFICATION KINETICS

---

Owing to the great importance of the Kraft pulping and the fact that a lot of the raw material is consumed during the process a lot of research has been performed to describe the delignification process for optimisation of the cooking. Many models have been set up and they are all subject to certain assumptions and simplifications which limit their generality. The complex morphology of wood yields a very heterogeneous raw material which makes the investigation and modelling of the kinetics of delignification challenging.

An early description for the cooking is the H-factor model proposed by Vroom (Vroom, 1957). In this model the combined effect of temperature and time on the delignification are accounted for and it is commonly used in process control. However, it is only applicable when the other cooking conditions are kept constant since it does not take the chemistry of the pulping into account. The H-factor model is calibrated for each pulping system to describe the delignification, i.e. what H-factor value a certain degree of delignification corresponds to. Hence, effective alkali concentration, liquor to wood ratio etc. need to be the same for predictions of delignification degree to be valid (Sixta, 2006). The H-factor model is further described in section 4.3.2.

More developed models are classified by Sixta as pseudo first-principle models as opposed to the pure empiric models such as the H-factor (Sixta, 2006). These pseudo first-principle models include more reaction conditions, such as concentration of hydroxide and hydrosulphide ions, temperature and reactivities, of different species in the wood than the empiric models. Hence, they are more complex but have a wider applicability. A large numbers of studies have been conducted. For instance, Wilder and Daleski set up a model on the delignification kinetics which took the concentration of hydroxide and hydrosulphide ions into consideration (Wilder and Daleski, 1965). Another model was set up by LéMon and Teder, again dependent on hydroxide and hydrosulphide but in a more elaborate way (LéMon and Teder, 1973). The model of Wilder and Daleski fail to predict a zero reaction rate when the hydroxide ion concentration reach zero and hence LéMon and Teder developed the model further. Olm and Tistad investigated the initial stage of the delignification and concluded it to be independent of hydrosulphide and effective alkali concentration. Instead their model for this phase is a first order kinetic expression with regards to residual lignin in the wood and a rate constant solely dependent on temperature according to the Arrhenius equation. The authors suggest that the limiting factor in this phase is the diffusion of alkali into or reaction products out from the chips (Olm and Tistad, 1979).

In a later model, integrating several delignification models for different parts of the cook, Gustafson et al. also included mass transfer in wood the chips to achieve a better model (Gustafson et al., 1983). In this model the concept of three delignification phases, previously described in section 2.5.3.1, was employed with LéMon and Teder's model being used as the bulk delignification model. Olm and Tistad's work was used to model the initial phase of the delignification. Carbohydrate degradation in the different phases was also included in the model and was described as functions of the delignification. The inclusion of mass transfer made the model even more apt. However, detailed mechanisms for the solubilisation of lignin from the wood matrix was not included.

The three phases in the model of Gustafson et al. was modelled as occurring consecutive steps with clear breaking points in which the next delignification phase took place. Another description, is that of the delignification phases occurring in parallel. The mechanisms associated with the each delignification phase dominate that phase whereas the other still occur but to a lower extent (Teder, 2009). The Purdue model describes the delignification phases to occur in parallel and includes a detailed description of the different species in the wood and their reactions paired with mass transfer equations

(Sixta, 2006). The model only describes the initial and bulk phase, but Lindgren and Lindström have developed it further to include also the residual phase of the delignification (Lindgren and Lindström, 1996).

The three phase description of the delignification, described in section 2.5.3.1, is very common. The different phases have different dependencies on the active cooking chemicals and also different activation energies and are related to the different delignification reactions taking place (Teder, 2009). Remarkably, when the amount of removed non-lignin constituents, such as carbohydrates, is plotted against the dissolved amount of lignin in the wood the three different phases of the delignification are clearly visible almost independently of operation conditions or wood species (Sixta, 2006). For the different phases first order kinetics with respect to lignin is employed and have been shown to work well in many studies when the concentration of hydroxide and hydrosulphide is held constant, most often by applying a high liquor to wood ratio. However, even though the model fits well with experimental data it has not been shown that the phenomena described in the model are the ones actually controlling the overall delignification kinetics. Generally the delignification is considered to be limited by the reaction kinetics (Dang et al., 2016a). However, as many authors note, the wood structure is very complex and hence mass transfer resistance ought to be significant and impact the delignification kinetics. Inclusion of the mass transfer have thus been made in models, but mainly on larger scale, i.e. wood chips.

Recent studies by Bogren et al. and Dang et al. have investigated the mass transfer on a smaller scale, namely the dissolution of lignin from the cell wall of the wood. This has been done by cooking wood meal in a flow-through reactor to reduce the mass transport resistance from diffusing in chips and also control the cooking liquor of the cook. A “memory” effect of the delignification when changing the concentration of active cooking chemicals was proposed. A high concentration of active cooking chemicals in the start of the cook delignifies the wood extensively. However, the dissolution of this degraded lignin takes time. When the concentration of active cooking chemicals was lowered, slowing the chemical reactions, lignin was still released from the wood and this yielded a higher delignification degree than if the concentration was low all along (Bogren et al., 2009b).

Investigations of the impact of ionic strength, with constant concentration of active cooking chemicals, on the Kraft cooking delignification kinetics of Scots pine, *Pinus Sylvestris*, has been conducted by Dang et al. and resulted in the conclusion that the delignification rate reduces when the ionic strength is increased. Furthermore, results from Mattson et al. suggest that the delignification reactions under the conditions employed by Dang occur very rapidly (Mattsson et al., 2017). The findings made by Dang suggest that the rate of Kraft delignification at the fibre wall level is governed by solubility and /or mass transport of lignin (Dang, 2017). The rate of the delignification reactions was considered not to be affected by the ionic strength of the cooking liquor (Dang et al., 2016a). Dang did not investigate the impact of ionic strength on larger length scales, i.e. chips (Dang et al., 2013).

Santos et al. on the other hand investigated the delignification of eucalyptus wood on both saw dust and wood chips and came to the conclusion that there is no notable difference in delignification kinetics between the two length scales. The conclusions were that the delignification kinetics is solely governed by chemical reactions not mass transport (Santos et al., 2011). The analyses of the cook of wood chips were conducted on homogenized pulp and not on the black liquor.

The delignification kinetics thus have been studied extensively and a quite good understanding of the impact of different parameters on the delignification on a macroscopic scale exists. However, all the mechanisms of the delignification are not fully described, for instance the mass transport of the wood constituents through the wood are not fully known (Dang et al., 2016a). The delignification is mostly

regarded as limited by the chemical reactions, but recent studies have shown that mass transport may be rate determining. These studies have been made on Scots pine, a softwood. The differences between hardwood and softwood in terms of chemical composition and wood structures makes the transferability of these conclusions difficult. Similar investigations on wood meal as those performed by Dang et al. is thus of interest. The great importance of eucalyptus for the pulp industry calls for investigations on eucalyptus wood meal. Since there is a clear conflict between the findings of Santos et al. on eucalyptus which conclude mass transport to be unimportant and Dang et al. which found mass transport to be important for softwood, investigations on eucalyptus with Dang's method are of great interest.

## 4 METHOD

---

To distinguish between the kinetics related to the reactions and mass transport in the cell wall to those occurring in whole wood chip, both delignification of wood meal and whole wood chips was studied. Moreover, cooking liquors with different ionic strengths but the same concentration of active cooking chemicals were employed. The first part of experimental investigation was performed in a small continuous flow-through reactor and the second part in an autoclave batch reactor. Characterisation of the products was made by standard measurements on lignin and carbohydrates. These included composition and molecular weight, by chromatographic and spectroscopic methods, as well as structural investigations of lignin fractions with NMR. In order to produce comparable results, the methods used by Dang were also used in this project (Dang, 2017). However, the investigated wood species was *Eucalyptus Urograndis* instead of Scots pine (*Pinus Sylvestris*). The following sections describe the continuous flow-through reactor as well as the batch reactor. Moreover, the characterisation methods are presented.

### 4.1 COOKING LIQUOR PREPARATION AND ABC-TITRATION

The cooking liquor was prepared in two steps. First a stock liquor was prepared by dissolving solid  $\text{Na}_2\text{S}$  in water. The composition of this liquor was determined with ABC-titration, after which the cooking liquor could be prepared by dilution of the stock liquor. In the cases where a high ionic strength was desired sodium carbonate was added. The reason for using sodium carbonate to regulate the ionic strength was to produce comparable results to those of Dang (Dang, 2017).

The  $\text{Na}_2\text{S}$  salt contained an unspecified amount of crystal water which made the determination of the composition directly from the added amount of salt impossible. Therefore, step A and B of the standard ABC titration test for white liquor was used to determine the concentration of active cooking chemicals in the stock liquor. The test is designed to, in several steps, give the concentration of the different active ions (Biermann, 1996). The titration equipment used was a *SI Analytics TritroLine 7000*. The steps are described below.

- A. To 10 g liquor 50 g water was added followed by addition 30 ml  $\text{BaCl}_2$  solution, 200 g/l. Barium chloride was added to the stock liquor to precipitate carbonates present in the liquor. However, the amount should be almost zero since no carbonates have been added to the stock liquor. Then the liquor was titrated with HCl 1M until pH 11 was reached. Thereafter, the amount of added HCl was noted, and this was the “A-value”. Then the liquor was titrated to a pH of around 3. Step A is designed for liquors containing carbonates, i.e. white liquor, but even if no carbonates are present, it needs to precede step B. At the end of step A, when pH is 3, all the  $\text{OH}^-$  ions and half of the  $\text{SH}^-$  ions have been consumed.
- B. Formaldehyde was added to the liquor which complexes the remaining  $\text{SH}^-$  ions to yield  $\text{OH}^-$  ions and S-methylene complexes. Hence, all  $\text{SH}^-$  ions are consumed and replaced with  $\text{OH}^-$  ions. The pH value increased during this process. Titration with HCl to pH 9 gave the “B-value” as the amount of HCl added. Only the A and B parts of the ABC test were run. Using the “B-value” the concentration of active cooking chemicals in the stock liquor could be calculated according to the method presented in Appendix I.
- C. Is employed to measure the amount of carbonates in the cooking liquor. This was not utilised during this project since the stock liquor did not contain any carbonates. These were added after the ABC-titration (Biermann, 1996).

## 4.2 WOOD MEAL IN CONTINUOUS FLOW-THROUGH REACTOR

A small continuous flow-through reactor was used for the first part of the project in order to maintain a constant concentration of cooking chemicals during the cook and to prevent the resorption of lignin and xylan onto the pulp. The flow-through reactor also enable change of cooking liquor during the cook. This was utilised to change the ionic strength of the cooking liquor during the cook. Furthermore, wood meal was used to minimise the effects of mass transport on larger length scales, which occur during cooking of wood chips (Dang et al., 2013).

### 4.2.1 Continuous flow-through reactor

The continuous flow-through reactor consisted of a column filled with wood meal submerged in a heating bath of PEG. Pipe coils before the inlet of the column enabled preheating of cooking liquor, and a cooling bath after the column outlet cooled the cooking liquor. A simplified scheme of the reactor is shown in Figure 13. Cooking liquor was pumped through the reactor by a high pressure pump and a relief valve was located in the end of the system (Bogren et al., 2009b).

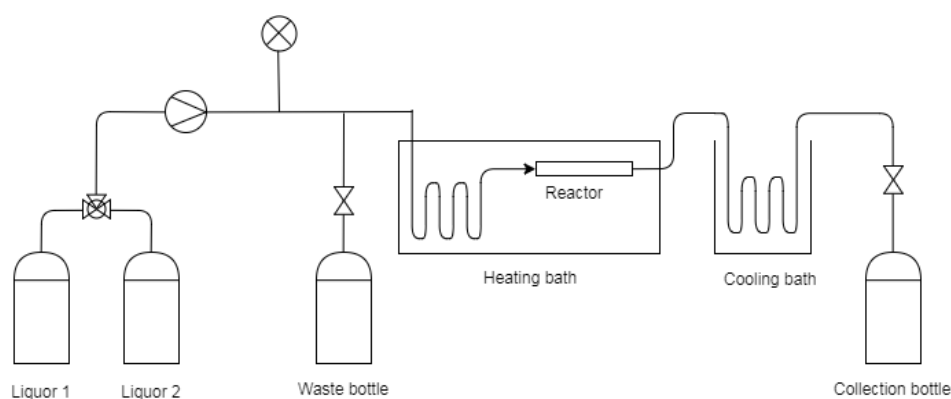


Figure 13. Simplified scheme of the continuous flow-through reactor used in the experiments.

#### 4.2.1.1 Preparation

Approximately 4,5 g of wood meal was carefully packed in the column of the flow-through reactor to avoid lumps and plugs, with the objective to enable an even flow of cooking liquor. The wood meal was prepared with a Wiley mill equipped with a <1mm sieve. Prior to every cook the dry content of the wood meal was measured with a *Satorius MA30 Moisture Analyzer*.

#### 4.2.1.2 Impregnation

Around 3-4 free column volumes of cooking liquor at r.t. was pumped through the reactor to obtain good impregnation of the wood meal. The flow rate was increased stepwise during the impregnation to avoid packing of the wood meal which would result in pressure exceeding the limit of the equipment.

#### 4.2.1.3 Cooking

A PEG heating bath was preheated to 115°C before submerging the column, after which the temperature was set to 158°C and the timing of the cook started. The bath reached the temperature of 158°C after approximately 22 min and the temperature was then kept constant. The cooking liquor was continuously pumped through the reactor throughout the cook according to Table 4.

Table 4. Scheme over changes between flowrates during cook. The time presented in brackets is used during the shorter cooks.

Flow rate change [ml/min]	Exchange time [min]	
2,5 → 5	2	} Impregnation cycle
5 → 8	3	
8 → 10	4	
10	5	
10 → 8	12	} Cooking cycle
8 → 2,5	22	
2,5 → 1	180 (90)	

Initially a lot of alkali is consumed which requires compensation with a higher flow rate to achieve an even cooking liquor concentration. The protocol presented in Table 4, have previously been established to yield a uniform delignification throughout the column (Bogren, 2008).

Fractions were collected between the times presented in Table 5. Since the fractions of black liquor were cooled prior to collection, further reactions in the black liquor fraction were assumed to be quenched, as opposed to a batch-wise cooking, such as the autoclave described in section 4.3. Each cook yielded one sample of pulp and between 3 and 8 samples of black liquor, depending on the total cooking time. A total cooking time of 40 min yielded 3 black liquor samples, 90 min yielded 5 samples and 180 min yielded 8 samples.

Table 5. Time intervals for collection of black liquor.

Fraction	Cooking time interval [min]	Sample volume [ml]
1	0-10	100
2	10-20	84
3	20-40 (+10 min cooling for C-cook)	61 (+ 10 ml for C-cook)
4	40-60	50
5	60-90 (+10 min cooling for A-cook)	75 (+ 10 ml for A-cook)
6	90-120	75
7	120-150	75
8	150-180 (+10 min cooling for B-cook)	75 (+10 ml for B-cook)

After the cook, the pulp was removed from the column, homogenised with 300 ml of deionized water. The pulp was thereafter filtered and washed with additionally 700 ml of deionized water. The filter cake was left to dry for a minimum of 24h at 105 °C and was then weighed.

#### 4.2.2 Chosen experiment parameters

The parameters investigated were cooking time and ionic strength of the cooking liquor. The ionic strength was varied with inactive ions, i.e. ions not directly active the delignification reactions. Rather, the concentration of active cooking chemicals was kept constant at all times, while the concentration of inactive ions was varied. Since comparison with previous softwood experiments were of interest, the parameter values was based on experiments performed on softwood by Dang (Dang, 2017). Whereas Dang investigated the effect of changing the ionic strength of the cooking liquor at both 30 and 60 min in the same cook, the change of ionic strength in this project was only changed once in each cook according to Table 6. The results of Dang when changing the ionic strength twice during the cook was not considered to provide additional information of the impact of ionic strength on delignification, compared to single change of ionic strength. Ionic strength is difficult to determine when organic anions appear in the reactions system. Hence, sodium ion concentration was used as a representation of ionic strength (Dang et al., 2013). The concentration of sodium ions was varied during the cook by changing to or from a liquor with higher ionic strength. The concentration of sodium ions was not measured explicitly, rather regulated with addition of known amount of sodium carbonate to the cooking liquor.

Two levels of ionic strength were used. High versus low ionic strength corresponding to  $[\text{Na}^+]=3$  mol/kg cooking liquor and  $[\text{Na}^+]=0.52$  mol/kg cooking liquor respectively.

Table 6. Cooking conditions used during the wood meal experiments. The series names were based on ionic strength (H=high, L=low), Total cooking time (A=90 min, B=180 min, C=40 min) and exchange time of ionic strength (30 min or 60 min). For instance LH\_B\_30 means that the cook starts at low ionic strength. After 30 min this was changed to high ionic strength and the total cooking time was 180 min.

Series	Initial compositions mol/kg solvent			Temperature (°C)	Salts added	Exchange time (min)	$[\text{Na}^+]$ mol/kg cooking liquor	Cooking time (min)		
	[OH <sup>-</sup> ]	[HS <sup>-</sup> ]	[Na <sup>+</sup> ]					A	B	C
LH_A/B_30	0.26	0.26	0.52	158 °C	Na <sub>2</sub> CO <sub>3</sub>	30	0.52→3.00	90	180	-
LH_A/B_60	0.26	0.26	0.52	158 °C	Na <sub>2</sub> CO <sub>3</sub>	60	0.52→3.00	90	180	-
HL_A/B_30	0.26	0.26	3.00	158 °C	Na <sub>2</sub> CO <sub>3</sub>	30	3.00→0.52	90	180	-
HL_A/B_60	0.26	0.26	3.00	158 °C	Na <sub>2</sub> CO <sub>3</sub>	60	3.00→0.52	90	180	-
L_B/C	0.26	0.26	0.52	158 °C	Na <sub>2</sub> CO <sub>3</sub>	-	0.52	-	180	40
H_B/C	0.26	0.26	3.00	158 °C	Na <sub>2</sub> CO <sub>3</sub>	-	3.00	-	180	40

### 4.3 WOOD CHIPS IN BATCH REACTOR

A batch autoclave reactor, shown in Figure 14, was used in the second part of the project. This enabled studies of the influence of mass transport on larger length scales, i.e. chip level rather than cell wall level. Both cooking time and ionic strengths were varied between these experiments. The cooking conditions were chosen to match those of the flow-through reactor cooks.

#### 4.3.1 Batch autoclave reactor

The batch autoclave reactor consists of six autoclaves attached to a rotating beam and partly submerged in a PEG-oil heating bath. A drawing of the oil bath and a more detailed drawing of an autoclave is shown in Figure 14. Cooking of chips was performed in six 1.2 l autoclaves at a time to facilitate two samples at three different cooking times.

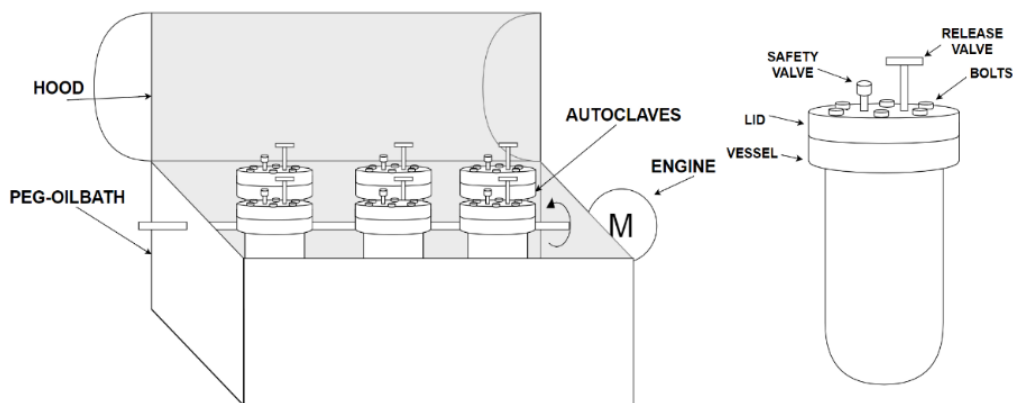


Figure 14. Schematic drawing of the oil bath and placement of the autoclaves to the left and detailed a drawing of an autoclave to the right.

##### 4.3.1.1 Preparation

Preparation of the cooking liquor was performed in the same manner as for the flow-through reactor.

Approximately 200 g of cooking liquor and 25 g of wood chips was added to the autoclaves, thus the liquor to wood ratio was 8/1 corresponding to the ratio in the flow-through reactor cooked for 180 minutes. The concentration of OH<sup>-</sup> ions for the longest cook are estimated to change from 0,26 mol/kg solvent to 0,15 mol/kg solvent at the end of the cook, which implies that the concentration of active cooking chemicals is not constant. This estimation is based on the values in (Rohrer, 2012, Sixta, 2006) and the method for calculating hemicelluloses and celluloses used by (Dang et al., 2013). Hydrogen

sulphide contributes greatly to the delignification but only shows a small decrease in concentration during the cook (Brännvall, 2009b).

#### 4.3.1.2 Impregnation

Before submerging the autoclaves in a bath of PEG at 115°C they were pressurised up to 5 bars for three minutes with nitrogen gas to impregnate the chips.

#### 4.3.1.3 Cooking

After submerging of the autoclaves in the PEG bath, the temperature was increased to the desired temperature of 158°C. This temperature was reached after approximately 50 minutes, which was slower than the 22 min temperature increase in the flow-through reactor. To overcome this difference in heating time the concept of H-factor was used to convert the cooking times for the flow-through reactor to those used for the autoclaves. A further explanation on this is found in section 4.3.2. The cooking time was measured from the point when the temperature increase was started. Two autoclaves were taken out of the oil bath at each of the three cooking times presented in Table 7 and submerged in cooling water for 10 minutes prior to outtake of sample.

Table 7. Cooking conditions and parameters for autoclave cook.

Batch	Salts added	[Na <sup>+</sup> ] mol/kg solvent	Cooking time (min)	Corresponding cooking time in flow-through reactor (min)
L_D	Na <sub>2</sub> CO <sub>3</sub>	0,52	33	18
L_E	Na <sub>2</sub> CO <sub>3</sub>	0,52	43	22,5
L_F	Na <sub>2</sub> CO <sub>3</sub>	0,52	83	60
H_D	Na <sub>2</sub> CO <sub>3</sub>	3,00	33	18
H_E	Na <sub>2</sub> CO <sub>3</sub>	3,00	43	22,5
H_F	Na <sub>2</sub> CO <sub>3</sub>	3,00	83	60

An important difference compared the flow-through reactor is that the same black liquor is used during the whole cook since it is a batch cook. The amount of active cooking chemicals will, thus, be reduced during the cook and all the dissolved matter from the wood ends up in one single black liquor sample instead of several fractions. Moreover, the lignin and carbohydrates dissolved during the process will continue to react for the entire cooking time until the reactions are quenched at the very end of the entire cook. The black liquor from the flow-through reactor was quenched directly after exiting the column, not after the whole cook. Each cook in the autoclave yielded one pulp and one black liquor sample for each autoclave.

#### 4.3.2 Chosen experiment parameters

The cooking times for the autoclave cook were based on the results where the delignification reactions were prominent in the flow-through cook, i.e. after short cooking times. However, due to the increase in scale and difference in temperature increase profile, the cooking times had to be scaled. This was done using the concept of H-factor calculated with Eq. (4). This factor, developed by Vroom, combines the effect of temperature and cooking time on the delignification (Vroom, 1957). Both cooking time and temperature influences the degree of delignification achieved. The cooking temperature is the same in the autoclave, but the temperature profile during the heating of the autoclaves is different.

$$H = \int_{t_0}^t e^{(43.2 - \frac{16113}{T})} dt \quad (4)$$

The H-factor relates reaction rates of lignin at different temperatures using the Arrhenius equation (Brännvall, 2009b). Hence, the activation energy for the delignification reactions is used. Moreover, the factor does not describe the absolute delignification rate, but rather the reaction rate relative to that at 100°C (Vroom, 1957). The activation energy for this reaction was calculated from soda cooking of softwood with data from Laroque and Maass under an assumption of a first order reaction (Larocque and Maass, 1941). Thus, the factor is not developed with data Kraft cooking which makes the usage uncertain since other activation energies could be viable owing to the other reaction paths of Kraft cooking compared to soda cooking. Furthermore, in Eq. (4) a constant activation energy is assumed during the whole delignification and it is based on softwood. Since many different reactions is involved in the delignification, the assumption that one activation energy may be used over the whole cook is questionable. However, regarding the usage of softwood data it has been established that hardwood activation energies are almost the same (Santos et al., 2011). Hence, the Eq. (4) was used although there are issues with it. The H-factor is widely accepted and used, but it must be noted that it does not in itself yield information on the delignification degree. However, models may be set up which relates the H-factor to the degree of delignification (Vroom, 1957). These models are only valid with the other cooking parameters preserved.

In the autoclave the cooking parameters was chosen to be similar to those of the flow-through reactor to yield comparable results, e.g. liquor-to-wood ratio and start concentration of active cooking chemicals. However, differences are present such as batch wise cooking rather than flow-through which changes the concentration of active cooking chemicals over time and also allows reactions to continue in the black liquor as well as resorption of species on to the wood to occur.

The H-factor for the cooks in the flow-through reactor was calculated and then aiming at achieving the same H-factor for the autoclave cooks. To use the H-factor the temperature profile first had to be established through a test cook where the temperature was noted every 15 minutes when heating from 115°C until 158°C. Using this temperature profile to calculate the H-factor the total cooking time in the autoclave, presented in Table 7, was determined. The H-factor calculations are presented in Appendix II.

### 4.3.3 Choice of chip dimensions

Dimensions were specified and chips selected accordingly in order to limit the variations in size, thus reducing the variation between each batch. Chip thickness has been shown to be the most important of dimension as far as delignification is concerned (Dang, 2017). Therefore, the thickness (c) was set to a narrow interval, between 3 and 6 mm. The other dimensions, width and length, were set to an interval based on the available lengths and widths. Both width (a) and length (b) were set to 15-27.5 mm. Figure 15 present how the dimensions were defined.

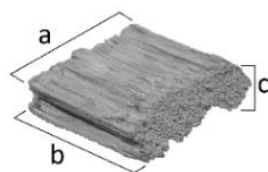


Figure 15. Picture of an *E. Urograndis* chip. a: width, b:length, c:thickness.

### 4.3.4 Separation of BL

Black liquor and pulp were separated by filtration through a polypropylene filter. The black liquor was recirculated once over the chips so as to retain small wood fibres. The pulp was then washed with 10 l of water whilst the black liquor was stored. The pulp was then homogenised.

### 4.3.5 Homogenisation of the pulp

In the first step, the washed pulp was disintegrated in 2 l of water at 30000 revs, then filtrated through a finer polypropylene filter than that used in the separation of BL and pulp. The filtrate was recirculated once over the pulp, followed by additional washing with 5 l of water. The second step of the homogenisation was mixing of the pulp with 1.25 L of water followed by filtration with the same finer polypropylene filter, recirculation of the filtrate and subsequent washing with additional 5 l of water. The black liquor remaining in the pulp after homogenization and washing was to some degree leached out of the pulp into neutral water overnight. This water was then filtered off, recirculated and the pulp was washed with 5 l of water. The pulp was finally dried overnight in 105°C.

## 4.4 ANALYTICAL METHODS

The characterization of the wood, pulp and black liquor from the cooks is outlined in Figure 16, and described in detail in the following section. All samples were characterised with all methods except the NMR. These tests were only run on six black liquor samples from two cooks due to expense of the NMR test.

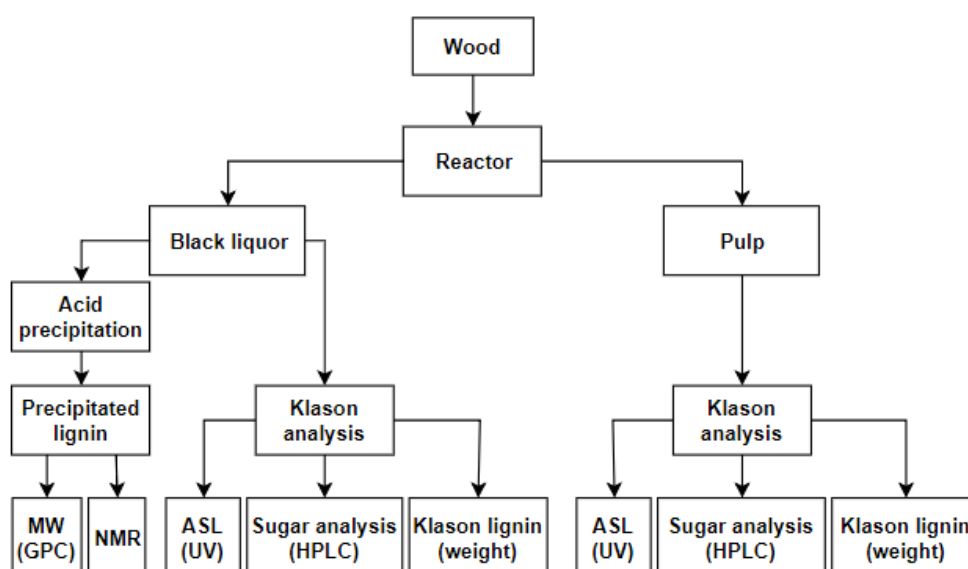


Figure 16. Outline of the experimental work. Starting with the raw material, proceeding to cooking in reactor and then on to the characterisation steps.

### 4.4.1 Klason lignin content

The methods described below served to measure the content of residual lignin in the pulp and black liquor after cooking. By lowering the pH lignin was precipitated. Hydrolysis in an autoclave followed to break the bonds between lignin and carbohydrates and degrade the polysaccharides to monosaccharides (Gellerstedt, 2009c). The lignin was then filtered off and weighed whereas carbohydrates remained in the filtrate. Pulps from the flow-through reactor cooks were easily disintegrated and contained few shives. The autoclave pulps on the other hand were coarser with a lot of shives. Hence, these were milled with an analytical grinder, *Yellowline A10* 20 000 revs/min, prior to Klason lignin measurement.

#### 4.4.1.1 Pulp and wood meal

Approximately 200 mg, dry weight, of wood meal or pulp was weighed into 150 ml beakers and 3 mL of 72 vol-% sulfuric acid was added. The mixture was first stirred for a few minutes and then evacuated for 15 min. The samples were then placed in a water bath at 30°C for 1 hour and stirred each 20 min,

followed by addition of 84 grams of deionised water. Next, lids were put on the beakers which were then moved to a pre-heated autoclave at 125°C for 1 hour. After hydrolysis, the mixture was filtrated onto a glass microfiber filter and the filtrate diluted to 100 ml. The solid residue remaining after filtration and drying, Klason lignin, was measured gravimetrically after drying at least 15 hours in 105°C (Theander and Westerlund, 1986).

#### 4.4.1.2 Black liquor

The method to isolate Klason lignin from black liquor was adapted by Dang from the method used on pulp and wood meal. Approximately 10 ml of each black liquor fraction was weighed into 150 ml beakers and 72 vol-% H<sub>2</sub>SO<sub>4</sub> was added to reach a pH between 1 and 1.5. After thorough stirring the samples were first left to stand for 30 min and then placed in a water bath at 30°C for 1 hour, with stirring each 20 min. Addition of 8.93 ml of deionized water was then made and the samples were moved to an autoclave at 125°C for 1 hour of treatment. Thereafter, the mixture – the hydrolysate – was filtrated onto a glass microfiber filter and 4 ml of fucose solution, 200 mg/L, was added to the filtrate followed by dilution to 100 ml. The solid residue remaining after filtration, the Klason lignin, was dried for at least 15 hours in 105°C and then measured gravimetrically.

#### 4.4.2 Carbohydrate analysis

The carbohydrate content of the wood, pulp and black liquor was measured using high performance anion exchange chromatography with pulsed amperometric detection (HPAEC-PAD). The machine used was a *Dionex ICS-5000 HPIC System* equipped with *Dionex CarboPac® PA1* columns and a gold electrode in the detector, with which monomers of arabinose, galactose, glucose, xylose and mannose were measured. Three eluents were used, one with 170 mM NaAc and 200 mM NaOH, one with 200 mM NaOH and the final one with MilliQ-water. The first of these eluents was used to wash the columns between the samples. The pH during operation was around 13.

The wood, pulp and black liquor required pre-treatment with acid hydrolysis prior to running in the HPAEC. Hence, the filtrate from the Klason lignin content methods were used for carbohydrate analysis. The filtrate was run in the HPAEC machine in three different concentrations: undiluted, 10 times dilution (1/10) and 50 times dilution (1/50). The best results, with clearest peaks in the chromatograms, were obtained for the 1/10 dilutions. An exception was the peaks for glucose in pulps which were clearest for the 1/50 dilution. Fucose was used as the internal standard with a concentration of 8 mg/ml in the samples. Data was analysed with *Chromeleon® 7, Chromatography Data System software, Dionex Chromeleon, Vers. 7.1.3.2425*.

The amount of sugar monomers measured with the HPAEC-PAD was corrected to account for the anhydrous character of sugars when present as carbohydrate chains in pulp, i.e. the weight of one molecule of water was withdrawn from each sugar unit. Consequently, pentose amounts, such as xylose and arabinose were multiplied by 0.88 whereas hexose amounts, such as galactose, glucose and mannose were multiplied with 0.90. Furthermore, the yield of monomers from polysaccharides in the acid hydrolysis was considered using yield values from Wigell et al., presented in Table 8 (Wigell et al., 2007).

Table 8. Correction factors for yield of sugar monomers from acid hydrolysis (Wigell et al., 2007).

Sugar unit	Yield during acid hydrolysis
Arabinose	0,94
Galactose	0,95
Glucose	0,97
Xylose	0,90
Mannose	0,93

#### 4.4.3 Acid soluble lignin content

Although most of the lignin in the black liquor, pulp and wood meal precipitates as Klason lignin when subjected to acid hydrolysis, some lignin and fragments of lignin remain soluble in the hydrolysate and is consequently called acid soluble lignin, ASL. It contains a mixture of products from degradation reactions such as depolymerised lignin of low molecular weight and various hydrophilic derivatives of lignin (Yasuda et al., 2001). Yasuda et al, mentions that ASL is formed predominantly from syringyl lignin and that it is the reason for hardwood having a higher ASL content than softwood. The lignin of the softwood does not contain any syringyl. Santos et al. writes that eucalyptus is high in syringyl units and hence we ought to expect quite high amounts of ASL (Santos et al., 2011). Also, Karr and Brink found that Klason lignin may be broken down to ASL during repeated hydrolysis (Kaar and Brink, 1991).

UV spectroscopy, using a *Specord 205* from *AnalytikJena*, was used for determination of amount of acid soluble lignin, ASL, in the hydrolysate from the Klason lignin content measurement. The samples were run against a reference of deionised water at 205 nm. The dilutions made for carbohydrate analysis were used here which meant there was fucose added to the samples. However, upon testing a pure sample of fucose it was evident that fucose is not detectable at 205 nm.

Values between 0.1 and 1 were used, else another dilution was used. Most often the 1/50 dilution was used. *WinASPECT Software Vers. 2.3.10* was used to analyse the data. The absorptivity constant used was 110 l/g\*cm (Lin et al., 1992).

#### 4.4.4 Precipitated lignin from BL

Dissolved lignin in black liquor samples was precipitated by addition of concentrated sulfuric acid to reach pH 2,5. The samples were agitated at r.t. and left over night in a freezer at -18°C. The samples were then thawed at room temperature and the lignin filtrated on a glass filter of size #4 followed by washing with acid water, pH 2,5. The lignin was dried at 40°C for three days where after it was run in GPC and NMR (Dang et al., 2016b).

#### 4.4.5 Molecular weight distribution (MWD)

Dried acid precipitated lignin samples were dissolved in dimethyl sulphoxide, DMSO, containing 10 mM of LiBr. 10 mg of lignin was dissolved in 1 ml DMSO. 100 µl of this solution was diluted with 4 ml DMSO and filtered with a 0,2 µm filter on a syringe into a vial. In some cases the amount of lignin available was too low to scrape out from the filter after the acid precipitation. In these cases the DMSO was added to the filter so that it amounted to 1 ml/10 mg lignin. This dissolved the lignin so that it dripped through the filter.

The MWD and weight average molecular weight ( $M_w$ ) of the samples were determined by gel permeation chromatography, GPC. The GPC system used in this case was a *PL-GPC 50 Plus Integrated GPC system*, equipped with a UV detector operating at 280 nm. One *PolarGel-M (50×7,5 mm)* column and two *PolarGel-M (300×7,5 mm)* columns were employed during the analysis. The instrument was calibrated with ten pullulan polysaccharide standards with MW:s ranging from 180 to 708000 Da and the results were analysed with *Cirrus™ GPC/SEC Software Vers. 3.2*.

#### 4.4.6 Nuclear magnetic resonance (NMR)

The selection of the samples to be analysed by NMR were made after the Klason lignin content analysis based on findings on the delignification rate, appearance of the acid soluble lignin and ionic strength of the cooking liquor used. Further discussion on the choice of samples is presented in section 5.4.

The acid precipitated material was dissolved in DMSO-d<sub>6</sub>. Most of the samples were dissolved as 70-100 mg/0.75 ml DMSO-d<sub>6</sub>. For some of the samples too little acid precipitated lignin was available, and these were dissolved as 20-50 mg/0.25 ml DMSO-d<sub>6</sub>. The samples were analysed at the Swedish NMR centre in Gothenburg. <sup>1</sup>H-<sup>13</sup>C HSQC, heteronuclear single quantum coherence spectroscopy, NMR tests were conducted at 800 MHz with a *Burker Advance III HD 18.8T* spectrometer at 25°C. The spectra were recorded for 4 h in case of 70-100 mg/0.75 ml DMSO-d<sub>6</sub> samples and up to 8 h for the 20-50 mg/0.25 ml DMSO-d<sub>6</sub> samples. The processing of the spectra was done with *MestReNova Vers. 10.0.0* using the default processing template and automatic phase and baseline correction.

#### 4.4.7 Number of samples

In general each cook was performed only once, but some cooks were rerun. Consequently, calculations of the pooled standard deviation of the amounts of the main components in the pulps and black liquors for these cooks were performed and these results are assumed to be transferrable to the single cooks. Furthermore, the wood was characterised six times and pooled standard deviations was calculated for those samples as well. The results are presented as percent on wood in Table 9.

Table 9. Pooled standard deviation of the main components of the wood, pulp and black liquor.

	<b>Pulp</b>	<b>Black liquor</b>	<b>Wood meal</b>
Klason [% on wood]	0,21	0,02	2,11
ASL [% on wood]	0,01	0,15	0,13
Glucose [% on wood]	2,81	0,14	1,10
Xylose [% on wood]	0,54	4,26	0,34

## 5 RESULTS AND DISCUSSION

In the following section, the results will be presented and discussed. The flow-through reactor results on *E. Urograndis* wood meal will be compared to the results from the investigations performed by Dang on pine wood (Dang, 2017) and the results from the cooking of *E. Urograndis* wood chips in autoclaves respectively. These comparisons between soft- and hardwood enables a more thorough mechanistic investigation, by studying of the impact of length scales on the delignification of *E. Urograndis*.

### 5.1 KLASON LIGNIN

In the following section, the results from cooking of wood meal in a flow-through reactor and cooking chips in an autoclave reactor will be presented. The main focus will be on the impact of ionic strength on the amount of Klason lignin in both black liquor and pulp. The amount of Klason lignin in wood meal, pulp and each BL fraction was determined by the Klason method described in the section 4.4.1.

#### 5.1.1 Flow-through reactor

Both cooks with constant ionic strength, L\_B and H\_B, and cooks with changed ionic strength: first high, then low, HL, and also first low, then high, LH, were investigated and are presented in sections 5.1.1.1 and 5.1.1.2 respectively.

##### 5.1.1.1 Constant ionic strength

The amount of Klason lignin in each BL fraction was directly measured, divided by the Klason lignin content of the wood meal and plotted in Figure 17. Since pulp only was taken out at three different times (40, 90 and 180 minutes), the remaining Klason lignin values of the pulp were calculated by subtracting Klason lignin value in each fraction from that of the wood meal, and adding Klason lignin value in each BL fraction to that of the pulp. The mean value of these values gave a good approximation of the Klason lignin amount in the pulp, the result is presented in Figure 18. This explains why the value in Figure 18 does not start at 1 for the H\_B cook. A similar behaviour can be observed in several of the following results for Klason lignin in pulp. An example of how the theoretical amount of Klason lignin in the pulp was calculated is presented in Appendix III.

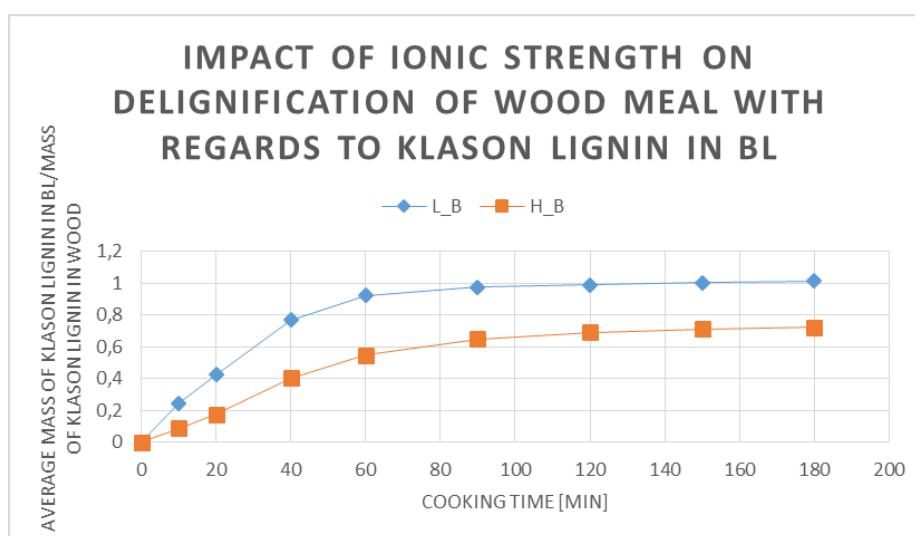


Figure 17. Impact of constant ionic strength on the delignification of wood meal in a flow-through reactor with regards to Klason lignin in BL.

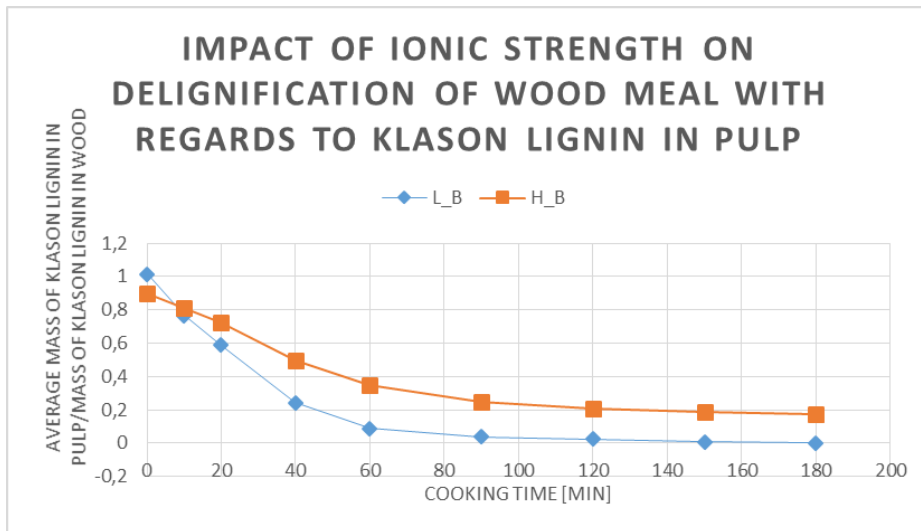


Figure 18. Klason lignin content in pulp from the flow-through reactor presented as portion of the Klason lignin content of the wood meal. L\_B is a cook with low ionic strength at 180 min, whereas H\_B is a cook at high ionic strength for 180 min.

It is apparent from both Figure 17 and Figure 18 that increased ionic strength reduces the delignification rate of wood meal in the flow-through reactor, possibly due to reduced solubility of lignin. This corresponds with the results of Dang (Dang, 2017). This can also be observed in Figure 19, where the pulps from H cooks are much darker and contains more lignin.

It is also notable that the delignification occurs fast early in the cook and then slows down during cooking of eucalyptus. That also corresponds with Dang's work on Scots pine (Dang, 2017). After 120 min almost no further delignification occurs, which can be seen in Figure 18. Compared to the results of (Dang, 2017) a faster delignification is seen for eucalyptus than Scots pine. This corresponds well to the general behaviour of hard- and softwood delignification where the former is more rapid.

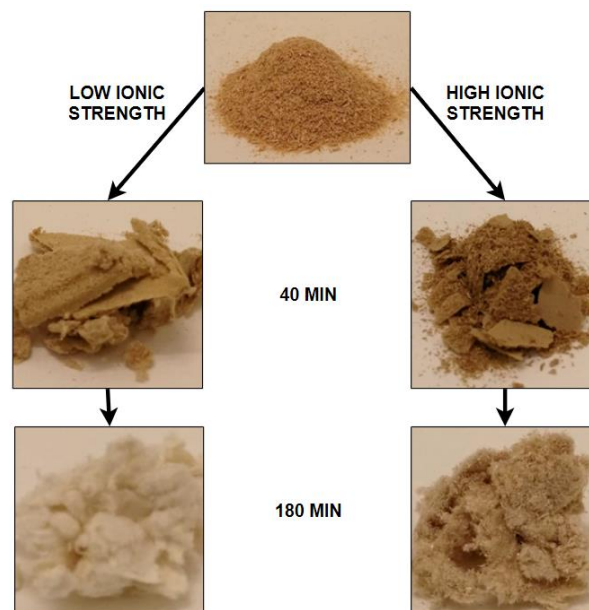


Figure 19. The path from wood meal to pulp. First pulp from 40 min of cooking and then 180 min of cooking. H cook on the right side and L cook on the left. Note how much whiter and hence more extensively delignified the pulp from the L cook is.

In Figure 19, it is possible to observe two major differences between the L and H cooks. Firstly, the pulp from H cooks are, as previously mentioned, darker as a result of higher lignin content. Secondly, the fibres from the wood meal can be easily seen in the H cooks, due to poorer delignification.

### 5.1.1.2 Changed ionic strength

Cooks with changed ionic strength were performed with two different exchange times and two different cooking times. The chosen parameters are presented in Table 6. Cooks with the same exchange time were combined, which is indicated by “...” in the plot titles. Thus, the mean Klason lignin amount of the two different cooking times was used at each point to ensure a better statistical security. However, the number of cooks was few. Since the cooks had different cooking times, only points between 0 to 90 min are mean values of two cooks, after that the values are solely from the long cooks.

In Figure 20 to Figure 23 below, the profile of cooks with changed ionic strength is compared with those with constant ionic strength. The profile with changed ionic strength is consistently marked in blue.

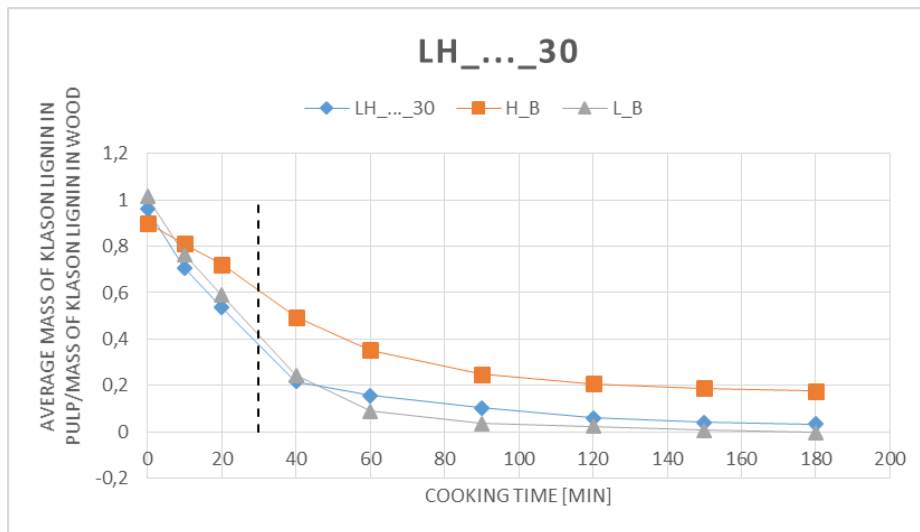


Figure 20. Cooks with change of ionic strength from low (L) to high (H) at 30 min. The dashed line indicates the point at which the ionic strength of the cooking liquor was exchanged.

In Figure 20, the delignification profile for LH\_...\_30 follows that of the L\_B cook until the change of ionic strength is introduced, then the profile flattens out and shifts towards the profile of the H\_B cook.

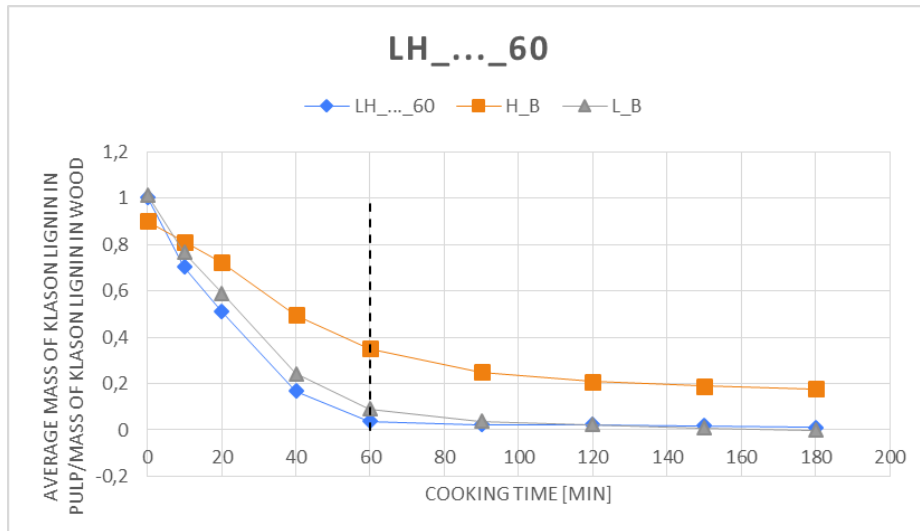


Figure 21. Cooks with change of ionic strength from low (L) to high (H) at 60min. The dashed line indicates the point at which the ionic strength of the cooking liquor was exchanged.

In Figure 21, the delignification profile for LH\_...\_60 follows that of L\_B until the change of ionic strength is introduced and also beyond this point. The profile does not change since most of the lignin has already been removed and not enough is left for the profile to change to the profile of H\_B.

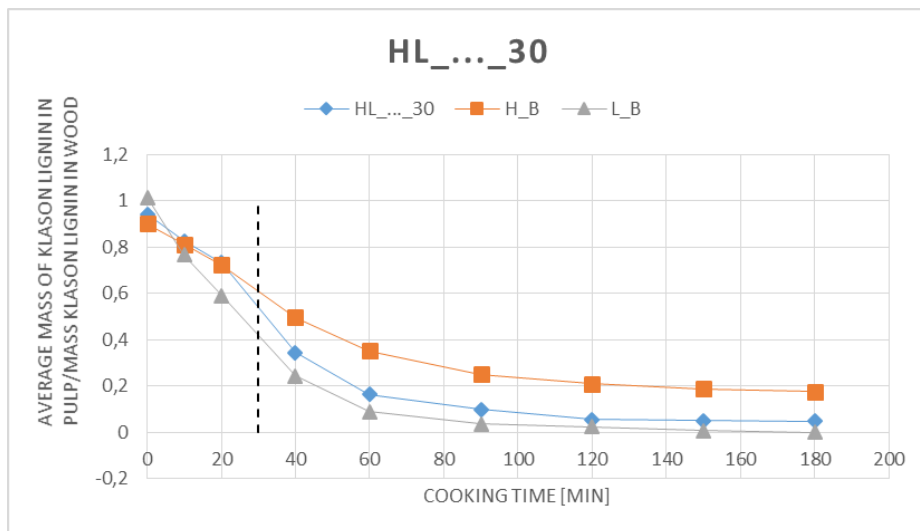


Figure 22. Cook with change of ionic strength from high (H) to low (L) at 30 min. The dashed line indicates the point at which the ionic strength of the cooking liquor was exchanged.

In Figure 22, the delignification profile for HL\_...\_30 follows that of H\_B until the change in ionic strength is introduced after which it shifts towards the profile of L\_B.

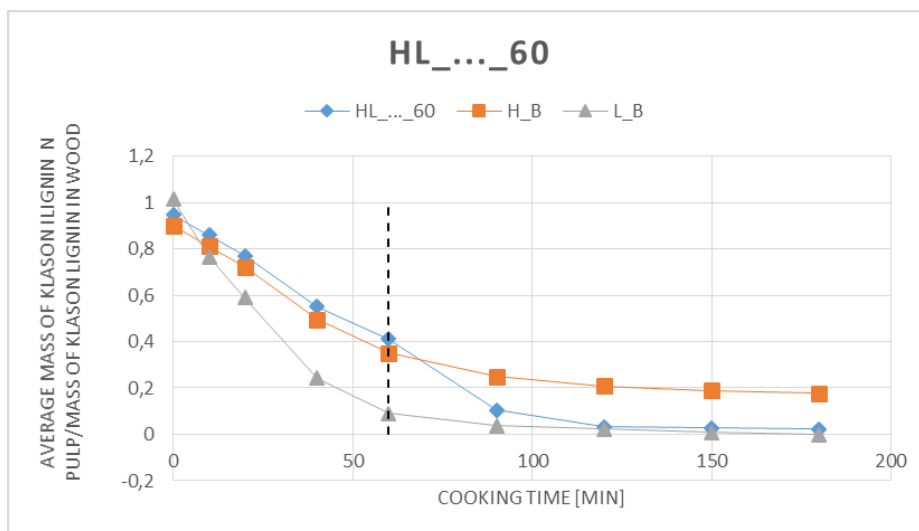


Figure 23. Cooks with change in ionic strength from high (H) to low (L) at 60 minutes. The dashed line indicates the point at which the ionic strength of the cooking liquor was exchanged.

In Figure 23, the delignification profile for HL\_...\_60 follows that of H\_B until the change in ionic strength is introduced. In contrast to LH\_...\_60 in Figure 21, the profile of HL\_...\_60 follows the profile of L\_B after the ionic strength exchange. This difference between HL\_...\_60 and LH\_...\_60 is due to that HL\_...\_60 has much more lignin left in the wood when the change is introduced and can therefore change profile to that of L\_B.

In general, a clear response to exchange of ionic strength can be seen for all samples with enough residual lignin left in the pulp when the change was introduced. I.e. exchange to low ionic strength shifts the profile to that of L\_B, whereas exchange to high ionic strength shifts the profile to that of H\_B. Hence, a swift response to ionic strength exchange is seen most likely due to the change of solubility of lignin.

### 5.1.2 Autoclave reactor

In the following section, the results from the autoclave cooks on wood chips are presented and discussed. The ionic strength was not exchanged during these experiments and the effect of ionic strength exchange during the cook on the chip morphological length scale will therefore not be discussed. For ease of comparison between the flow-through and autoclave reactor cooks, the cooking times for the autoclave cooks are presented as the corresponding cooking time in the flow-through reactor. This is in accordance with the method presented in section 4.3.2. However, the two lowest cooking times were so short that they ended during the heating period of the autoclave cooks. This made the conversion imperfect, which explains the cooking times close to each other, 18 and 22,6 min. Hence, 18 min cooking time corresponds to 33 min of actual cooking time in the autoclave and 22,6 min corresponds to 43 min and 60 min to 83 min. Furthermore, it is important to note that the active cooking chemicals are consumed during the cook and will therefore decrease over time, thus the concentration of active cooking chemicals will decrease.

It is apparent from Figure 24, which shows pulps from the L cook, that the degree of delignification is low after 18 minutes of cook as the pulp resembles defibrillated wood and not regular pulp. The amount of shives in this pulp is great and the texture is rough. The pulp obtained after 60 minutes cook has a structure resembling that of regular pulp with a smoother texture, but some shives are present.



Figure 24. The path from wood chip to pulp during the L cook. First 18 min cook and then 60 min. The 22,6 min cook is not included since there are no visual difference between that and the pulp cooked for 18 minutes.

Two cooks were performed at each cooking time and ionic strength and the values presented in Figure 25 and Figure 26 are mean values of these.

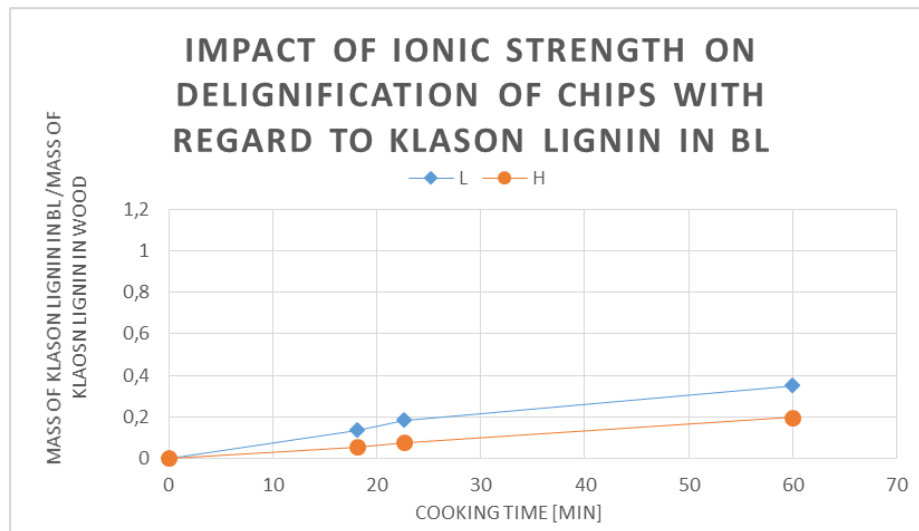


Figure 25. Klason lignin content in black liquor from cooks with constant either high (H) or low (L) ionic strength.

In Figure 25, showing the Klason lignin content in the black liquor, a clear difference is observed between cooks with high, H, and low, L, ionic strength. No such difference can be seen in Figure 26, showing the Klason lignin content of the corresponding pulps.

From Figure 25 and Figure 26, conclusions regarding the impact of ionic strength can be made. First, the lignin in the chips have reacted in both cooks since it is soluble with water when the chips are defibrillated. Hence, the chemical reactions are not affected by the ionic strength. Secondly, the mass transport of lignin out of the chip is affected by the ionic strength, which is indicated by the difference in Klason lignin content in the BL:s, Figure 25. The harsh treatment of the pulps after the cook, i.e. the disintegration and washing, means lignin is washed out from *lumen* and vessels in the wood chips. It is possible that a lot of lignin resides in *lumen*, vessels and the cell walls in H cooks. The increased ionic strength decreases the solubility of lignin in the BL (Bogren et al., 2009a, Dang, 2017). Hence, the driving force of the removal of lignin fragments from the wood is reduced. The lignin does not migrate from the wood to the BL, but rather remains inside the wood and is lost during washing and disintegration. This indicates that mass transport influences the delignification.

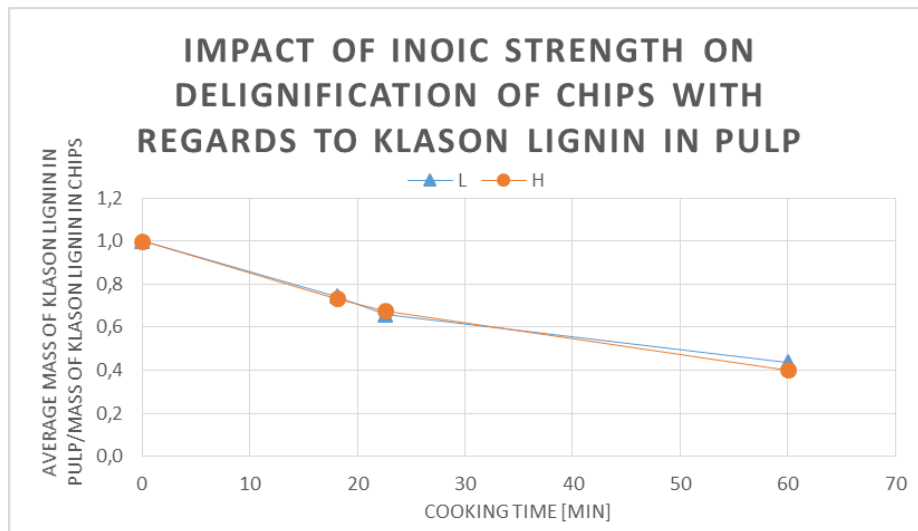


Figure 26. Klason lignin content in washed pulp from cooks with constant either high (H) or low (L) ionic strength.

### 5.1.3 Comparison between autoclave and flow-through cooks

A major difference between autoclave cooks and flow-through cooks regarding Klason lignin content is that there is no effect of mass transport through *lumen* and/or vessels in the flow-through reactor due to the small length scale. *Lumen* and vessels are destroyed during milling so that the only transport of lignin to be considered is that through the cell wall out to the black liquor. Due to the extensive disintegration and washing of the pulp required in the autoclave cooks, the degree of delignification of pulp cannot directly be compared between pulp from the autoclave and the flow-through reactor. Considerable amounts of lignin, retained in the autoclave reactor pulp, are removed during the disintegration and washing. Therefore the Klason lignin content in BL, rather than the pulp, will be compared. The results are presented in Figure 27.

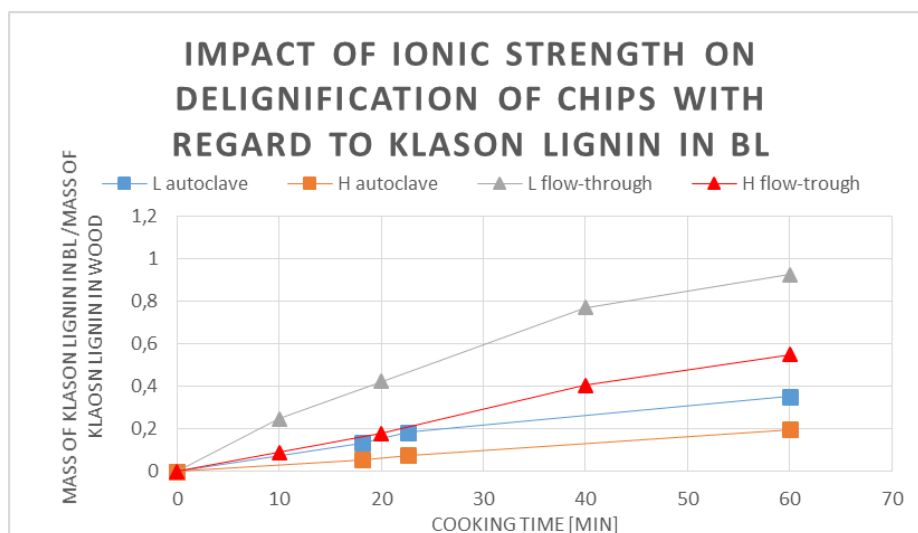


Figure 27. Comparison between Klason lignin in BL from autoclave and flow-through reactor with high and low ionic strength of the cooking liquor.

In Figure 27, two clear differences between the flow-through and the autoclave reactor in terms of Klason lignin in the black liquor can be seen. First, the content of Klason lignin in BL is larger in the flow-through reactor cooks. Secondly, the difference between cooks in low and high ionic strength cooking liquor is larger when using the flow-through reactor rather than the autoclave. Both differences may be ascribed to the additional mass transport resistance present in the chips compared to the wood meal. This additional resistance originates from the longer to the reaction sites in the chips. This extra

mass transport resistance decreases the amount of lignin released from the wood to the BL, hence the lower total delignification between the autoclave and the flow-through reactor. The effect of higher ionic strength in the cooking liquor is also reduced. The extra mass transport resistance in the wood chip adds to the mass transport resistance on cell wall level, which is affected by the ionic strength. This combined effect of mass transport resistances makes the effect of ionic strength less pronounced. A comparison between high and low ionic strength cooks in both autoclave and flow-through reactor is presented in Table 10. It is evident that a higher degree of delignification can be reached in flow-through than in autoclave since the degree of delignification is 95% vs 50%. This difference in degree of delignification between flow-through and autoclave may be due to the mass transport of cooking chemicals to the reactive sites. In the wood chips the distance between the surface and the reaction site is longer. Hence, the concentration of cooking chemicals will be lower at the reactive sites. This effect is important to note, the delignification is not only dependent on the mass transport of lignin out of the chip but also dependent on the mass transport in of cooking chemicals. Also, the effect of ionic strength is more pronounced in the flow-through cooks since the difference in delignification degree between L and H is greater.

Table 10. Degree of delignification in cooks performed in both Autoclave and Flow-through at high (H) or low (L) ionic strength.

<b>Lignin content BL after 60 min cook</b>	<b>L</b>	<b>H</b>
<b>Autoclave</b>	35%	20%
<b>Flow-through</b>	95%	50%

## 5.2 CARBOHYDRATES

In this section the amount of carbohydrates in the pulps from the different cooks are presented. Unlike the Klason lignin measurement no approximation of the amounts of sugar units in the pulp during the course of the cook was made. Hence, the carbohydrate amounts are only presented from measurement on pulp which means there is less time resolution than in the Klason lignin results.

The relative amounts of sugar units left in the pulps after cooking are displayed in Figure 28 and Figure 30. It is clear that a longer cooking time implies a lower amount of sugar units left in the pulp, i.e. hemicelluloses and cellulose are degraded. The difference between 40 and 90 min of cooking is greater than that for 90 and 180 min of cooking which implies that the degradation of carbohydrates occurs early in the cook, in good agreement with (Gellerstedt, 2009a). Galactose, Gal, and arabinose, Ara, are particularly sensitive, whereas glucose, Glu, and xylose, Xyl, are more resilient which may be explained by the crystallinity of cellulose and side groups of xylan that protects against peeling. Readsorption onto the cellulose may also occur during the autoclave cooks, but not in the flow-through cooks since the BL is continuously replaced in the column.

It should be noted that the amounts of sugars presented in Figure 28 and Figure 30 are relative amounts.

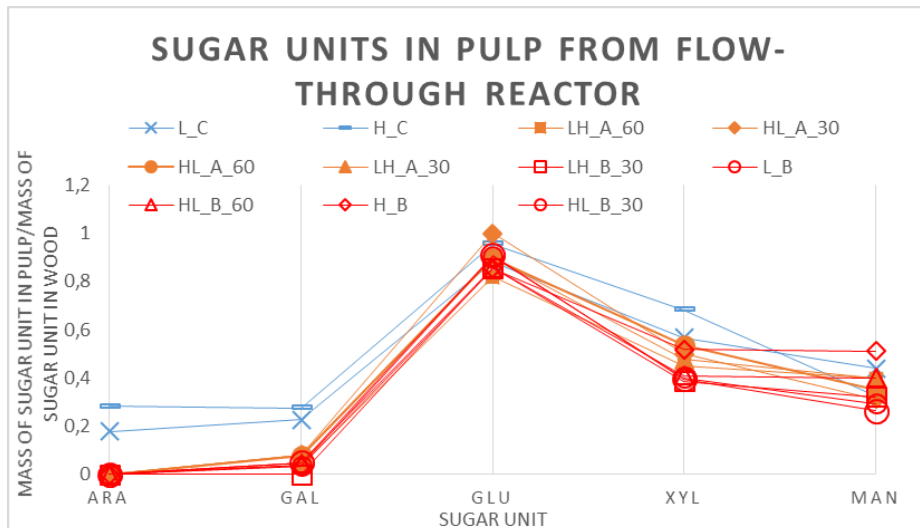


Figure 28. Relative amounts of sugars in pulp from flow-through reactor. Blue lines with lines/crosses as markers have been cooked 40min, yellow lines with filled markers have been cooked 90min and red lines with unfilled markers have been cooked 180min.

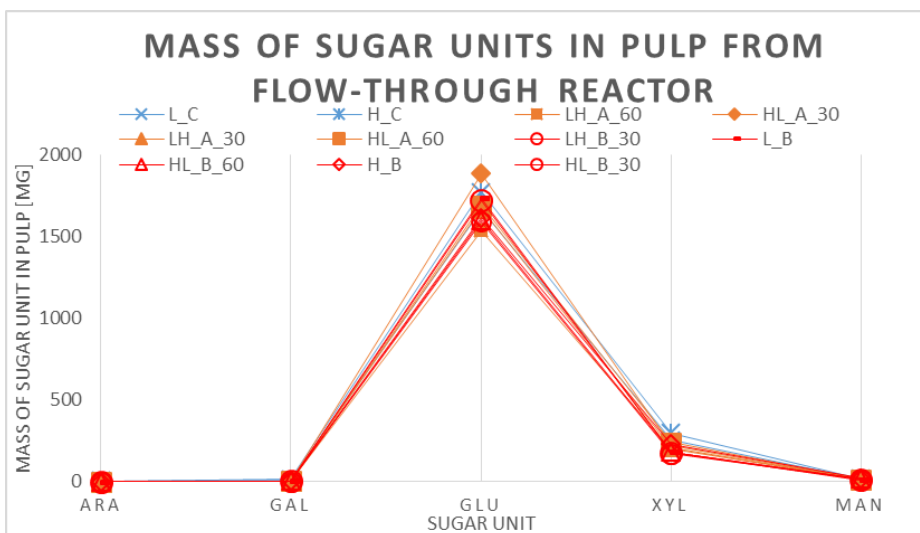


Figure 29. Absolute amount of sugar units in the pulp from the flow-through reactor. Blue lines with lines/crosses as markers have been cooked 40min, yellow lines with filled markers have been cooked 90min and red lines with unfilled markers have been cooked 180min.

The absolute amount of the sugars in the samples can be found in Figure 29 and Figure 31. It is difficult to draw any conclusions on the behaviour of mannose in the samples since the amount is very low, which can be seen in Figure 29 and Figure 31. The amounts of arabinose and galactose are also low, but somewhat larger than mannose. Furthermore, the results from the HPAEC-PAD indicates presence of rhamnose in the samples. Quantification of this was not possible, since the separation from the galactose peak was inadequate. This means that the amount of galactose consequently is slightly overestimated since a part of the peak of rhamnose is counted as galactose. However, the amount of galactose in the pulp is very low, as shown in Figure 29 and Figure 31, and the amount of rhamnose was even lower. Hence, it was concluded that the exclusion of rhamnose was viable.

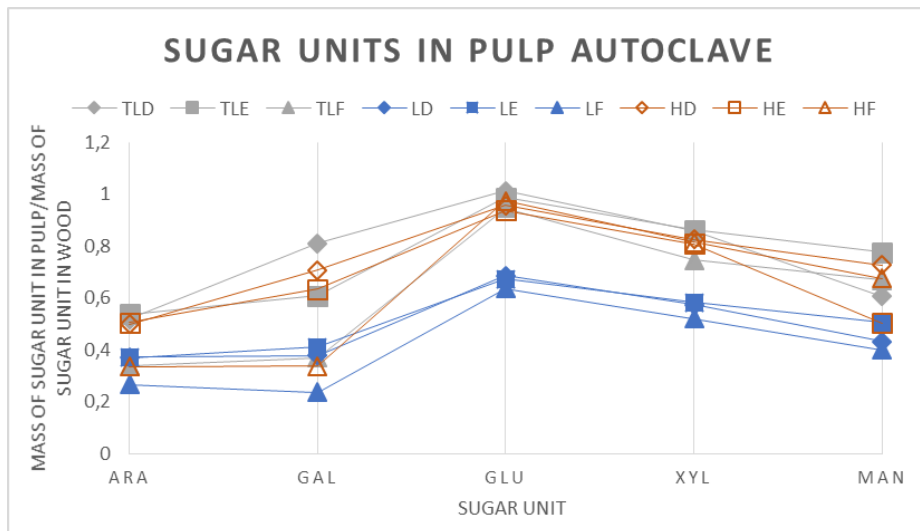


Figure 30. Relative amounts of carbohydrates in the pulp from the autoclave. D samples, diamond markers, have been cooked for a time corresponding to 10min in the flow-through reactor, E samples, square markers, 20min and F samples, triangles, 60min.

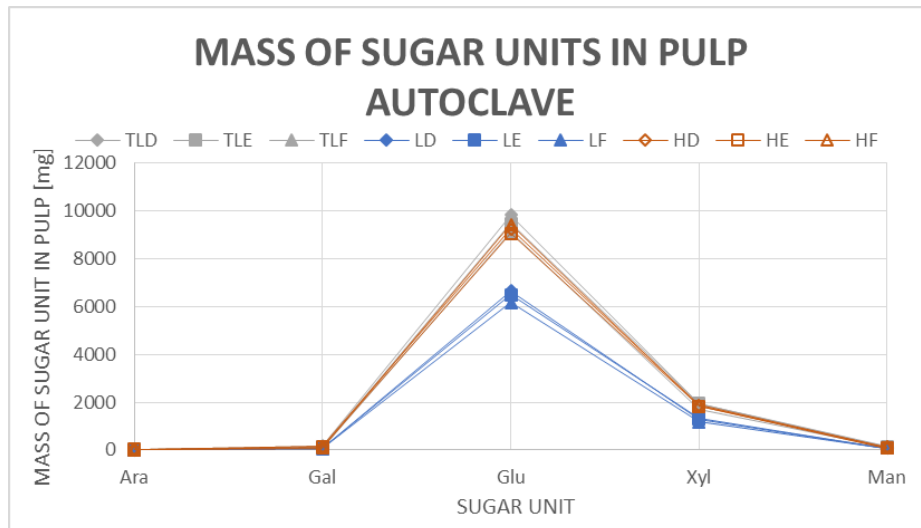


Figure 31. Absolute amount of carbohydrates in the pulp from the autoclave. D samples, diamond markers, have been cooked for a time corresponding to 10min in the flow-through reactor, E samples, square markers, 20min and F samples, triangles, 60min.

Comparing Figure 30 to Figure 28, it is evident that the degree of carbohydrate degradation is less extensive in the autoclave compared with the flow-through reactor. This may be explained by the shorter cooking times of the autoclave pulps presented.

The amount of sugars in the L and TL (duplicate run of L) samples, shown in Figure 30 and Figure 31, are quite different although they were cooked and characterized in the same way which is peculiar. Figure 26 show a clear similarity in the delignification degree behaviour between cooks with high and low ionic strength in the autoclave. The degradation and dissolution of carbohydrates during the cook ought to correlate with the degree of delignification. It hence could be argued that the amount of sugars in the low ionic strength cooks, TL and L, should be similar to that of a high ionic strength cook, H, in the autoclave since they display the same degree of delignification. By that reasoning it appears to be something strange with the L cooks in Figure 30 and Figure 31 since they do not follow the behaviour of the H cooks. How the difference between L and TL has arisen remains unclear.

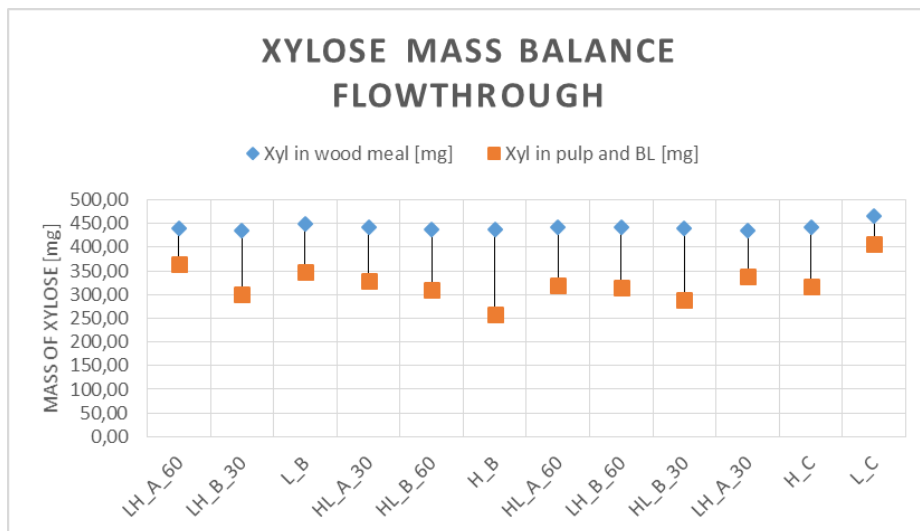


Figure 32. Mass balance of xylose between wood and pulp and BL from flow-through cooks. The residual xylose, not found in BL or pulp, is assumed to have reacted in the BL and formed sugars acids.

The xylose mass balances for the flow-through and autoclave reactor cooks are presented in Figure 32 and Figure 33 respectively. Xylose from the wood ends up either in the pulp or the BL. In the BL it may react further to form alkali stable meta-saccharinic acid (Gellerstedt, 2009a). The difference between the xylose in the wood and the xylose detected in pulp and black liquor is hence considered to be alkali stable sugar acids. The degree of peeling that have occurred during the cook may thus be connected with the difference between the amount of xylose in wood meal and the amount in pulp and BL. It was expected that the amount of sugar acids would increase with increased cooking time since more xylose would have been released and had time to react. However, no clear correlation between amount of sugar acids and the cooking conditions can be observed. This remains therefore to be investigated further, but may be the result of stabilising side groups. Important to note is that the L autoclave cooks show peculiar behaviour with regards to carbohydrates compared to the other cooks, which have been mentioned previously. Furthermore, there is no significant difference in the percentage of xylan in the wood that have been converted to sugar acids between the autoclave cook and flow-through cook. The fraction of xylan converted to sugar acids is slightly higher in the flow-through but the difference is too small to draw any conclusions.

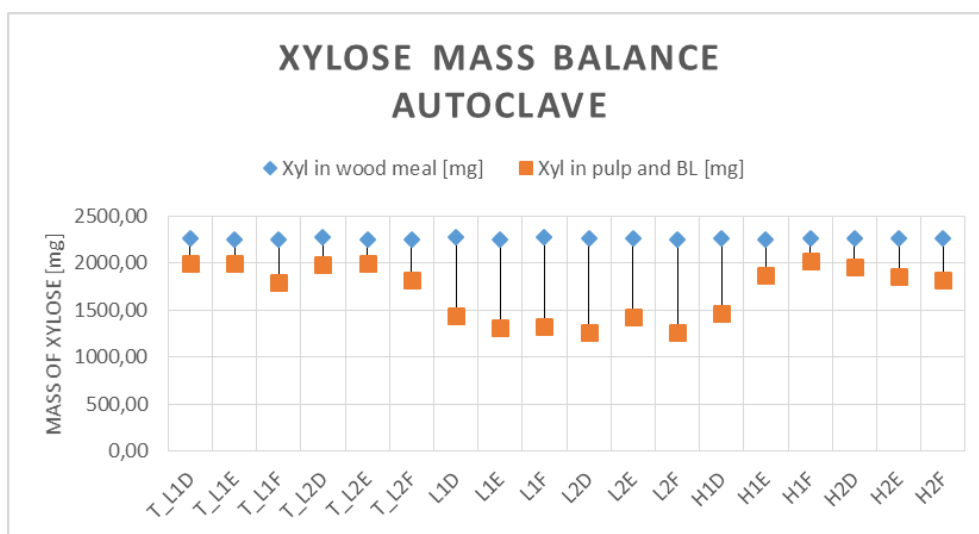


Figure 33. Mass balance of xylose between wood and pulp and BL from autoclave cooks. The residual xylose, not found in BL or pulp, is assumed to have reacted in the BL and formed sugars acids.

### 5.3 COMPOSITION

The composition of pulps from the flow-through reactor is presented in Figure 34 together with the composition of the wood meal. The latter was characterised six times, and the presented results are the averages of these measurements. Shorter cooking times, such as in HC and LC cooks, results in poorly delignified pulps with much remaining Klason lignin. High ionic strength of the cooking liquor increases this effect, which is evident when comparing HC with LC cooks. Also, the cooks with short cooking times have more ASL in the pulps, than the cooks with longer cooking time, which is an expected result.

There is much xylose in the wood meal which indicates a high xylan content in the eucalyptus wood. The content of xylose remains quite stable in all pulp samples, regardless of cooking time and ionic strength. This corresponds well with the notion of xylans being quite resilient to degradation in Kraft cooking.

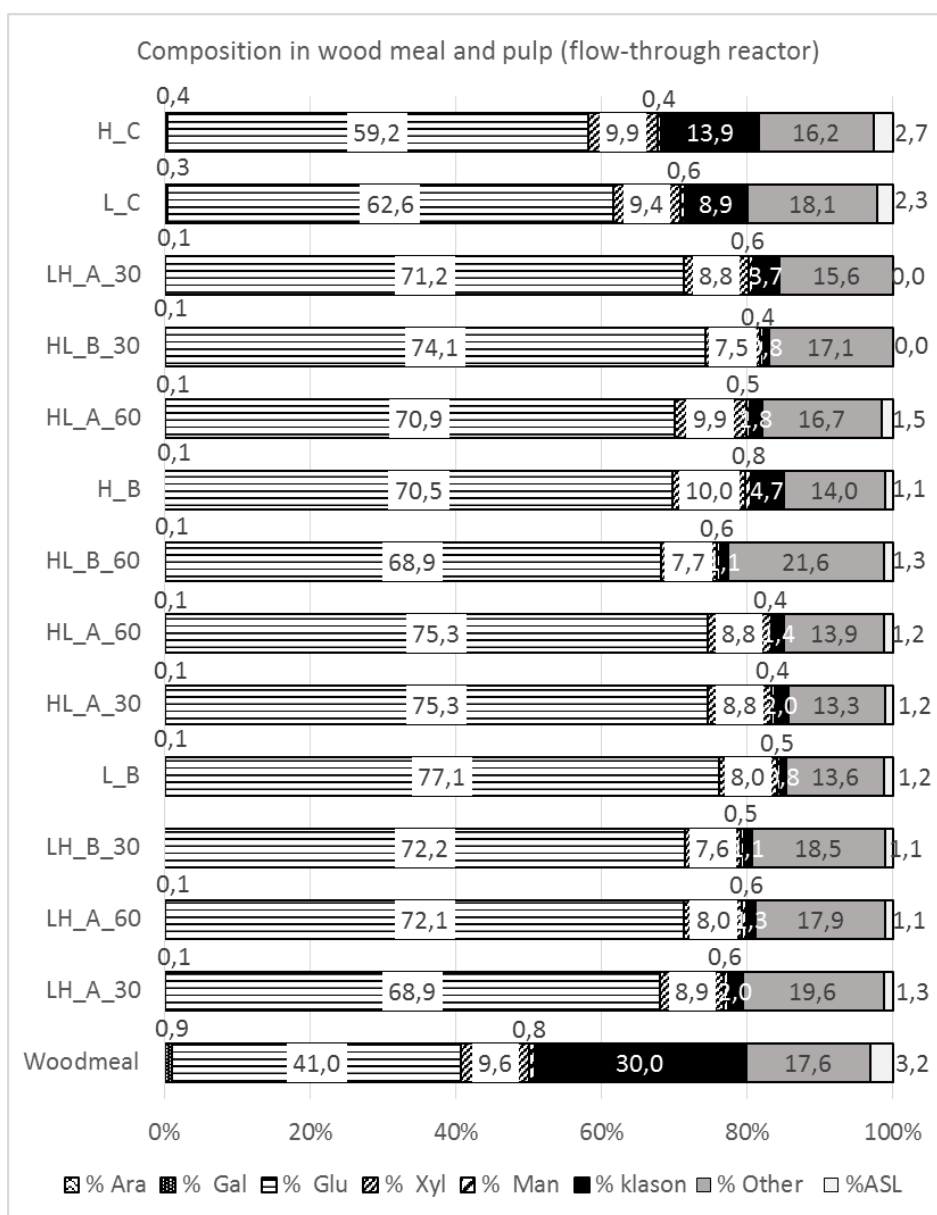


Figure 34. Composition of wood meal and pulp in terms of Klason lignin, ASL and various sugar monomers. "Other" components include extractives, ash, glucuronic acid, acetyl groups, rhamnose, sugar acids and unidentified matter.

In Figure 35, it is evident that the degree of delignification is lower in the autoclave cooks. Notable is that L has a peculiar behaviour with low contents of carbohydrates, which corresponds to the results and discussion in section 5.2. As discussed in section 5.1.2, the ionic strength does not seem to have a major effect on the autoclave pulps, which is also evident from the composition in Figure 35, where TL and H have similar composition.

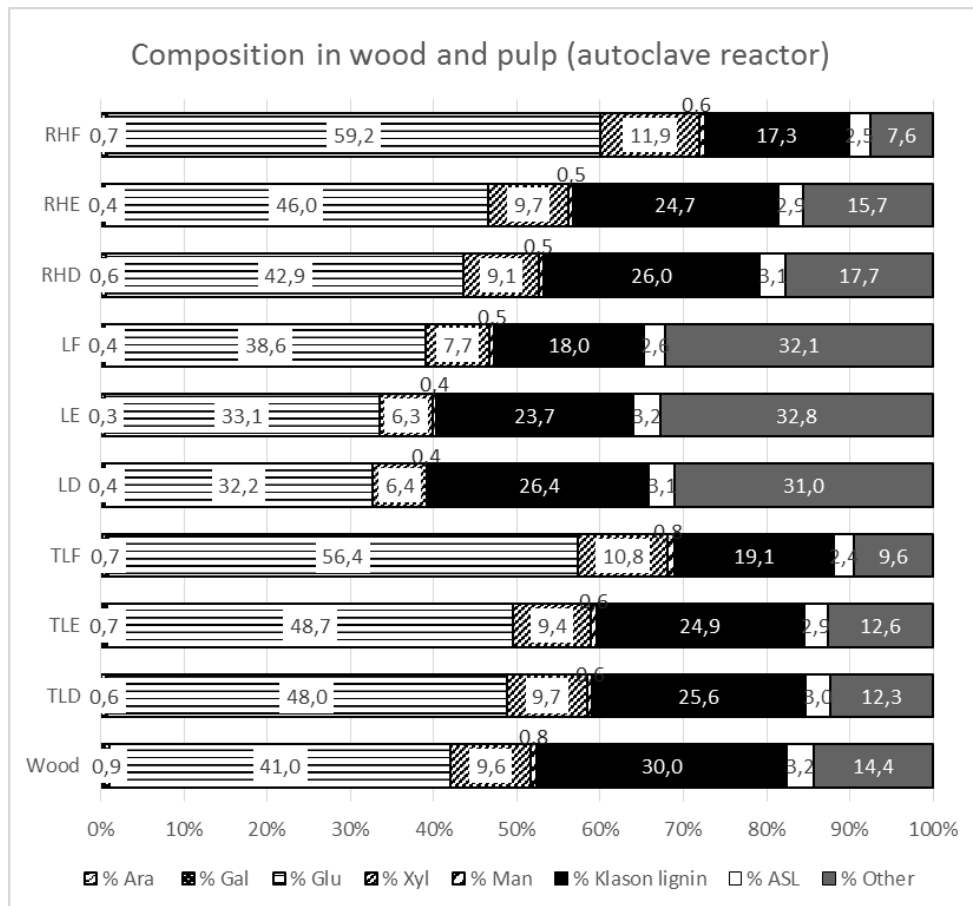


Figure 35. Composition of wood meal and pulp in terms of Klason lignin, ASL and various sugar monomers. "Other" components include extractives, ash, glucuronic acid, acetyl groups, rhamnase, sugar acids and unidentified matter.

In Table 11, composition data of *E. Urograndis* from the literature and the measurements on the wood meal are presented. More literature values for the composition, obtained with other characterisation methods, are presented in Appendix IV.

Some differences are present but the values generally corresponds well. Notable is the glucose value, which differs the most. However, the small differences between the values from the literature and the values from the experiments is probably due to different characterisation methods used, especially the method used for characterisation of carbohydrates.

The amount of acid soluble lignin in the wood meal was found to be 3,2% which corresponds well to previously reported values of ASL content in hardwood, 3-4% (Lin et al., 1992, Maekawa et al., 1989). Furthermore, the part called "other" in Figure 34 and Figure 35 corresponds to the sum of extractives, ash, glucuronic acid, acetyl groups, rhamnase, sugar acids and unidentified matter. The percentage identified in this work, 14,4 %, corresponds to the findings of Magaton et. al. (Magaton et al., 2009) and Lopez et. al. (López et al., 2015), for which the "others" was reported as 14,5 %.

Table 11. Comparison between the compositions of *E. Urograndis* found in literature and the composition detected in experiments. The values are given as percentage of wood. The amounts of extractives and rhamnose were not investigated during this work and are therefore left blank.

	<i>Values from literature (Pinto et al., 2005)</i>	<i>Values from experiments</i>
<b>Klason lignin</b>	27.9 %	30 %
<b>Extractive</b>	1.91 %	--
<b>Glucose (Glu)</b>	52.1 %	41 %
<b>Xylose (Xyl)</b>	11.4 %	9.6 %
<b>Rhamnose (Rha)</b>	0.2 %	--
<b>Arabinose (Ara)</b>	0.4 %	0.2 %
<b>Mannose (Man)</b>	0.7 %	0.8 %
<b>Galactose (Gal)</b>	1.2 %	0.9 %

## 5.4 MOLECULAR WEIGHTS

The molecular weights of the acid precipitated lignin from BL are presented as the weight average molecular weight,  $M_w$ . No measurements of  $M_w$  for the residual lignin in the pulp were made, since that lignin was locked in the wood matrix. The  $M_w$  for lignin from cooks with low ionic strength is higher than that of lignin from high ionic strength. In Figure 36 and Figure 37, the  $M_w$  of cooks when exchanging the ionic strength of the cooking liquors are presented. L\_B and H\_B results, i.e. constantly high and low ionic strength, are included for comparison. In Figure 38, a comparison between flow-through and autoclave  $M_w$  is presented. The molecular weight distributions, from which the  $M_w$ 's were calculated, are presented in Appendix V.

### 5.4.1 Flow-through cooks

In investigations on Scots pine Dang concluded that the  $M_w$  of lignin increased constantly during the cook in the flow-through reactor both with low and high ionic strength in the cooking liquor (Dang, 2017). Although the cook with constant high ionic strength, H\_B, display this behaviour as shown in Figure 36, it is evident that the cook with low ionic strength, L\_B, does not. It reaches a maximum value after 90 min of cooking, where after it decreases. This may be explained by a too small sampling amount. In Figure 18 it is evident that the amount of lignin in the fractions after 90 min of cooking is very low. Hence, most of the lignin has already been removed from the wood, and the actual contents of the “acid precipitated lignin” in the remaining fractions are unclear. Hence, the  $M_w$  of these fractions (120, 150 and 180 min of cooking) is likely not representative. The same is true for the last fraction of LH\_A\_60 as well as last four fractions of HL\_B\_60. Another explanation to the decreasing  $M_w$  might be that the delignification is completed. The large fragments have already dissolved by the end of the cook and the fragments left are small residual fragments.

Compared to the results of Dang the  $M_w$  of the L\_B cooks are higher and the H\_B cooks are lower (Dang, 2017). In general, L\_B has a much larger average molecular weight than H\_B indicating that larger lignin fractions dissolve in cooking liquors with lower ionic strength. Exchange of ionic strength clearly effects the average molecular weight of the lignin released from the wood (Dang, 2017). At 60 min in the LH\_A\_60/LH\_B\_60 cooks the molecular weight decreases when the ionic strength is increased. Fractions 6-8 of LH\_B\_60 follows the profile of H\_B nicely. The same can be observed for LH\_A\_30/LH\_B\_30, but for fractions 4-8. The curves follows the L\_B curve until the change at 30min where they start approaching the HB line instead.

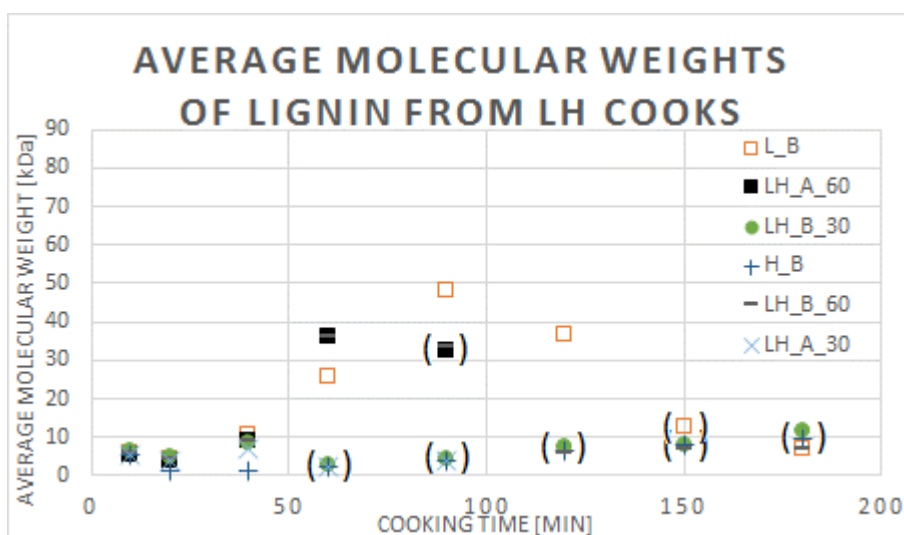


Figure 36.  $M_w$  of cooks in the flow-through reactor starting with low ionic strength and changing to high. As references the cooks with constant high and constant low ionic strength, i.e.  $H_B$  and  $L_B$ , are presented as well. Points marked with a parenthesis are based on samples with very low amount of lignin and may not be representative. However, the points for  $H_B$  are representative until 120 min, but have a parenthesis around them since they lay on top of points with to low amount of lignin.

$HL_B_{30}$ , in Figure 37, follows the curve of  $H_B$  until the ionic strength is decreased after 30 min, then it moves to the curve of  $L_B$ . Just as with the case of  $L_B$  the amount of lignin is low in the last fractions, see Figure 22, which – with the same reasoning as with  $L_B$  in Figure 36 – explains why the  $M_w$  drops after 90 min of cooking.

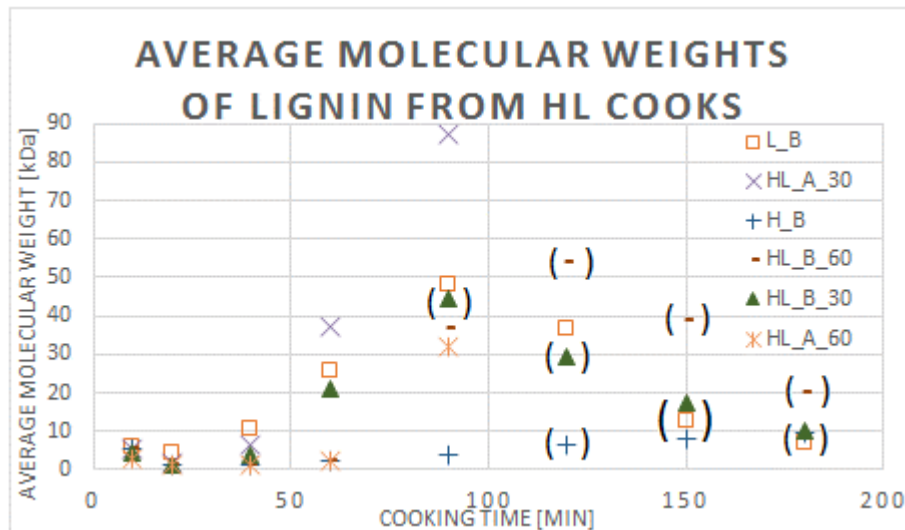


Figure 37.  $M_w$  of cooks in the flow-through reactor starting with high ionic strength and changing to low. As references the cooks with constant high and constant low ionic strength, i.e.  $H_B$  and  $L_B$ , are presented as well. Points marked with a parenthesis are based on samples with very low amount of lignin and may not be representative.

$HL_A_{60}/HL_B_{60}$  in Figure 37 follows the curve of  $H_B$  until the change and then rapidly moves to the curve of  $L_B$ . The result gives a curve similar to the  $L_B$  curve but shifted to the right. The last three fractions of  $HL_B_{60}$  contain very little lignin, which is seen in Figure 23, and hence the decreasing behaviour of the  $M_w$  in the last three fractions is seen here as well, like in  $L_B$ .

HL\_A\_30 show a clearly outlying behaviour. It follows the H\_B line until the change at 30 min, just as expected, but then it deviates. Rather than following the L\_B line, it increases a lot. Some undissolved matter remained in the sample of fraction five, i.e. the one at 90 min of cooking, before dilution with 4ml of DMSO. This incomplete dissolution could mean that large complexes existed in the sample which gave the high  $M_w$ . This is the most plausible explanation of the outlying behaviour since no other difference compared with other samples run in the GPC was noted. In opposition to this line of reasoning, must be mentioned that the first fraction of HL\_A\_30 also contained some undissolved material like the fifth fraction. This fraction have a  $M_w$  corresponding to that of similar cooks. Hence, the results of improperly dissolved samples are difficult to interpret.

#### 5.4.2 Comparison of $M_w$ of lignin between autoclave and flow-through reactor cooks

The average molecular weight in the autoclave cooks is low compared to those of the flow-through reactor, shown in Figure 38, since the lignin continues to be degraded in the BL after it has been dissolved. In the flow-through the BL is cooled after passing the sample which quenches degradation reactions of the lignin. Also, there is a larger difference between fractions with regards to average molecular weight in the flow-through reactor compared to the autoclave cooks due to the quenching of the BL. Differences in  $M_w$  are preserved when the reactions in the BL are quenched. Furthermore, the autoclave has very similar average molecular weights for the high and low ionic strength cooks in contrast to the flow-through reactor where higher ionic strength gives lower average molecular weight.

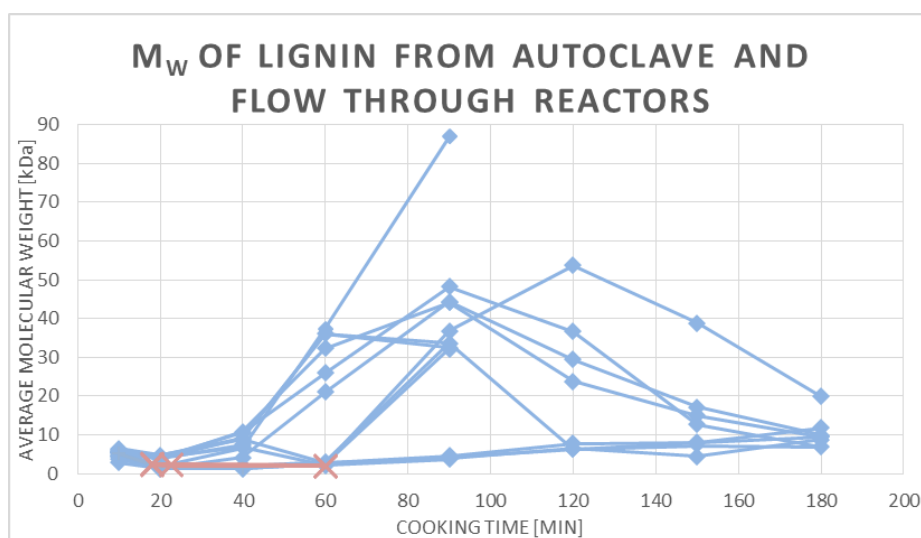


Figure 38. Comparison of  $M_w$  of lignin from autoclave cooks, red lines with cross markers, and flow-through cooks, blue lines with diamond markers.

## 5.5 NMR

The investigation of Klason lignin content suggests that the major part of the delignification occurs in the initial part of the cook as shown in Figure 18 and Figure 25. Hence, a lot of structural changes should be detectable with NMR in the lignin from early black liquor fractions. Acid precipitated lignin, APL, from six BL samples were thus chosen to be run in  $^1\text{H}$ - $^{13}\text{C}$  HSQC NMR. They are presented in Table 12. No samples from the autoclave cooks were chosen.

Carbohydrates present in the lignin samples are considered to be parts of lignin-carbohydrate complexes, LCC:s. Other kinds of sugars, such as shorter sugar chains and monomers are acid soluble and washed through the filter when filtering the APL.

Table 12. Samples run in NMR.

Sample	BL Fraction	Cooking time interval [min]	Colour of the lignin
L_B (10 min)	2	10-20	Brown-grey
L_B (20 min)	3	20-40	Brown-grey
L_B (40 min)	4	40-60	Brown-grey
HL_B_60 (10 min)	2	10-20	Green-grey
HL_B_60 (20 min)	3	20-40	Green-grey
HL_B_60 (40 min)	4	40-60	Green-grey

The 2D HSQC NMR spectra show the signal intensity of C-H bonds in different functional groups. The signal intensity of CH/CH<sub>3</sub> groups increase in the order of colour indication: green < yellow < orange < red, while CH<sub>2</sub> group increases in the order of: blue < indigo < violet. Three different regions in the 2D NMR spectra for the samples were analysed. Namely, the aliphatic region; the methoxy, linkages and carbohydrates region and lastly the aromatic and alkene region. Figure 39 show an example of a full spectrum of one sample with the different regions marked. The results are presented for each cook separately followed by a comparison of the two cooks. All the spectra are appended in Appendix VI.

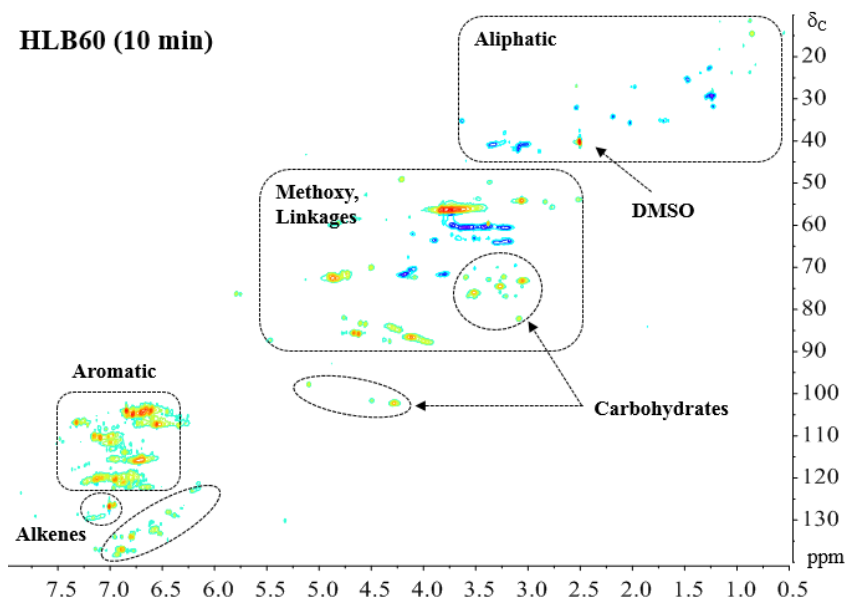


Figure 39. 2D NMR spectra for HL\_B\_60 fraction 1 where regions for different kinds of bindings are marked.

### 5.5.1 L\_B

In Figure 40 the aromatic regions of the lignin samples from the L\_B cook are presented. A further discussion on these regions are found in section 5.5.1.3. The other regions are presented in Appendix VI.

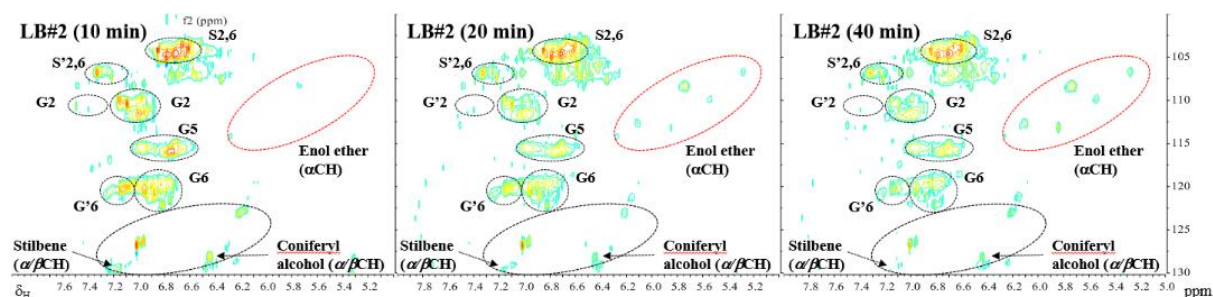


Figure 40. Aromatic region of the 2D HSQC NMR of L\_B. Notice how the “enol ether” signal increase, both in the number of peaks and the intensity of each peak; and how the “coniferyl alcohol” signal decreases.

#### 5.5.1.1 Aliphatic region

Reduced aliphatic structures are formed as a function of the cooking time, which is shown by a decreased signal of  $\gamma$ -CH<sub>3</sub> group and an increased signal for  $\beta$ -CH<sub>3</sub> groups. This could be explained by the propane parts of the phenylpropanes, which constitute the lignin, being shortened during the cook.

#### 5.5.1.2 Methoxy, Linkages and Carbohydrates region

The signals for  $\beta$ -O-4 and  $\beta$ - $\beta$  inter-unit linkages decrease as a function of the cooking time. The breaking of the  $\beta$ -O-4 bond conforms to the general explanations of the degradation of lignin during Kraft cooking.  $\beta$ - $\beta$  structures may be reduced by cleavage of the propane chain in the phenylpropane unit. This does not cleave the  $\beta$ - $\beta$  bond, but disconnects one of the  $\beta$  carbons from its propane chain through a base catalysed retrograde aldol reaction, meaning that the  $\beta$ - $\beta$  functionality is lost (Gierer, 1980).

Moreover, the signal for carbohydrates increase as a function of the cooking time which may indicate increased amounts of LCC. The formation of LCC:s transpires from the degradation of the larger lignin-carbohydrates network of wood during delignification, or alternatively, from the condensation of the quinone methides with polysaccharide peeling intermediates during cooking (Mattsson et al., 2017). These LCC increases of the M<sub>w</sub> of lignin which conforms with the results of M<sub>w</sub> for L\_B presented in Figure 36. In this figure it is evident that the M<sub>w</sub> values for the acid precipitated lignin increases as a function of the cooking time. A possible explanation of the delignification is that the  $\beta$ -O-4 bonds are broken which fragments the lignin. Smaller lignin fractions are released early. As time passes larger structures, including LCC:s leave the wood and are dissolved in the BL. Mass transport is hence important.

The higher M<sub>w</sub> of lignin observed with the longer elution time demonstrates the cleavage of inter-unit linkages, i.e.  $\beta$ -O-4 and  $\beta$ - $\beta$ , in lignin occurs at slower rate than the formation of LCC:s from breaking of the lignin-carbohydrate network in the wood during cooking. Another interpretation for this may be re-polymerization reactions of lignin and carbohydrates – forming lignin-carbohydrate, LC, bonds – taking place during the pulping. However, only very weak signals of ether LC-bonds<sup>3</sup>, ester LC-bonds<sup>4</sup>

<sup>3</sup>  $\delta$ C/ $\delta$ H (81.2-80.1)/(4.7-4.2) ppm and 81.7/5.0 ppm

<sup>4</sup>  $\delta$ C/ $\delta$ H 62.7/4.3 ppm

and phenyl glucoside LC-bonds<sup>5</sup> are found, which could indicate that the LCC:s are formed by LC carbon-carbon bonds. Fullerton and Wilkins report formation of carbon-carbon linkages between model compounds of lignin and carbohydrates (Fullerton and Wilkins, 1985). However, they also reported these bonds to be unstable during alkaline conditions. Hence, the increase of carbohydrate signals over the cooking time is hard to relate to LCC since there are very low signals for lignin-carbohydrate bonds in the NMR spectra. Carbon-carbon bonds are not visible, but such bonds between lignin and carbohydrates are unstable during the conditions employed in Kraft cooking according to Fullerton and Wilkins. Hence, a possible conclusion is that pure carbohydrate chains, e.g. xylans, are present in the lignin samples contrary to the previous assumption.

### 5.5.1.3 Aromatics and alkenes region

The signals for alkenes, aromatic CH and oxygenated aromatic CH decrease with increasing cooking time while the signals for enol ethers increase. These changes are shown in Figure 40, except the alkenes. These alkenes relate to conjugated bonds between the  $\alpha$ - and  $\beta$ -carbons in the phenylpropane chain with carbonyl groups present. The decrease of alkenes is probably due to some sort of oxidation. Condensation reactions could also decrease the amount of alkenes. However, no such condensations are present since no signals of restricted  $\alpha/\beta$ -CH<sup>6</sup> are found in the spectra. Thus, the reduction of the amount of alkenes is probably due to some sort of oxidation.

The presence of coniferyl alcohol and enol ether found in the spectra indicates elimination reactions of the  $\beta$ -O-4 linkages. Enol ether and coniferyl alcohol formation are two competing reactions from quinone methide originating from  $\beta$ -O-4 linkages. The formation of coniferyl alcohol starts early while the formation of stable enol ether starts later in the cook.

## 5.5.2 HL\_B\_60

In Figure 41 the aromatic regions of the lignin samples from the HL\_B\_60 cook are presented. A further discussion on these regions are found in section 5.5.2.3. The other regions are presented in Appendix VI.

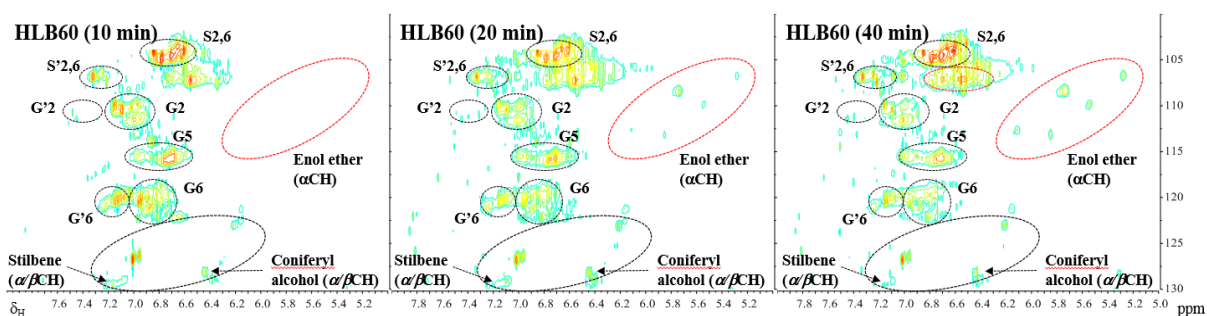


Figure 41. Aromatic region of the 2D HSQC NMR of HL\_B\_60. Notice how the “enol ether” signal increase, both in the number of peaks and the intensity of each peak; and how the “coniferyl alcohol” signal decreases.

### 5.5.2.1 Aliphatic region

Reduced aliphatic structures are formed as a function of the cooking time, which is shown by a decreased signal of  $\gamma$ -CH<sub>3</sub> group and an increased signal for  $\beta$ -CH<sub>3</sub> groups. There is also a strong signal for Ar-CO-CH<sub>2</sub>-CH<sub>2</sub>-OH, which was not present in the cook with low ionic strength. This signal decreases as a function of the cooking time. The reason for this signal being present in the high ionic strength cook but not in the low ionic strength cook remains unknown.

<sup>5</sup>  $\delta C/\delta H$  (104-99)/(5.3-4.8) ppm

<sup>6</sup>  $\delta C/\delta H$  55-40/4.6-2 ppm

### 5.5.2.2 *Methoxy, Linkages and Carbohydrates region*

The signals for  $\beta$ -O-4 and  $\beta$ - $\beta$  inter-unit linkages first decreases between “10 min” and “20 min”. Then they increase to more than the signal in the first fraction thus yielding a net increase of the  $\beta$ -O-4 signals as a function of the cooking time. This is quite unanticipated since the  $\beta$ -O-4 are expected to be cleaved during the course of Kraft cooking. However, results have been reported with the amount of  $\beta$ -O-4-bonds first increasing and then decreasing as the degree of delignification increases when cooking in a flow-through reactor (Gellerstedt, 2009a). Hence, it is possible that the net increase in  $\beta$ -O-4 signals seen over the three fractions is just the initial increase and that further cooking would decrease the  $\beta$ -O-4 signals. A possible explanation for the increase of  $\beta$ -O-4 signals is the fact that the fast formation of stable enol ethers may result in the prevention of the cleavage elimination of  $\beta$ -O-4 linkage in the last fraction. The  $M_w$  of the fractions increase over time, but to a much lower extent than the L\_B cook which is seen in Figure 37.

The signal for carbohydrates increases as a function of the cooking time, just as in the L\_B cook. Just as in that case there are no clear signals for linkages between lignin and carbohydrates present.

### 5.5.2.3 *Aromatics and alkenes region*

The signal for alkenes decrease as a function of the cooking time. This may again be ascribed to oxidation, as in L\_B due to the same lack of restricted  $\alpha/\beta$ -CH signals. Moreover, the signals for aromatic CH decrease while aromatic oxygenated CH increases which is shown in Figure 41. The increase of aromatic oxygenated CH signals over time could be due to oxidation of lignin fragments, or that oxygenated lignin fragments present in the wood meet larger transport resistance and hence requires longer time to be released. Moreover, the signals for enol ether increase as a function of the cooking time just as in the L\_B cook.

### 5.5.3 *Comparison between L\_B and HL\_B\_60*

The lignin from L\_B and HL\_B\_60 show many similarities. During the cooks reduced aliphatic structures form and enol ether signals increase. Coniferyl alcohol is present in all fractions but the signals decrease with cooking time. The coniferyl alcohol forms at early stage of delignification whereas the enol ether forms at later stage. This observation is in good agreement with the data from Mattsson et al. (Mattsson et al., 2017). Moreover, ionic strength gives no effect on the formation of coniferyl alcohol and/or enol ethers.

Carbohydrate signals become stronger as a function of the cooking time. However, the signals for LCC complexes are very weak. Furthermore, there are no signs of lignin condensation reactions occurring at the  $\alpha$ -carbon in either of the cooks because the tertiary aliphatic methine groups (CH)<sup>7</sup>, which would signify such condensations, are only found with relatively low signals. Finally, aromatic CH-groups decrease as a function of the cooking time, and so does the signals for alkenes.

The differences between the cooks are that  $\beta$ -O-4 and  $\beta$ - $\beta$  signals decrease for the L\_B cook, whereas they increase for the HL\_B\_60 cook. Moreover, there are no Ar-CO-CH<sub>2</sub>-CH<sub>2</sub>-OH signals in the L\_B cook but there are clear signals in the HL\_B\_60 cook. Finally the oxygenated aromatic CH-groups increase for the HL\_B\_60 cook while decreasing for the L\_B cook.

According to Mattsson et al. coniferyl alcohol is the major intermediate from phenolic  $\beta$ -O-4 cleavage and since it reacts in many different ways it is not accumulated in the BL (Mattsson et al., 2017). When investigating acid precipitated lignin from Scots pine cooked under the same conditions as the L\_B samples Mattsson et al. found coniferyl alcohol in the early fractions of the cook. This supported a

---

<sup>7</sup>  $\delta C/\delta H$  55-40/4.6-2.0 ppm

conclusion on the major delignification reactions taking place in the early part of the cook (Mattsson et al., 2017). The coniferyl alcohol in L\_B and HL\_B\_60 forms at an early stage of delignification whereas the enol ether forms a later stage. This observation is in good agreement with the data from Mattsson et al. even though they used softwood, which is less reactive than hardwood used in the present investigation. Hence, it would seem as though the phenolic  $\beta$ -O-4 bonds are cleaved early in the cook also for *E. Urograndis* which could strengthen the hypothesis that the delignification is limited by solubility and or mass transport rather than reaction kinetics.

The decrease of coniferyl signals are paired with increasing signals for enol ethers which according to Mattsson et al. may indicate  $\beta$ -O-4 conversions (Mattsson et al., 2017). The formation of enol ether from quinone methide is a competing reaction to the formation of coniferyl alcohol from phenolic  $\beta$ -O-4 cleavage. The desired reaction is for the quinone methide to form a thioalcohol with  $\text{SH}^-$  which later on forms coniferyl alcohol by expelling the sulphur. The reaction is an equilibrium reaction meaning that a shortage of  $\text{SH}^-$  reduces the amount of the desired thioalcohol formation and instead enable the quinone methide to use other reaction paths which increases the formation of enol ethers. Since the amount of  $\text{SH}^-$  is high in the cooking liquor there is no shortage of it in the liquid bulk. Instead the increase of enol ethers could be explained as local shortage of  $\text{SH}^-$  within the wood cells. If so, mass transport phenomena are important also on a cell wall level, not only on larger scale such as transport in wood chips.

## 6 CONCLUSIONS

---

The hypothesis when commencing this project was that the delignification of *E. Urograndis* not only is controlled by chemical reaction kinetics but rather also on mass transport phenomena similarly to the results of Dang on *Pinus Sylvestris*. Using the same flow-through reactor and cooking conditions, comparisons were made possible. Both wood meal and chips of *E. Urograndis* were cooked to investigate the influence of mass transport also on larger scale. The chips were cooked in an autoclave reactor. Furthermore, the ionic strength of the cooking liquor was varied, while at the same time keeping the concentration of active cooking chemicals constant. Thus, the influence of mass transport on cell wall level could be investigated since the solubility of lignin decreases with increasing ionic strength of the cooking liquor.

The results indicate a more rapid delignification of the eucalyptus compared to the pine which is consistent with established delignification rates of soft- and hardwood. A higher ionic strength of the cooking liquor reduces the delignification rate. This is especially clear when cooking wood meal as opposed to wood chips. A difference in lignin content in BL was observed between the H cook and L cook of chips. The difference may probably be ascribed to the higher mass transport resistance out of the chip with higher ionic strength in the cooking liquor. However, no difference in delignification degree was observed after washing of the pulp between the cooks with low and high ionic strength. This leads to the conclusion that the chemical reaction of delignification is not affected by ionic strength.

The impact of ionic strength was found to be higher on the delignification of wood meal than on wood chips. This may be due to the difference in mass transport of cooking chemicals to the reactive sites. In the wood chips the distance between the surface and the centre is longer, hence the concentration of cooking chemicals will be lower at the reactive sites. This effect is important to note, the delignification is not only dependent on the mass transport of lignin out of the chip but also dependent on the mass transport in of cooking chemicals. The final conclusion regarding delignification of *E. Urograndis* is thus that the mass transfer plays a significant role.

Analyses of carbohydrates indicate a large portion of xylose in the wood which is quite stable as a function of the cooking time. The major part of the carbohydrates are glucose, and the content is quite stable with increasing cooking time. Arabinose, galactose and mannose are only present in minor amounts and are degraded during the cook. Rhamnose was detected but not quantified. These results is in accordance with common knowledge of composition of hardwoods and the behaviour of carbohydrates during Kraft pulping.

The weight average molecular weight,  $M_w$ , of the lignin increases with the cooking time. Furthermore, high ionic strength decreases the solubility of the lignin meaning that large lignin fragments moves slower out of the wood. Thus more lignin remains in the wood when the cooking liquor has high ionic strength. This concurs with the results of the lignin content analyses.

NMR results show presence of coniferyl alcohol in the black liquor early in the cook which suggest major delignification reactions occurring rapidly. Furthermore, enol ethers form over time which could suggest lack of  $HS^-$  ions locally in the cell wall during the cook of wood meal.

## 7 FUTURE WORK

---

Some recommendations for future work is listed below.

- Perform shorter cooks so that pulp is taken out at each time BL fractions are sampled in the flow-through reactor, i.e. 10, 20, 40, 60, 90, 120, 150 and 180 min. This would enable better lignin balances since pulp would be available at all cooking times.
- Cooks with a higher liquor to wood ratio should be performed to ensure a higher excess of active cooking chemicals, especially if longer cooks are to be performed since a more extensive delignification is expected. This to enable the assumption that the concentration of active cooking chemicals are constant during the cook. During the experiments performed in this work, approximately 42 % of the active cooking chemicals were consumed during the longest cooks, therefore the concentration could not be considered constant for these autoclave cooks.
- More experiments needs to be performed at each cooking time in the autoclave to confirm if the findings of this thesis is solid.
- Perform cooks with longer cooking time in the autoclave to investigate how the later part of the delignification appears.

## Bibliography

- BIERMANN, C. J. 1996. 16 - Pulping Calculations. *Handbook of Pulping and Papermaking (Second Edition)*. San Diego: Academic Press.
- BJÖRKLUND JANSSON, M. & NILVEBRANT, N.-O. 2009. 7. Wood Extractives. *Wood Chemistry and Wood Biotechnology*.
- BOGREN, J. 2008. *Further insights into kraft cooking kinetics*, Chalmers University of Technology.
- BOGREN, J., BRELID, H., BIALIK, M. & THELIANDER, H. 2009a. Impact of dissolved sodium salts on kraft cooking reactions. *Holzforschung*, 63, 226-231.
- BOGREN, J., BRELID, H., KARLSSON, S. & THELIANDER, H. 2009b. Can the delignification rate be affected by previously applied cooking conditions? *Nordic Pulp and Paper Research Journal*, 24, 25-32.
- BROWN, R. M. J. & SAXENA, I. M. 2007. *Cellulose: Molecular and Structural Biology: Selected Articles on the Synthesis, Structure, and Applications of Cellulose*, Springer Netherlands.
- BRÄNNVALL, E. 2009a. 1. Overview of Pulp and Paper Processes. *Pulping Chemistry and Technology*.
- BRÄNNVALL, E. 2009b. 6. Pulping Technology. *Pulping Chemistry and Technology*.
- BRÄNNVALL, E. & ANNERGREN, G. 2009. 16. Pulp Characterisation. *Pulping Chemistry and Technology*.
- CHEN, H. T., FUNAOKA, M. & LAI, Y. Z. 1997. Attempts to understand the nature of phenolic and etherified components of wood lignin. *Wood Science and Technology*, 31, 433-440.
- CHRISTIAN, G. D. & O'REILLY, J. E. 1978. *Instrumental analysis*, Boston, Allyn and Bacon.
- DANG, B., BRELID, H. & THELIANDER, H. What do we know regarding the kinetics of delignification in kraft cooking? Autrans, France, 14th European Workshop on Lignocellulosics and Pulp, 2016a. 5-8.
- DANG, B. T., BRELID, H., KÖHNKE, T. & THELIANDER, H. 2013. Impact of ionic strength on delignification and hemicellulose removal during kraft cooking in a small-scale flow-through reactor. *Nordic Pulp & Paper Research Journal*, 28.
- DANG, B. T., BRELID, H. & THELIANDER, H. 2016b. The impact of ionic strength on the molecular weight distribution (MWD) of lignin dissolved during softwood kraft cooking in a flow-through reactor. *Holzforschung*, 70, 495-501.
- DANG, B. T. T. 2017. *On the course of kraft cooking: the impact of ionic strength*. 4306., Chalmers University of Technology.
- DANIEL, G. 2009. 3. Wood and Fibre Morphology. *Wood Chemistry and Wood Biotechnology*.
- EK, M., GELLERSTEDT, G., HENRIKSSON, G. & DE, G. 2009. *Wood Chemistry and Wood Biotechnology*, Berlin ;Boston, De Gruyter.
- EVTUGUIN, D. V. & NETO, P. Recent advances in eucalyptus wood chemistry: Structural features through the prism of technological response. 2007.
- FENGEL, D. & WEGENER, G. 2011. 16. Pulping Processes. *WoodChemistry, ultrastructure, reactions*.
- FULLERTON, T. J. & WILKINS, A. L. 1985. The mechanism of cleavage of b-ether bonds in lignin model compounds by reducing sugars. *Journal of wood chemistry and technology*, 5, 189-201.
- GELLERSTEDT, G. 2009a. 5. Chemistry of Chemical Pulping. *Pulping Chemistry and Technology*.
- GELLERSTEDT, G. 2009b. 8. Cellulose Products and Chemicals from Wood. *Wood Chemistry and Wood Biotechnology*.
- GELLERSTEDT, G. 2009c. 9. Analytical Methods. *Wood Chemistry and Wood Biotechnology*.
- GIERER, J. 1980. Chemical aspects of kraft pulping. *Wood Science and Technology*, 14, 241-266.
- GONZALEZ, R., TREASURE, T., PHILLIPS, R., JAMEEL, H., SALONI, D., ABT, R. & WRIGHT, J. 2011. Converting Eucalyptus biomass into ethanol: Financial and sensitivity analysis in a co-current dilute acid process. Part II. *Biomass and Bioenergy*, 35, 767-772.

- GUSTAFSON, R. R., SLEICHER, C. A., MCKEAN, W. T. & FINLAYSON, B. A. 1983. Theoretical model of the kraft pulping process. *Industrial & Engineering Chemistry Process Design and Development*, 22, 87-96.
- HENRIKSSON, G. 2009. 6. Lignin. *Wood Chemistry and Wood Biotechnology*.
- HENRIKSSON, G., BRÄNNVALL, E. & LENNHOLM, H. 2009. 2. The Trees. *Wood Chemistry and Wood Biotechnology*.
- HENRIKSSON, G. & LENNHOLM, H. 2009. 4. Cellulose and Carbohydrate Chemistry. *Wood Chemistry and Wood Biotechnology*.
- KAAR, W. E. & BRINK, D. L. 1991. Simplified analysis of acid soluble lignin. *Journal of wood chemistry and technology*, 11, 465-477.
- KHOPKAR, S. M. 2011. *Basic Concepts of Analytical Chemistry*, Kent, UNITED KINGDOM, New Academic Science.
- LAROCQUE, G. L. & MAASS, O. 1941. The mechanism of the alkaline delignification of wood. *Canadian Journal of Research*, 19b, 1-16.
- LEE, D. P. & BUNKER, M. T. 1989. Carbohydrate analysis by ion chromatography. *Journal of Chromatographic Science*, 27, 496-503.
- LÉMON, S. & TEDER, A. 1973. Kinetics of the delignification in kraft pulping. I. Bulk delignification of pine. *Svensk papperstidning*.
- LEONARDI, G. D. A., CARLOS, N. A., MAZZAFERA, P. & BALBUENA, T. S. 2015. Eucalyptus urograndis stem proteome is responsive to short-term cold stress. *Genetics and molecular biology*, 38, 191-198.
- LIN, S. Y., DENCE, C. W., SPRINGERLINK, A. & SPRINGERLINK 1992. *Methods in Lignin Chemistry*, Berlin, Heidelberg, Springer Berlin Heidelberg.
- LINDGREN, C. & LINDSTRÖM, M. E. 1996. The kinetics of residual delignification and factors affecting the amount of residual lignin during kraft pulping. *Journal of Pulp and Paper Science (JPPS)*, 22, J290-J295.
- LÓPEZ, F., TRINIDAD GARCÍA, M., MENA, V., MAURICIO LOAIZA, J., ZAMUDIO, M. A. M. & GARCÍA, J. C. 2015. Can acceptable pulp be obtained from eucalyptus globulus wood chips after hemicellulose extraction? *BioResources*, 10, 55-67.
- MAEKAWA, E., ICHIZAWA, T. & KOSHIJIMA, T. 1989. An evaluation of the acid-soluble lignin determination in analyses of lignin by the sulfuric acid method. *Journal of wood chemistry and technology*, 9, 549-567.
- MAGATON, A. D. S., COLODETTE, J. L., GOUVÊA, A., GOMIDE, J. L., MUGUET, M. & PEDRAZZI, C. 2009. Eucalyptus wood quality and its impact on kraft pulp production and use. *Tappi J*, 8, 32-39.
- MATTSSON, C., HASANI, M., DANG, B., MAYZEL, M. & THELIANDER, H. 2017. About structural changes of lignin during kraft cooking and the kinetics of delignification. *Holzforschung*, 71, 545-553.
- OLM, L. & TISTAD, G. 1979. Kinetics of the initial stage of kraft pulping. *Svensk papperstidning*.
- PINTO, P. C., EVTUGUIN, D. V. & NETO, C. P. 2005. Structure of hardwood glucuronoxylans: modifications and impact on pulp retention during wood kraft pulping. *Carbohydrate Polymers*, 60, 489-497.
- ROHRER, J. 2012. Analysis of Carbohydrates by High-Performance Anion-Exchange Chromatography with Pulsed Amperometric Detection (HPAE-PAD). *Thermo Fisher Scientific, Technical Note*, 20.
- SANTOS, R. B., CAPANEMA, E. A., BALAKSHIN, M. Y., HOU-MIN, C. & JAMEEL, H. 2011. Effect of hardwoods characteristics on kraft pulping process: emphasis on lignin structure. *BioResources*, 6, 3623-3637.
- SILVERIO, F. O., BARBOSA, L. C. A., SILVESTRE, A. J. D., PILO-VELOSO, D. & GOMIDE, J. L. 2007. Comparative study on the chemical composition of lipophilic fractions from three wood tissues of Eucalyptus species by gas chromatography-mass spectrometry analysis. *Journal of Wood Science*, 53, 533-540.
- SIXTA, H. 2006. *Handbook of Pulp*, vol. 1, Wiley-VCH.
- SREEVANI, P. & RAO, R. 2015. Wood anatomical structure of the clones of Eucalyptus Tereticornis Sm.(Mysore Gum). *International Journal of Scientific & Technology Research*, 4, 156-159.

- TEDER, A. 2009. 7. Kinetics of Chemical Pulping and Adaptation to Modified Processes. *Pulping Chemistry and Technology*.
- TELEMAN, A. 2009. 5. Hemicelluloses and Pectins. *Wood Chemistry and Wood Biotechnology*.
- THEANDER, O. & WESTERLUND, E. A. 1986. Studies on dietary fiber. 3. Improved procedures for analysis of dietary fiber. *Journal of Agricultural and Food Chemistry*, 34, 330-336.
- THELIANDER, H. 2009. 12. Recovery of Cooking Chemicals: the Treatment and Burning of Black Liquor. *Pulping Chemistry and Technology*.
- WIGELL, A., BRELID, H. & THELIANDER, H. 2007. Degradation/dissolution of softwood hemicellulose during alkaline cooking at different temperatures and alkali concentrations.
- WILDER, H. D. & DALESKI, E. J. 1965. Delignification rate studies. Part II of a series on kraft pulping kinetics. *Tappi*, 48, 293-297.
- WIMMER, R., DOWNES, G., EVANS, R. & FRENCH, J. 2008. Effects of site on fibre, kraft pulp and handsheet properties of *Eucalyptus globulus*. *Annals of Forest Science*, 65, 602-602.
- VROOM, K. 1957. The "H" factor: a means of expressing cooking times and temperatures as a single variable. *PPMC*, 58, 228-231.
- YASUDA, S., FUKUSHIMA, K. & KAKEHI, A. 2001. Formation and chemical structures of acid-soluble lignin I: sulfuric acid treatment time and acid-soluble lignin content of hardwood. *Journal of Wood Science*, 47, 69-72.

## APPENDIX I

---

### CALCULATIONS PERFORMED DURING ABC-TITRATION

$$[HS^-] = \frac{pH9}{m}$$

Where  $pH9$  stands for the volume [ml] of HCl 1M needed to reach pH9. This is the “B-value” in the ABC-test described in section 4.1.  $m$  is the mass of the white liquor sample and  $[HS^-]$  is the concentration of  $HS^-$  ions.

$$m_{liq} = \frac{0,26}{[HS^-]} * 1000 \text{ (gives 1000 g of cooking liquor)}$$

$m_{liq}$  stands for amount of mother liquor needed to receive 1000 g of cooking liquor with the desired concentration 0,26 mol  $HS^-$  /kg liquor.  $m_{water}$  corresponds to the amount needed to dilute the mother liquor to the desired concentration.

$$m_{water} = 1000 - m_{liq}$$

### CALCULATIONS ON WHICH THE ADDED AMOUNT OF $Na_2CO_3$ WAS BASED

$$m_l = 1 \text{ kg liquid}$$

$$\frac{\frac{2m_s}{M_s} + 0,52}{1 + m_s} = 3 \frac{\text{mol}}{\text{kg liquid}}$$

$$m_t = m_l + m_s$$

$$m_s = ?$$

$$\frac{2m_s}{M_s} - 3m_s = 3 + 0,52$$

$$Na_l = 0,52 \text{ [mol]}$$

$$m_s \left( \frac{2}{M_s} - 3 \right) = 2,48$$

$$Na_s = ?$$

$$m_s = \frac{2,48}{\frac{2}{106} - 3} = 0,15629 \text{ kg}$$

$$\frac{Na_t}{m_t} = 3 \frac{\text{mol}}{\text{kg liquid}} = \frac{Na_s + Na_l}{m_t}$$

$$m_t = 1,16$$

$$Na_s = \frac{2m_s}{M_s}$$

Where  $m_l$ ,  $m_t$  and  $m_s$  are the masses of liquid, liquid and salt, and  $Na_2CO_3$  respectively.  $Na_l$  is the amount of sodium ions in one kilogram of cooking liquor prior to the addition of sodium carbonate. This sodium comes from the sodium sulphide.  $Na_s$  is the amount of sodium ions to be added in order to achieve the desired concentration.  $Na_t$  is the desired final amount of sodium ions in the cooking liquor.  $M_s$  is the molar mass of sodium carbonate.

To 1 kg of liquid 156,29 g of  $Na_2CO_3$  is added

## APPENDIX II

---

### CALCULATIONS OF H-FACTOR

The cooking time in the autoclave was calculated using the H-factor values for the corresponding cooks in the flow-through reactor. To establish the temperature profile during the heating of the autoclave reactor the temperature of the PEG-bath in which the autoclaves were immersed was measured during a test cook. The temperature data thus collected was interpolated to yield the temperature increase as a linear function. Calculation of the cooking time for the autoclave cooks was performed with the following Matlab code:

```
clear all, clc, clf,
%%%%%% Temperature profile interpolation parameters for the autoclave %%%
%Temperature increase measured for 45 min each 15min
t1=[0 15 30 45]; %Measuring times
T1=[115 127 140 153]; %Measured temperatures
plot(t1,T1)
hold on
ki=polyfit(t1,T1,1) %Interpolation parameters for temp. increase in the
%autoclave.

%H-factor calculations
T=[115 159]+273.15; %Start temperature, and cooking temperature.
runtime=20; %Cooking time in the autoclave reactor for which the autoclave
%times is searched.
%%%%%%%%%%%%%%%%%%%%%%%%%%%%%%%%%%%%%%%%%%%%%%%%%%%%%%%%%%%%%%%%%%%%%%%% Flow-through Reactor %%%%%%%%%%%%%%%%%%%%%%%%%%%%%%%%%%%%%%%%%%%%%%%%%%%%%%%%%%%%%%%%%%%%%%%%%
%H-factor during temperature increase, first 22 min
T_ramp=@(t)2*t+T(1); %Temperature profile for the FT-reactor
A_ramp=@(t)exp(43.2-16115./T_ramp(t)); %Integrand in the expression for H
H_ramp=integral(A_ramp,0,22); %H-factor for the temperature increase.

%H-factor after 22 min the temperature is constantly 159C.
T22=@(t)T(2)+0.*t; %Temp. after 22 min
A22=@(t)exp(43.2-16115./T22(t)); %Integrand in the expression for H-factor
H22=integral(A22,22,runtime); %H-factor for the cooking at constant T.

Htot=H_ramp+H22 %H-factor for the FT-reactor
%%%%%%%%%%%%%%%%%%%%%%%%%%%%%%%%%%%%%%%%%%%%%%%%%%%%%%%%%%%%%%%%%%%%%%%% Autoclave %%%%%%%%%%%%%%%%%%%%%%%%%%%%%%%%%%%%%%%%%%%%%%%%%%%%%%%%%%%%%%%%%%%%%%%%%
%H-factor during the temperature increase
T(3)=ki(2)+273.15; %Interpolated autoclave start-temp.
k=ki(1); %Interpolated autoclave temp-rise slope
t_ramp_autoclave=(T(2)-T(3))/ki(1); %After this time the temp is constantly
%159C given the interpolation.
T_ramp_aut=@(t)k.*t+T(3); %Temperature profile for the autoclave
A_ramp_aut=@(t)exp(43.2-16115./T_ramp_aut(t)); %Integrand for H calc.
H_ramp_aut=integral(A_ramp_aut,0,t_ramp_autoclave); %H during heating

%After t_ramp_autoclave min the temperature is constantly 159C.
T52=@(t)T(2)+0.*t; %Temp. after heating
A52=@(t)exp(43.2-16115./T52(t)); %Integrand for H calc.

Hauto=@(tau)integral(A_ramp_aut,0,t_ramp_autoclave)+integral(A52,t_ramp_aut
oclave,tau); %H-factor for autoclave.
%Find the cooking time in the autoclave
fun=@(tau)Htot-Hauto(tau); %Function for finding the H-factor so that it is
the same for autoclave and reactor.
guess=70; %Starting guess for the solver.
koktid=fzero(fun,guess) %Cooking time in the autoclave
```

## APPENDIX III

### CALCULATIONS OF KLASON LIGNIN IN THEORETICAL PULP

All masses of Klason were divided by the mass of Klason in the wood meal. The plotted values are therefore mass of Klason per mass of Klason put in the reactor.

$$\text{Klason lignin in wood meal [mg]} = m_{MW}$$

$$\text{Klason lignin in Bl fraction 1 [mg](10 min)} = m_{BL1}$$

$$\text{Klason lignin in Bl fraction 2 [mg](20 min)} = m_{BL2} \dots \dots \dots$$

$$\text{Klason lignin in pulp [mg]} = m_p$$

By subtraction the Klason lignin in each BL fraction from wood meal, this calculations were called forward (F) calculations:

$$\text{At 0 minutes: } m_{P0,F} = m_{MW}$$

$$\text{At 10 minutes: } m_{P1,F} = m_{MW} - m_{BL1}$$

$$\text{At 20 minutes: } m_{P2,F} = m_{MW} - m_{BL1} - m_{BL2}$$

$$\text{At 40 minutes: } m_{P3,F} = m_{MW} - m_{BL1} - m_{BL2} - m_{BL3}$$

....

$$\text{At 180 minutes: } m_{P8,F} = m_{MW} - m_{BL1} - \dots - m_{BL8}$$

The values were then divided by the initial Klason amount  $m_{MW}$ :

0 min	10min	20 min	40 min	60min	90 min	120 min	150 min	180 min
$\frac{m_{P0,F}}{m_{MW}}$	$\frac{m_{P1,F}}{m_{MW}}$	$\frac{m_{P2,F}}{m_{MW}}$	$\frac{m_{P3,F}}{m_{MW}}$	$\frac{m_{P4,F}}{m_{MW}}$	$\frac{m_{P5,F}}{m_{MW}}$	$\frac{m_{P6,F}}{m_{MW}}$	$\frac{m_{P7,F}}{m_{MW}}$	$\frac{m_{P8,F}}{m_{MW}}$

By adding the Klason lignin in each BL fraction to pulp, this calculations were called Backward (B) calculations:

$$\text{At 180 minutes: } m_{P8,B} = m_p$$

$$\text{At 150 minutes: } m_{P7,B} = m_p + m_{BL8}$$

$$\text{At 120 minutes: } m_{P6,B} = m_p + m_{BL8} + m_{BL7}$$

$$\text{At 90 minutes: } m_{P5,B} = m_p + m_{BL8} + m_{BL7} + m_{BL6}$$

....

$$\text{At 0 minutes: } m_{P0,B} = m_p + m_{BL8} + \dots + m_{BL1}$$

The values were then divided by the initial Klason amount  $m_{MW}$ :

0 min	10min	20 min	40 min	60min	90 min	120 min	150 min	180 min
$\frac{m_{P0,B}}{m_{MW}}$	$\frac{m_{P1,B}}{m_{MW}}$	$\frac{m_{P2,B}}{m_{MW}}$	$\frac{m_{P3,B}}{m_{MW}}$	$\frac{m_{P4,B}}{m_{MW}}$	$\frac{m_{P5,B}}{m_{MW}}$	$\frac{m_{P6,B}}{m_{MW}}$	$\frac{m_{P7,B}}{m_{MW}}$	$\frac{m_{P8,B}}{m_{MW}}$

Then the mean values between forward and backward were plotted.

## APPENDIX IV

---

### LITERATURE VALUES FOR COMPOSITION IN *E. UROGRANDIS*

The values presented below have not been obtained with the same methods used in this project, but they give a good approximation of the composition.

Table i. (Evtuguin and Neto, 2007)

	Lignin	Cellulose	Hemicelluloses (Pentosans)	Extractives	Ashes
<i>E. Urograndis</i>	26.7	48.6	11.3	1.91	0.53

Table ii: From (Gonzalez et al., 2011)

	Cellulose		Hemicelluloses				Extractives		Other	
	Glucans	Xylans	Galactans	Mannans	Arabinans	Uronic acid	Acetyl	Lignin	Resins	Ash
<i>E. Urograndis</i>	44.6 %	12.8%	0.5%	0.5%	0.3%	4.4%	2.9%	30.1%	3.6%	0.3%

## APPENDIX V

---

### MWD

The molecular weight distributions, MWD:s, measured with GPC are presented below. First the results from the flow-through reactor are presented in Figure I to Figure XII, followed by the autoclave results in Figure XIII to Figure XV. Some samples are marked with “star”, e.g. “LB#2-5star” in Figure I. This signifies samples which were difficult to dissolve. These were dissolved with more DMSO in the first dissolution. The following dilution ensured that these samples had the same concentration as the others when being analysed with the GPC. Furthermore, some samples are labelled with a “#2” indicating that a previous run had been run. All the presented samples correspond to the cooks for which the results have already been presented.

The samples are presented normalised according to Eq. (i).

$$X = \frac{x - y_{min}}{y_{max} - y_{min}} \quad (i)$$

Where  $x$  is the measured response at a given molecular weight,  $y_{min}$  is the minimum and  $y_{max}$  is the maximum response at a given molecular weight.  $X$  is the value used in the figures.

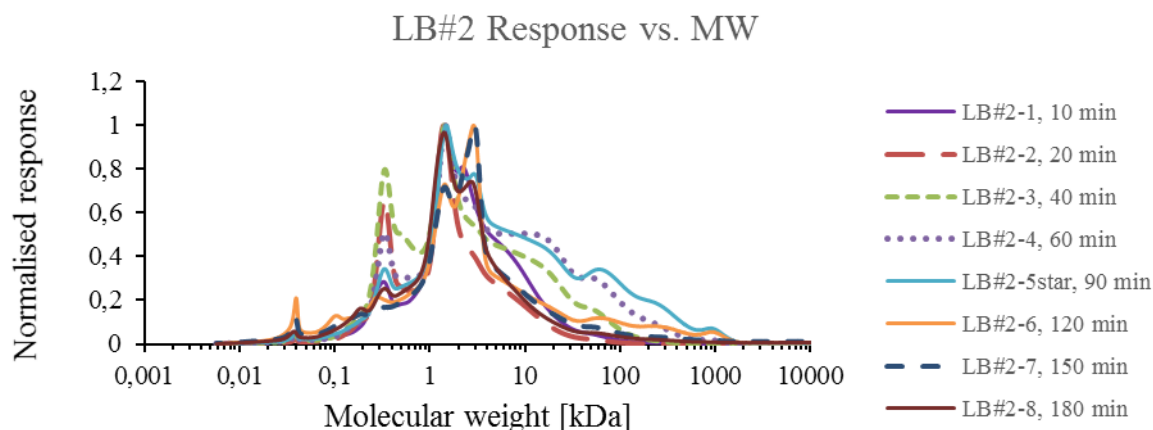


Figure I. MWD for LB. Sample 5 was dissolved in more DMSO than the other samples.

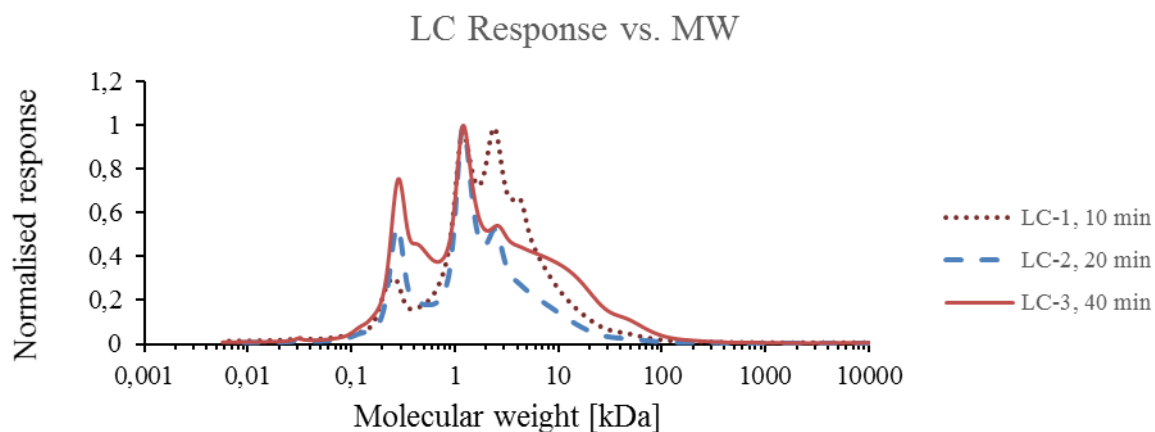


Figure II. MWD for LC.

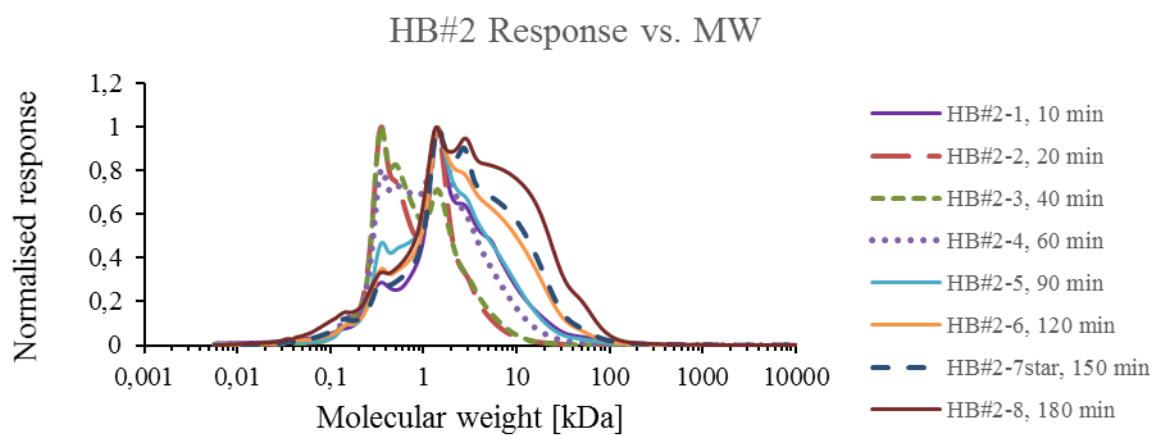


Figure III. MWD for HB. Sample 7 was dissolved in more DMSO than the other samples.

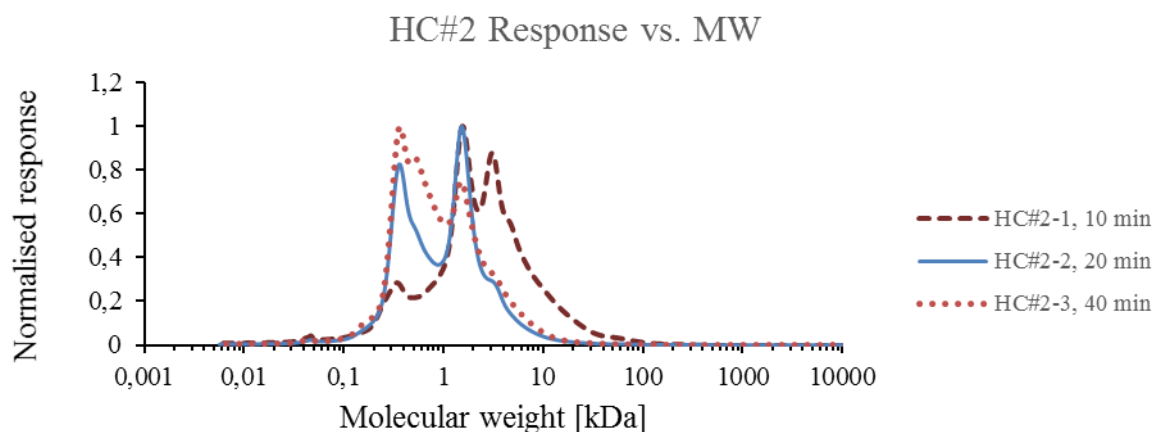


Figure IV. MWD for HC.

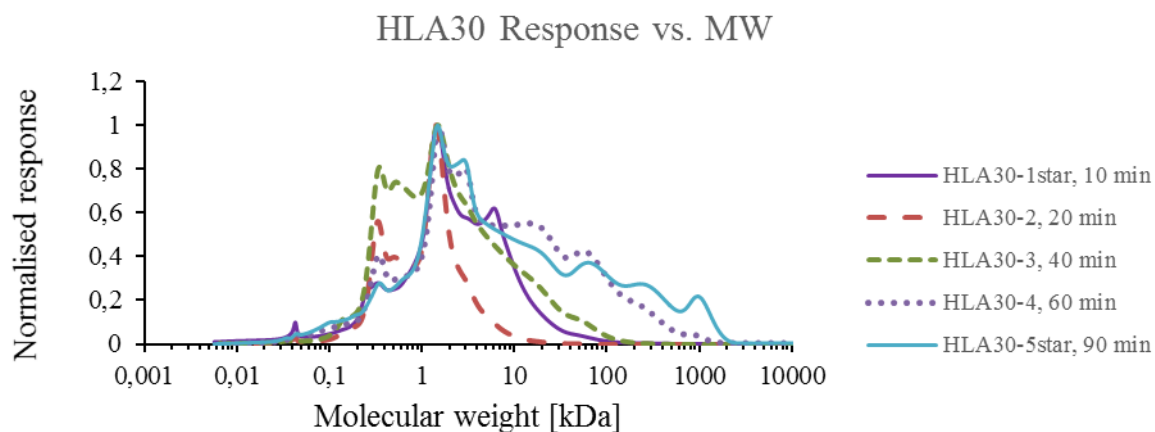


Figure V. MWD for HLA30. Samples 1 and 5 were dissolved in more DMSO than the other samples.

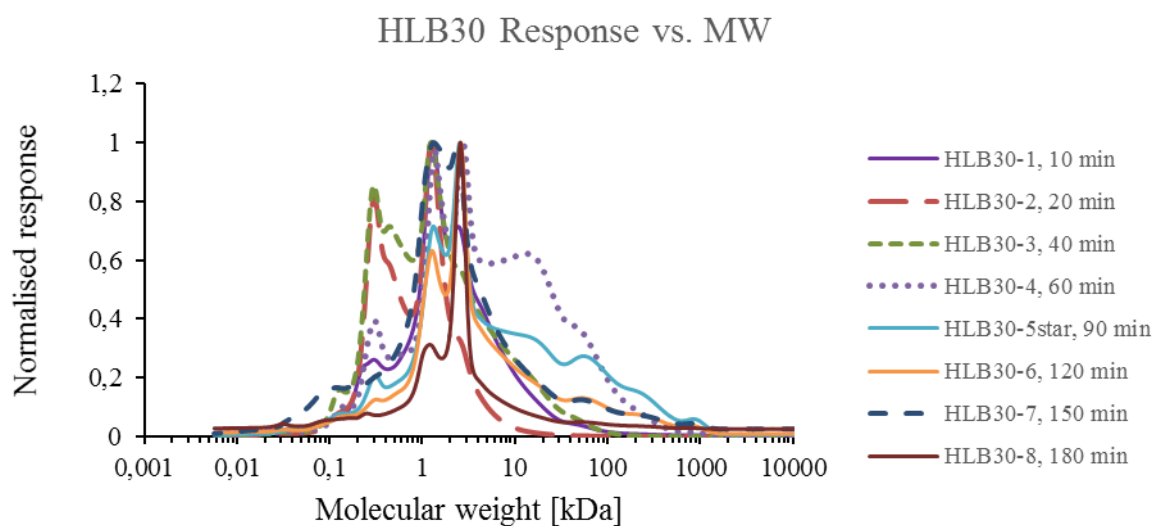


Figure VI. MWD for HLB30. Sample 5 was dissolved in more DMSO than the other samples.

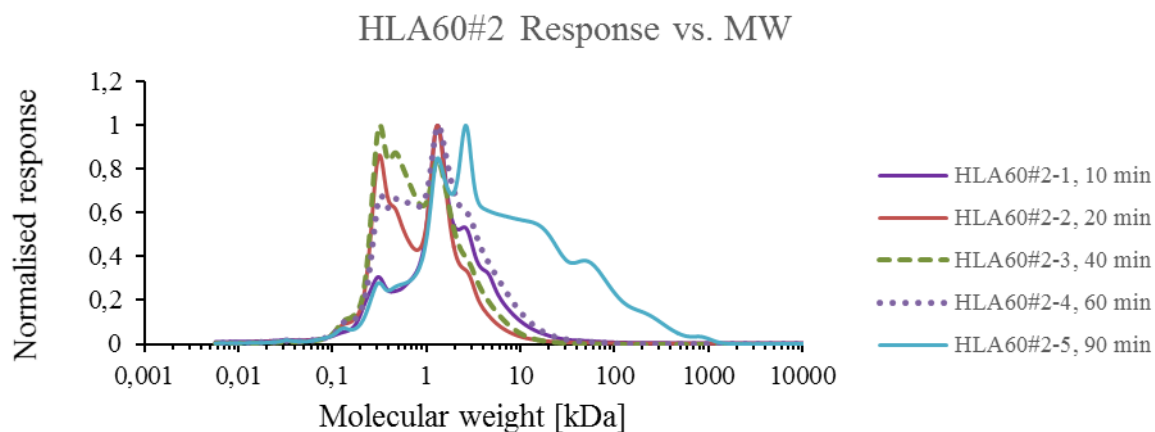


Figure VII. MWD for HLA60.

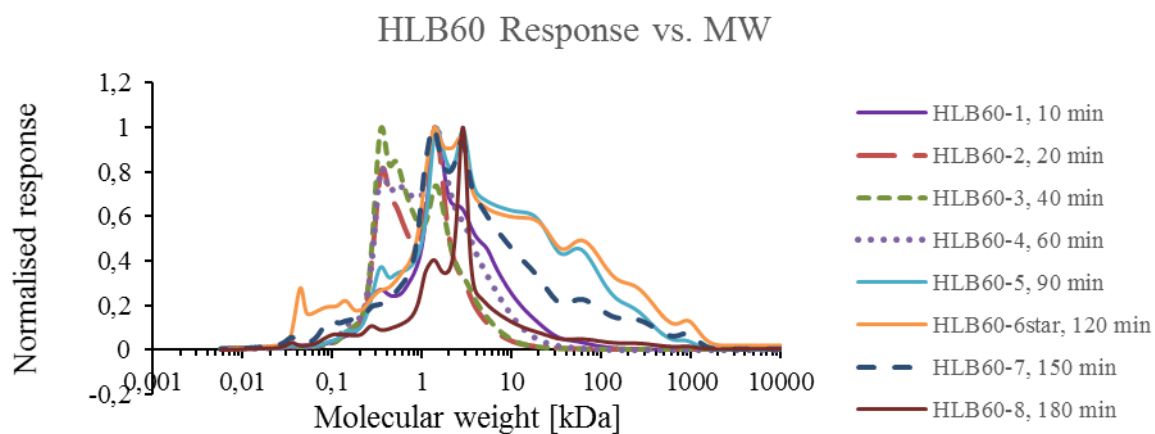


Figure VIII. MWD for HLB60. Sample 6 was dissolved in more DMSO than the other samples.

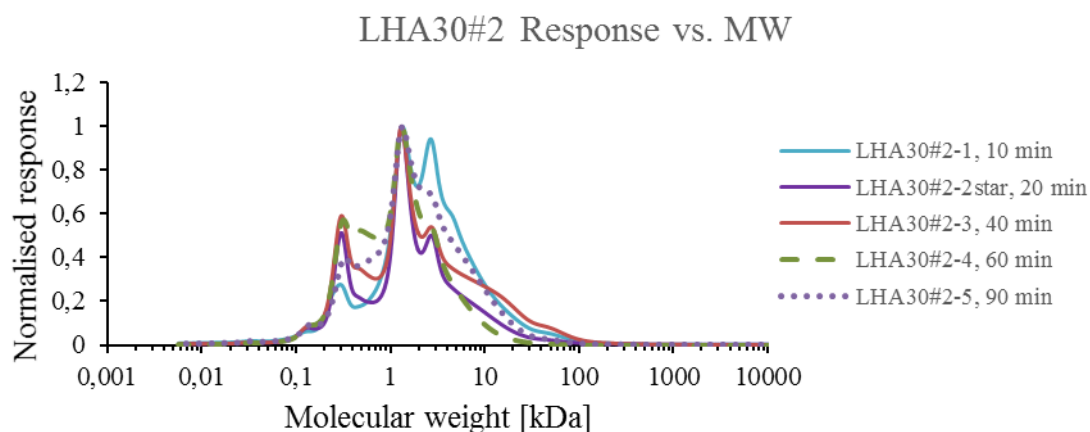


Figure IX. MWD for LHA30. Sample 2 was dissolved in more DMSO than the other samples.

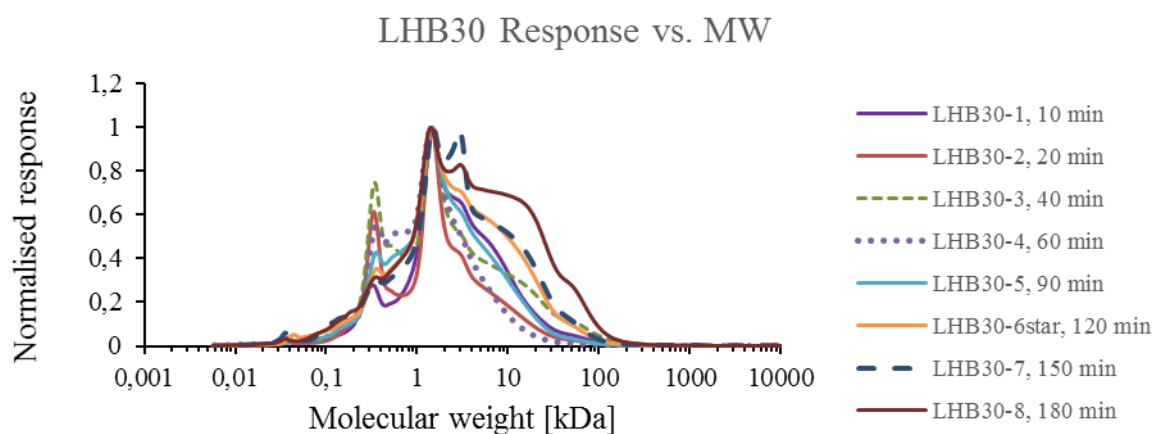


Figure X. MWD for LHB30. Sample 6 was dissolved in more DMSO than the other samples.

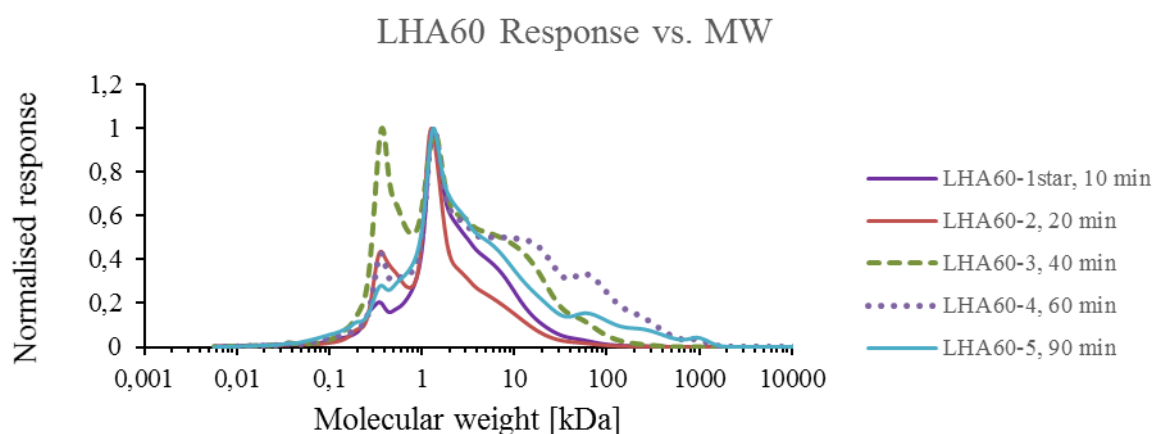


Figure XI. MWD for LHA60. Sample 1 was dissolved in more DMSO than the other samples.

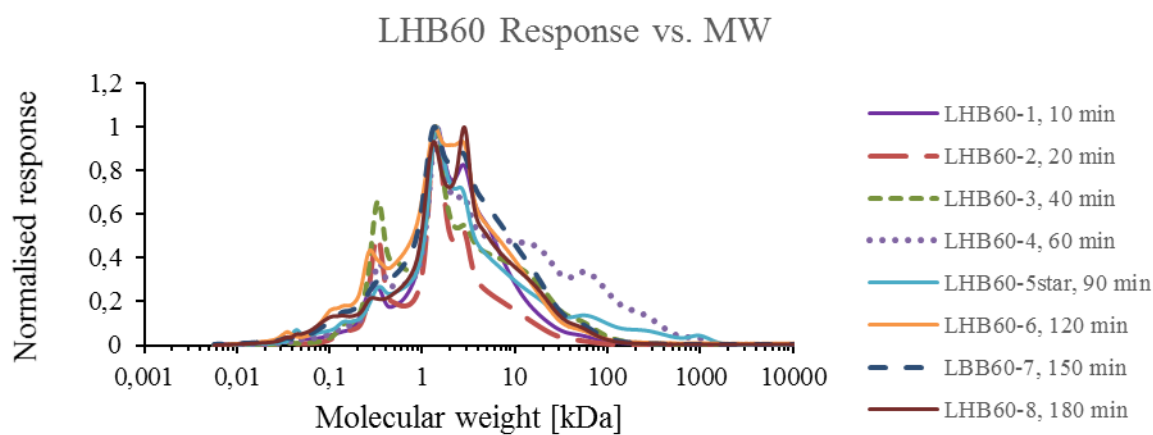


Figure XII. MWD for LHB60. Sample 5 was dissolved in more DMSO than the other samples.

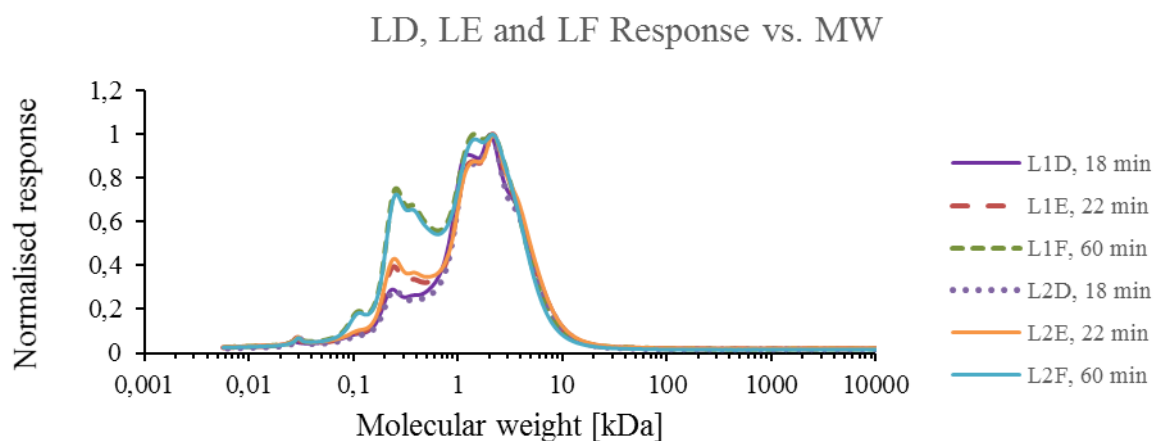


Figure XIII. MWD for LD, LE and LF.

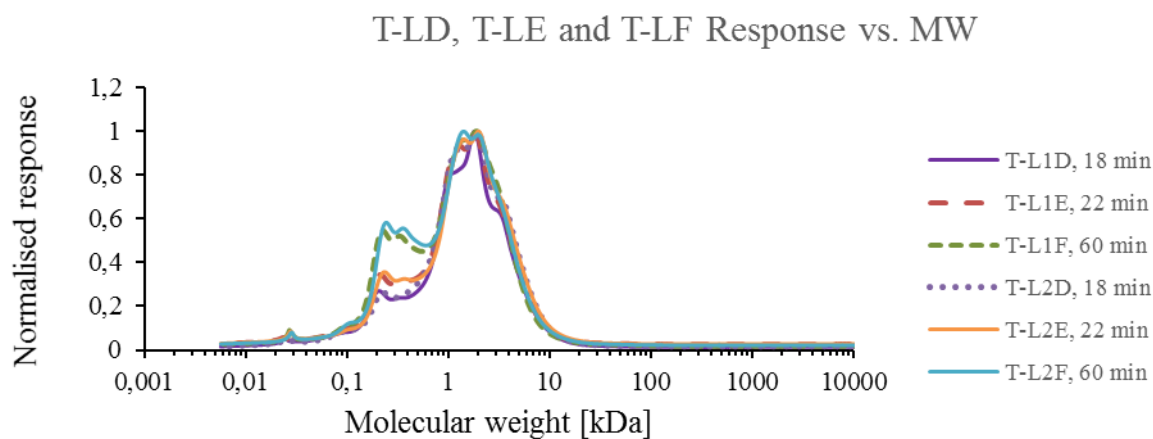


Figure XIV. MWD for T-LD, T-LE and T-LF.

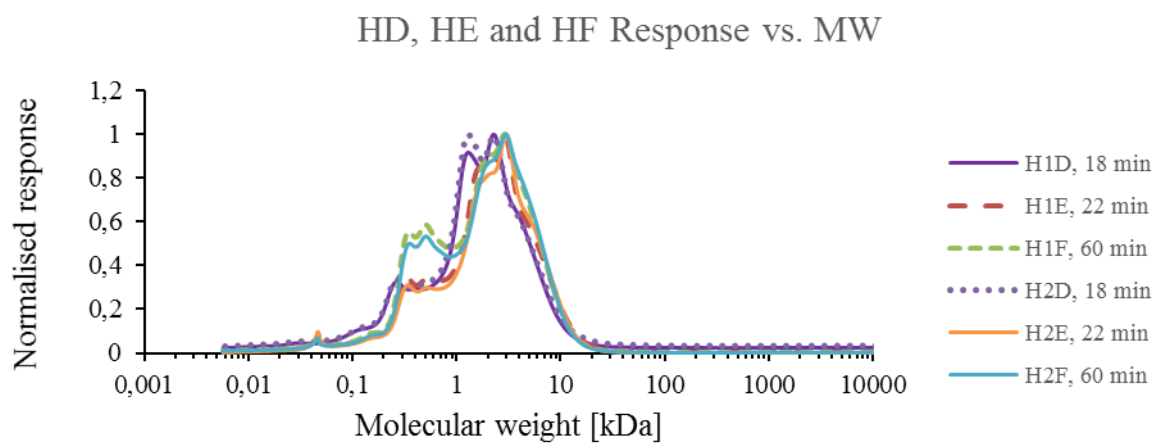


Figure XV. MWD for HD, HE and HF.

# APPENDIX VI

## 2D-NMR

An overview of the regions of the NMR spectra is presented in Figure XVI.

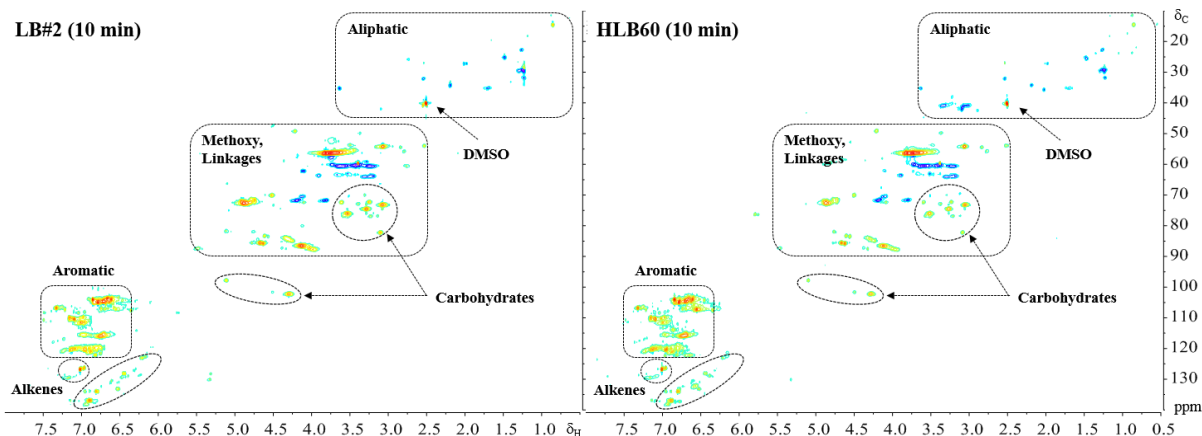


Figure XVI. Overview of the regions of the NMR spectra.

In Figure XVII, structures referred to in the NMR spectra are displayed. Conventional numbering of carbohydrates and lignin phenylpropanes is employed.

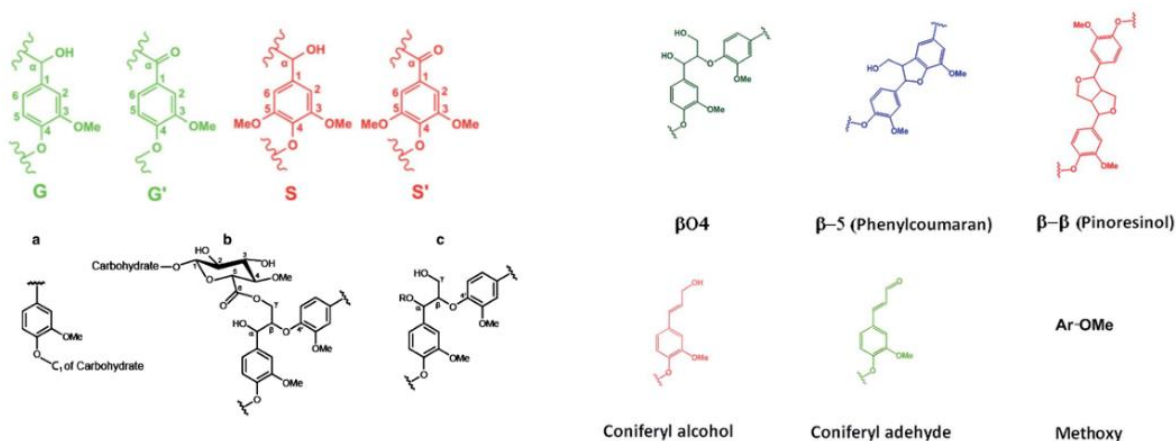


Figure XVII. The structures referred to in the NMR spectra.

### L\_B samples

The NMR spectra for the L\_B samples are presented below. In Figure XVIII the aliphatic and methoxy, linkages and carbohydrates regions are presented. The aromatic and alkene regions are presented in Figure XIX. Cooking time increase from left to right as indicated by the titles, “LB#2 (10min)” etc. Notice that although the title reads “LB#2” this is the same sample referred to as “L\_B” in the rest of the project.

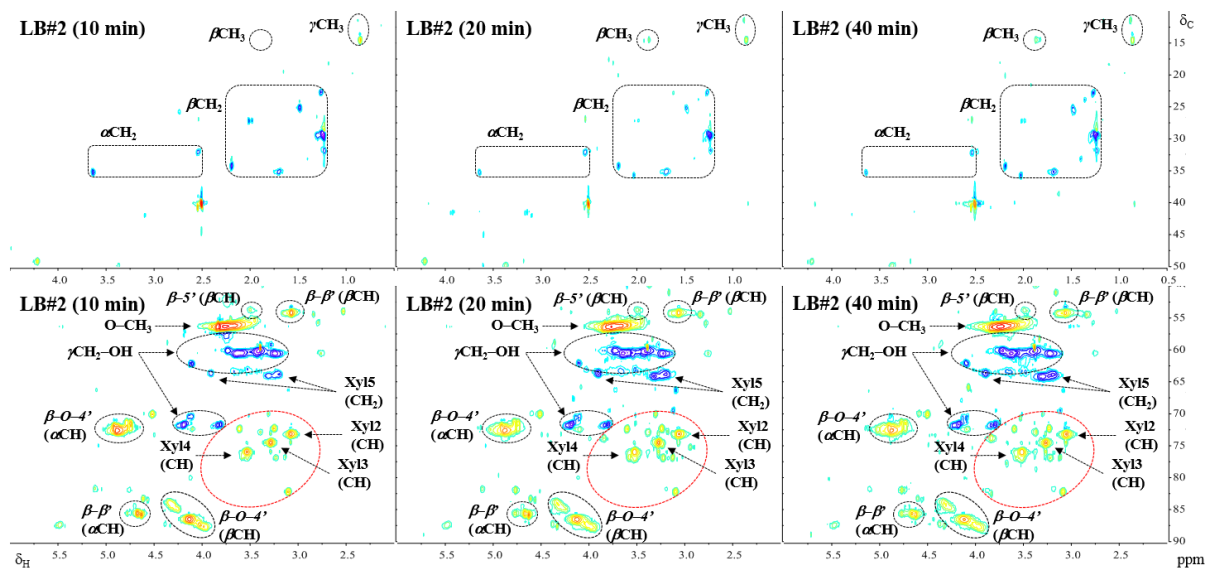


Figure XVIII. The aliphatic region of the NMR spectra for *L\_B* is presented in the top three squares. In the bottom three squares the methoxy groups, linkages and carbohydrate regions are presented.

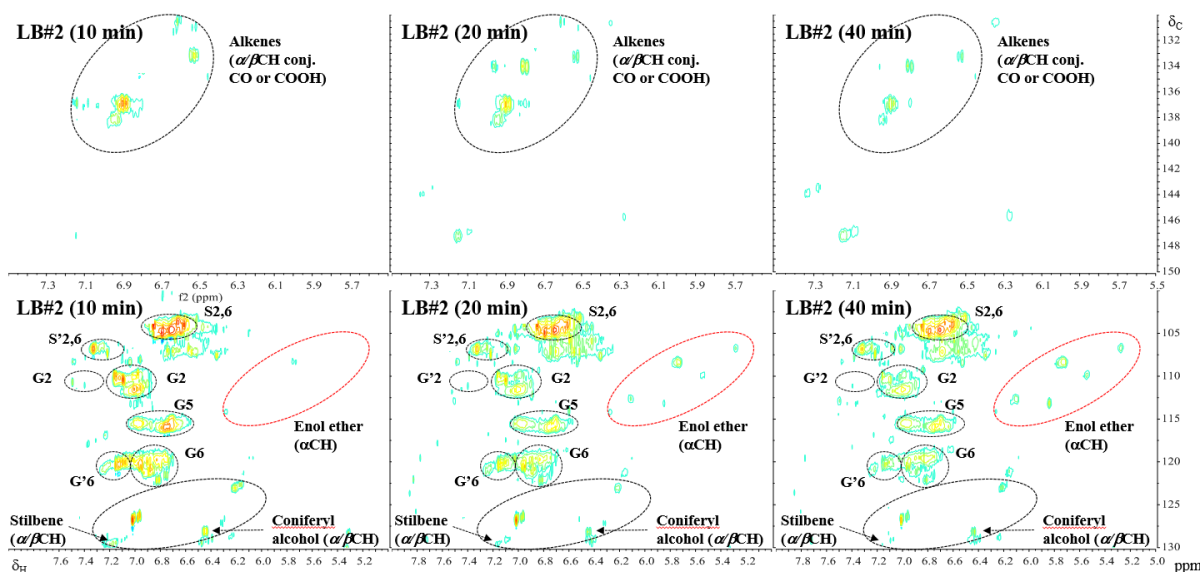


Figure XIX. The alkene region of the NMR spectra for *L\_B* is displayed in the upper three squares. In the bottom three squares the aromatic region is presented.

### HL\_B\_60 samples

The NMR spectra for the HL\_B\_60 samples are presented below. In Figure XX the aliphatic and methoxy, linkages and carbohydrates regions are presented. The aromatic and alkene regions are presented in Figure XXI. Cooking time increase from left to right as indicated by the titles, “HL\_B\_60 (10min)” etc.

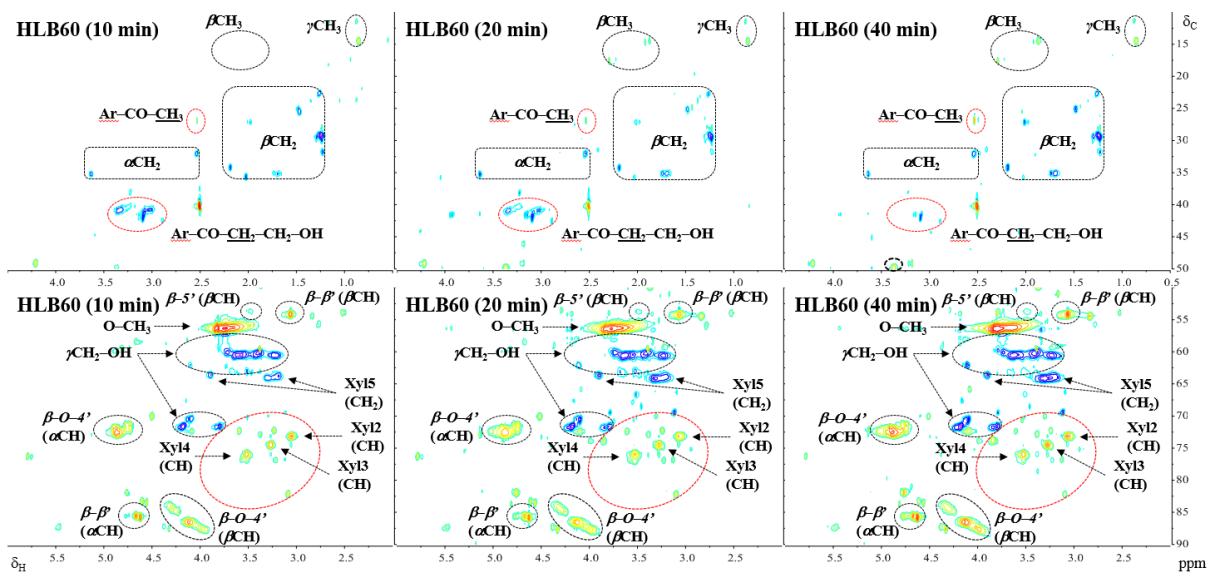


Figure XX. The aliphatic region of the NMR spectra for HLB<sub>60</sub> is presented in the top three squares. In the bottom three squares the methoxy groups, linkages and carbohydrate regions are presented.

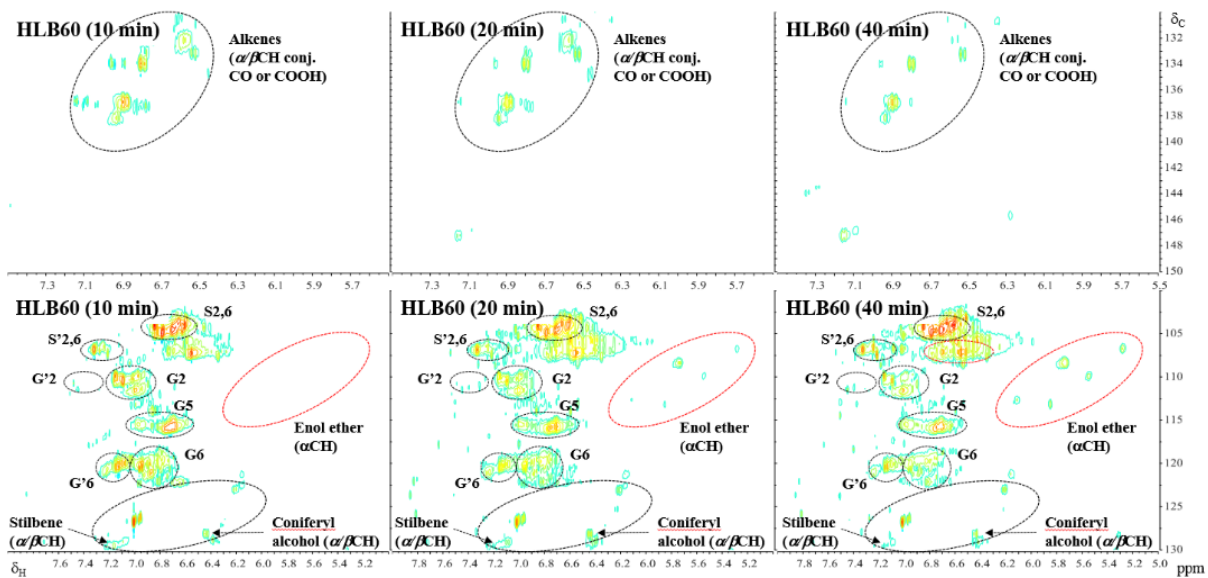


Figure XXI. The alkene region of the NMR spectra for HLB<sub>60</sub> is displayed in the upper three squares. In the bottom three squares the aromatic region is presented.